Norwegian University
of Life Sciences

Master's Thesis 2021 60 ECTS
Faculty of Environmental Sciences and Natural Resource Management

Waste-based sorbents for reducing the mobility and leaching of per- and polyfluoroalkyl substances (PFAS) in contaminated soil

Anny Qvale
Chemistry and Biotechnology (specialization: environmental chemistry)
Faculty of Chemistry, Biotechnology and Food Science

[This page has been left blank intentionally]

Acknowledgements

This thesis concludes my master's degree in environmental chemistry at the Norwegian University of Life Sciences (NMBU). The work was supported the earthresQue centre for research driven innovation (Rescue of Earth Materials and Wastes in the Circular Economy), which is partly funded by the Research Council of Norway, project number 310042/F40. The thesis is further associated with and funded by the PhD project *Use of waste-based sorbents for ex-situ and in-situ treatment of PFAS contaminated soil* (project number 5752 0000 02) at Lindum AS.

The completion of this work would not have been possible without all the fantastic support and assistance I received. First and foremost, I would like to thank my supervisors for their valuable feedback, guidance and enthusiasm. My sincere thanks to my main supervisor, Åsgeir R. Almås (NMBU), for being a constant source of support and knowledge. Your insight and availability have been greatly appreciated. I would also like to thank my co-supervisor, Karen Ane F. Skjennum (Lindum AS), for introducing me to the field of soil remediation and for all your invaluable help and advice. My special thanks go to Thomas Hartnik (Lindum AS) as well, for all your excellent guidance and input in the later stages of the work.

Secondly, I wish to express my sincere gratitude to the employees at Faculty for Environmental Sciences and Natural Resource Management (MINA). The expertise and laboratory assistance provided by Irene E. Eriksen Dahl, Valentina Zivanovic, Oddny Gimmingsrud, Christian Solheim, Eivind Molversmyr and Øyvind Enger was truly appreciated. I also overall want to thank all the MINA employees for being inclusive and making me feel welcome at the faculty's soil laboratory.

At last, I would like to thank my family and friends for their support and encouragement. Both the stimulating discussions and occasional joyful distractions have been very welcome. A great thanks to Hermann and Selma for proofreading my thesis. I would also like to extend my special thanks to Oscar for always being a source of encouragement and support.

Norwegian University of Life Sciences (NMBU)

Ås, December 2021

Anny Qvale

[This page has been left blank intentionally too]

Abstract

Per- and polyfluoroalkyl substances (PFAS) are a diverse group of anthropogenic, organic chemicals whose widespread use have caused contamination issues worldwide. Former use of PFAS-containing firefighting foams have generated many pollution hotspots, and a major concern is that the contaminants can spread from such contaminated sites and deteriorate drinking water. A number of waste-based products have great potential as binding materials (sorbents) for PFASs in contaminated soil, and these sorbents may prevent the substances from leaching out of such soils and reaching living organisms in the surrounding environment.

In this study, the suitability of seven different waste-based materials as PFAS sorbents was investigated for a contaminated soil sampled at a former firefighting training site. These potential sorbents were activated biochar, ash, bonemeal, chitosan, filter dust, LECA and slag. The materials' ability to sorb PFASs was explored by performing batch leaching tests on soil samples that contained different concentrations of the sorbents in question. In addition to determining the leached PFAS concentrations, the batch leachates were also analysed for additional geochemical parameters that the sorbents might influence—including pH, dissolved organic carbon (DOC), electrical conductivity, anions and various trace elements. The soil, which was characterized as *silty sand* with a low total organic carbon content, had a large overweight of perfluorooctanesulfonic acid (PFOS) among the Σ20 quantified PFASs. Of the seven sorbents tested, the activated biochar was most efficient and sorbed > 99 % of the measured PFASs in the samples added 0.1 % (soil dry weight) biochar. While activated biochar sharply reduced the concentrations of PFASs of different perfluorocarbon chain lengths and functional groups alike, the other sorbents mainly caused a reduction in long-chain PFASs. Bonemeal, which was the second most efficient sorbent, reduced the leached PFOS concentration by 87 % in the samples added 5 % (soil dw) bonemeal. However, bonemeal was not efficient for short-chain PFASs. The ability of the remaining sorbents was much lower (< 50 % reduction in leached PFOS concentration at the highest sorbent doses), and they were thus not considered good sorbents in this study. In conclusion, though not great sorption abilities were observed for all the materials investigated, waste-based materials still have great potential as economical and sustainable alternatives to commercial sorbents.

[This page has also been left blank intentionally]

Sammendrag

Per- og polyfluorerte alkylstoffer (PFAS) er en stor gruppe menneskeskapte, organiske forbindelser som grunnet sin utbredte bruk kan knyttes til forurensningsproblemer over hele verden. Tidligere bruk av PFAS-holdig brannskum har resultert i at mange «hotspots» for PFAS-forurensning har oppstått, og det fryktes at stoffene kan spre seg fra slike områder og forgifte drikkevann. En rekke avfallsbaserte produkter har et stort potensial som bindingsmaterialer (sorbenter) for PFAS i forurenset jord, og disse materialene kan dermed hindre stoffene i å lekke ut av jorden og komme i kontakt med levende organismer.

I denne studien ble syv avfallsbaserte materialer testet som PFAS-sorbenter for en forurenset jord prøvetatt ved et tidligere brannøvingsfelt. Disse potensielle sorbentene var aktivert biokull, aske, benmel, kitosan, filterstøv, LECA og slagg. Materialenes evne til å binde PFAS ble undersøkt ved å utføre ristetester av jordprøver tilsatt ulike konsentrasjoner av sorbentene. Eluatene ble både analysert for PFAS og ytterligere geokjemiske parametere som sorbentene kunne påvirke—inkludert pH, løst organisk karbon (DOC), elektrisk ledningsevne, anioner og ulike grunnstoffer. Jordprøven ble karakterisert som siltig sand med et lavt totalt organisk karboninnhold, og den inneholdt en stor overvekt av perfluoroktansulfonsyre (PFOS) blant de Σ20 kvantifiserte PFAS-ene. Den mest effektive sorbenten av de syv testede materialene var det aktiverte biokullet som sorberte > 99 % av de målte PFAS-ene i prøvene tilsatt 0,1 % (tørrvekt jord) biokull. Mens biokullet ga kraftige konsentrasjonsnedganger hos PFAS-er med både forskjellige perfluorkarbonkjedelengder og funksjonelle grupper, reduserte de andre sorbentene hovedsakelig langkjedede PFAS-er. Benmel, som var den nest mest effektive sorbenten, reduserte eluatkonsentrasjonen av PFOS med omtrent 87 % i prøvene tilsatt 5 % (tørrvekt jord) benmel. Dette organiske, avfallsbaserte materialet var imidlertid ikke effektivt for kortkjedede PFAS-er. Sorpsjonsevnen til de gjenværende sorbentene var mye lavere (< 50 % reduksjon i PFOS-konsentrasjon ved de høyeste sorbentdosene), og de ble derfor ikke ansett som gode sorbenter i denne studien. Selv om sorpsjonsevnene var små for de fleste av de undersøkte materialene, ble det konkludert med at avfallsbaserte materialer fortsatt har et stort potensial som økonomiske og bærekraftige alternativer til kommersielle sorbenter.

[This page has been left blank intentionally as well]

Table of Contents

Abbreviations and acronyms

AC	Activated carbon
AFFF	Aqueous film-forming foam
ANOVA	Analysis of variance
BIC	Bayes Information Criterion
CAS	Chemical Abstracts Service
Cl^-	Chloride
DOC	Dissolved organic carbon
DW	Dry weight
EC	Electrical conductivity
FASA	Perfluoroalkane sulfonamides
$FeSO_4 \cdot H_2O$	Iron sulphate monohydrate
$F_{leachable}$	The leachable fraction of a constituent
HF	Hydrofluoric acid
HNO_3	Nitric acid
IC	Ion chromatography
ICP-MS	Inductively coupled plasma mass spectrometry
K_d	The solid-water partitioning coefficient
K_{oc}	The carbon content-normalized partitioning coefficient
LC-MS/MS	Liquid Chromatography combined with mass spectrometry
LECA	Lightweight expanded clay aggregate
LOD	Limit of detection
LOI	Loss on ignition
LOQ	Limit of quantification
L/S ratio	Liquid-to-solid ratio
MeFOSA	N-Methylperfluorooctanesulfonamide (*compound*)
MINA	Faculty of Environmental Sciences and Natural Resource Management
NMBU	The Norwegian University of Life Sciences
NO_3^-	Nitrate
PBT	Persistent, bioaccumulative and toxic

PES	Polyethersulfone
PFAA	Perfluoroalkyl acids
PFAS	Per- and polyfluoroalkyl substances
PFBA	Perfluorobutanoic acid (*compound*)
PFBS	Perfluorobutane sulfonic acid (*compound*)
PFCA	Perfluoroalkyl carboxylic acids
PFHxA	Perfluorohexanoic acid (*compound*)
PFHxS	Perfluorohexane sulfonate (*compound*)
PFOA	Perfluorooctanoic acid (*compound*)
PFOS	Perfluorooctanesulfonic acid (*compound*)
PFOSA	Perfluorooctane sulfonamide (*compound*)
PFSA	Perfluoroalkyl sulfonic acids
pK_a	Acid dissociation constant (negative log of K_a)
PP	Polypropylene
PZC	Point of zero charge
rpm	Revolutions per minute
SOM	Soil organic matter
SO_4^{2-}	Sulphate
TC	Total carbon
TIC	Total inorganic carbon
TOC	Total organic carbon
VIF	Variance Inflation Factor
ρ	Spearman's rank-order correlation

1 Introduction

Per- and polyfluoroalkyl substances (PFAS) are synthetic organic chemicals that have hazardous effects on both the environment and human health (Høisæter et al., 2019; Silvani et al., 2019; Lindstrom et al., 2011). Anthropogenic activities have resulted in large-scale PFAS contamination issues worldwide, and pollution hotspots urgently need to be remediated to protect surrounding environments from contamination (Sörengård et al., 2019; Hale et al., 2017). The remediation of PFAS-contaminated soil is, however, extremely challenging due to the substances' high persistence and mobility in the environment, and traditional soil remediation techniques have so far been inefficient (Bolan et al., 2021; Mahinroosta & Senevirathna, 2020). Hence, alternative methods that are both cost-effective and environmentally benign for site remediation must be developed.

1.1 PFAS: a large, complex and challenging group

PFASs are defined as substances that contain alkyl moieties where the hydrogen atoms have either partly or completely been replaced with fluorine (European Commission, 2020a). The carbon-fluorine (C-F) bond is very strong, which causes PFASs to be highly physically and chemically stable (Zushi et al., 2012). This high stability has given PFASs numerous industrial and commercial applications, but also makes them resistant to environmental degradation (Mahinroosta & Senevirathna, 2020). In addition to being highly mobile in the environment, a persistent, bioaccumulative and toxic (PBT) nature has been demonstrated for several PFASs (European Commission, 2020a). Still, only a few PFASs are well studied, and much knowledge currently lacks about this highly diverse chemical group.

Due to the substances' variation in chain lengths and functional groups, a wide range of PFASs exist—both in polymeric and non-polymeric forms. So far, more than 6000 PFAS variants have been CAS-registered (U.S. EPA, 2020), but the real number of different PFASs is likely much higher. The physicochemical properties of separate PFASs often vary based on their structural elements, including carbon chain length, functional group and fluorination degree (Sörengård et al., 2020). Arranging the substances based on their structures can therefore be helpful, and such a classification of (non-polymer) PFASs is given in Figure 1.

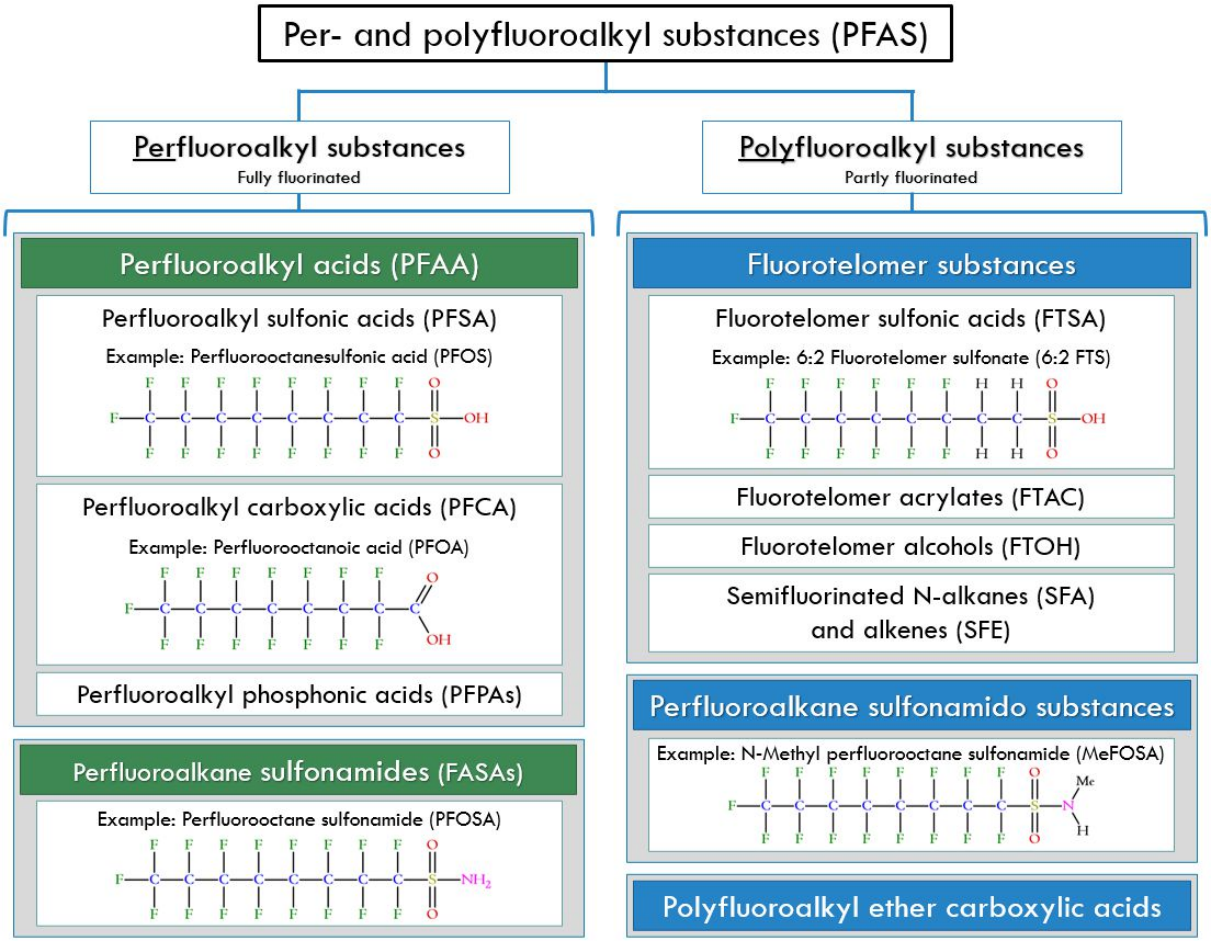

Figure 1. Overview of some environmentally relevant (non-polymer) PFAS groups, based on the classification hierarchy by Buck et al. (2011). Examples of different eight-carbon PFAS are given for both perfluoroalkyl substances (where the carbon chain is fully fluorinated) and polyfluoroalkyl substances (which contains at least one partially hydrogenated carbon).

A well-known PFAS class is the perfluoroalkyl acids (PFAA), where each compound consists of a fully fluorinated carbon chain attached to an acid functional group (Mahinroosta & Senevirathna, 2020). The two most important classes of PFAAs are the perfluoroalkyl sulfonic acids (PFSA), with sulfonic acid groups (–SO_2-OH), and the perfluoroalkyl carboxylic acids (PFCA), with carboxylic acid groups (–COOH). PFSAs, PFCAs and their precursors can also further be grouped into *short-chain* and *long-chain* PFAS. As recommended by Buck et al. (2011), long-chain PFASs are defined as PFSAs with ≥ 6 perfluorinated carbons and PFCAs with ≥ 7 perfluorinated carbons. Short-chain PFASs are then referred to PFSAs and PFCAs with fewer perfluorinated carbons than their long-chain homologues. Other perfluoroalkyl substances with perfluorinated chains of at least 7 carbons are considered "long-chain" as well (Buck et al., 2011).

Two of the most thoroughly studied PFASs are perfluorooctanesulfonic acid (PFOS) and perfluorooctanoic acid (PFOA), which are examples of PFSAs and PFCAs, respectively (fig. 1). Both PFOS and PFOA are long-chained, extremely persistent, soluble in water and useful as surfactants due to their lipid- and water-repellent properties (Mahinroosta & Senevirathna, 2020). As the chemicals are exceptionally stable, they also have numerous precursors: for instance, N-methyl perfluorooctane sulfonamide (MeFOSA) which is a PFOS-precursor (van Hees, 2017). Furthermore, all PFAAs either exist in an anionic, neutral or cationic state. The state is pH dependent, and due to their very low acid dissociation constants (pK_a), PFOA and PFOS usually occur as dissociated anions under natural environmental conditions (Vierke et al., 2013). While most analytically targeted PFASs to date also are anionic, differently charged PFASs and precursors can constitute a large portion of the chemicals at contamination sites (Nickerson et al., 2020). Altogether, with much knowledge lacking on most PFASs and their potential hazardous effects, the widespread use of these chemicals is of increasing concern.

1.2 PFAS contamination – historical use and contamination hotspots

Since production started in the early 1950s, anthropogenic activities have resulted in large-scale PFAS contamination issues worldwide. While numerous pollution hotspots exist, the substances are also found at remote locations and in wildlife far from human settlements (Lindstrom et al., 2011). The chemicals' ability to travel long distances and contaminate areas far from their release points thus makes for a complicated PFAS emission picture. Much is still unclear about the exposure of PFAS to humans and the environment, but some major exposure pathways have been identified and are summarized in Figure 2.

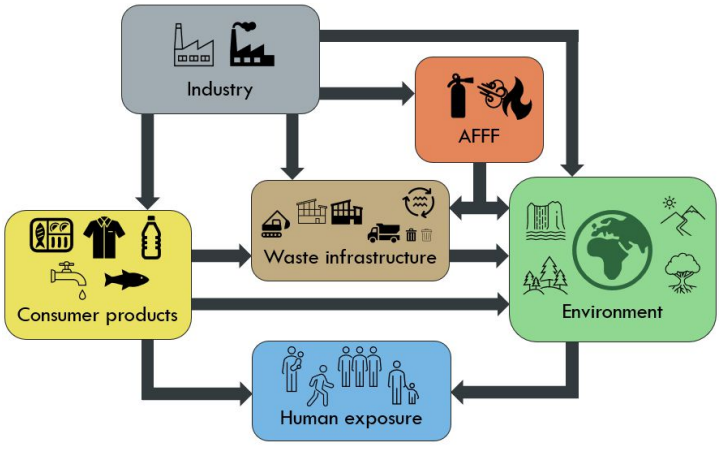

Figure 2. The main PFAS exposure pathways, adapted from Sunderland et al. (2019). Wastewater effluents, landfill leachate, biosolids and aqueous film forming foam (AFFF) are considered the major sources of PFAS contamination in water and soil (Bolan et al., 2021).

PFAS can enter the environment directly from industrial sites, aqueous film forming foam (AFFF), waste infrastructure and consumer products (fig. 2). Humans are then at risk of being exposed to PFAS through contaminated drinking water and food, in addition to exposure through contact with consumer products and dust/air in indoor environments (Sunderland et al., 2019; Lindstrom et al., 2011). More than 200 use categories for PFASs have been described recently, which shows how the chemicals are used in almost all industry sectors and a wide range of consumer products (Glüge et al., 2020). Among the most well-known PFAS uses are textile impregnation, food packaging and AFFF used in firefighting. Especially the latter is important in an environmental context; the extensive use of AFFFs is deemed a key reason for PFAS entering the environment (Bolan et al., 2021).

Former use of PFAS-containing AFFFs has caused many historical firefighting training sites to become contamination hotspots. A major concern is that PFAS from these contaminated sites can leach into groundwater and deteriorate drinking water (Bolan et al., 2021; Filipovic et al., 2015), which have already led to severe issues in Sweden (Banzhaf et al., 2017). In Norway, the sites of about 50 airports are polluted with PFASs due to firefighting training with AFFFs (Cappelen et al., 2016). Phasing out the production of harmful PFASs is an important measure to prevent further contamination. While the use of PFAS-containing firefighting foams was banned at most Norwegian airports in 2012—after a phaseout of PFOS back in 2001—many of the firefighting training facilities are still heavily contaminated with PFAS residues (Norconsult, 2019; Cappelen et al., 2016). The leaching of PFASs from such polluted areas can continue for decades (Ross et al., 2018), and clean-up is urgently needed to protect the surrounding areas. Previous regulations on specific PFASs have not been sufficient to deal with the pollution issue (European Commission, 2020a).

1.3 PFAS-regulations and the rise of short-chain PFASs

While the PFASs' high thermal stability and lipid-/water-repellence makes the chemicals useful as surfactants (surface active agents) in AFFFs, growing awareness of their hazardous effects has triggered the enactment of several regulations (European Commission, 2020a). Especially the ability of some PFASs to bioaccumulate and bind to protein has raised concerns (Cousins et al., 2020). As the strongest evidence of negative health effects have been obtained for PFOS and PFOA, most restrictions concern these two long-chain PFASs (Lindstrom et al., 2011). PFOS and PFOA are, for instance, internationally restricted through the Stockholm Convention on Persistent Organic Pollutants (UNEP, 2019), included in EU's revised directive on drinking

water (European Commission, 2020b) and newly proposed to get Norwegian soil normative values of 0.003 mg/kg dry weight (Norwegian Geotechnical Institute, 2020). Table 1 offers an overview of the current Norwegian quality standards for PFOS and PFOA in water.

Table 1. The Norwegian quality standard for PFOS and PFOA in both fresh water and coastal water. Only class II and some class III values are defined for these components (Norwegian Environment Agency, 2020).

	Class	**Class I**	**Class II**	**Class III**	**Class IV**	**Class V**
	Classification	Background	Good	Moderate	Bad	Very bad
PFOS	Fresh water (ng/L) Coastal water (ng/L)	*NA*	0–0.65 0–0.13	0.65–36000 0.13–7200	*NA*	*NA*
PFOA	Fresh water (ng/L) Coastal water (ng/L)	*NA*	0–9100 0–9100	*NA*	*NA*	*NA*

NA = not answered

The introduction of regulations on long-chain PFASs, such as PFOS and PFOA, have caused a shift to short-chain PFASs, despite little knowledge on these variants (European Commission, 2020a; Ateia et al., 2019). Perfluorobutane sulfonic acid (PFBS) is an example of a four-carbon PFAS developed to replace long-chain PFOS (U.S. EPA, 2018). However, using PFBS is now seen as highly concerning due to its high persistence and mobility, alongside its probable severe effects on human and environmental health (European Commission, 2020a). Moreover, the shift from long-chain to short-chain PFASs has also additionally complicated the remediation endeavours at polluted sites.

After the use of short-chain PFASs was adopted, the chemicals have been increasingly detected in the environment (Ateia et al., 2019). Perfluorobutanoic acid (PFBA) and PFBS are among the most frequently found short-chain PFASs in environmental matrices, and they are usually present in relatively high concentrations compared to the other short-chain compounds (Li et al., 2020). Among the long-chain PFASs, the most frequently detected substances in AFFFs are PFOS, PFOA and perfluorohexane sulfonate (PFHxS). These three chemicals are thus commonly treated as primary indicators for PFAS-pollution (Bolan et al., 2021; HEPA, 2018). Nevertheless, a much wider range of both long-chain and short-chain PFASs are normally present at contaminated sites—potentially somewhat due to impurities, reaction by-products or degradation products in the original industrial blend (Glüge et al., 2020). Together with the chemicals' high stability and dissimilar behaviour, this large variability of PFASs in a contaminated area makes remediation extremely challenging (Bolan et al., 2021).

1.4 Retention and leaching of PFAS in soil

The environmental distribution and fate of PFASs is determined by their binding to soils and sediments; hence, understanding the chemicals' behaviours in different environmental matrices is important in a remediation context. Both the PFASs' physicochemical properties and site-specific characteristics affect how easily the chemicals are transported through the environment (Mahinroosta & Senevirathna, 2020). Hydrophobic (van der Waals) and electrostatic interactions are main binding mechanisms of PFASs in soil (Bolan et al., 2021; Oliver et al., 2019; Du et al., 2014). Still, the exact mechanisms between PFAS and various solids are often unknown. The term *sorption* is therefore often used collectively as it encompasses both absorption (bound within a material) and adsorption (surface-bound) (Tan, 2011, p. 76).

Perfluorocarbon chain length and functional group are among the most important PFAS properties that affect sorption. These properties relate to the amphiphilic nature of many PFASs—which have a perfluorocarbon chain providing hydrophobicity and a functional group providing hydrophilicity (fig. 3). Long-chain PFASs are more hydrophobic and tend to sorb stronger than short-chain PFASs (Sörengård et al., 2020; Hale et al., 2017). For PFASs of the same length, PFSAs (sulfonic acids) sorb more strongly than PFCAs (carboxylic acids) (Sørmo et al., 2021; Li et al., 2020; Zhao et al., 2012). While these properties influence the binding strength and dominant binding mechanisms of distinct PFASs, various environmental factors further affect sorption.

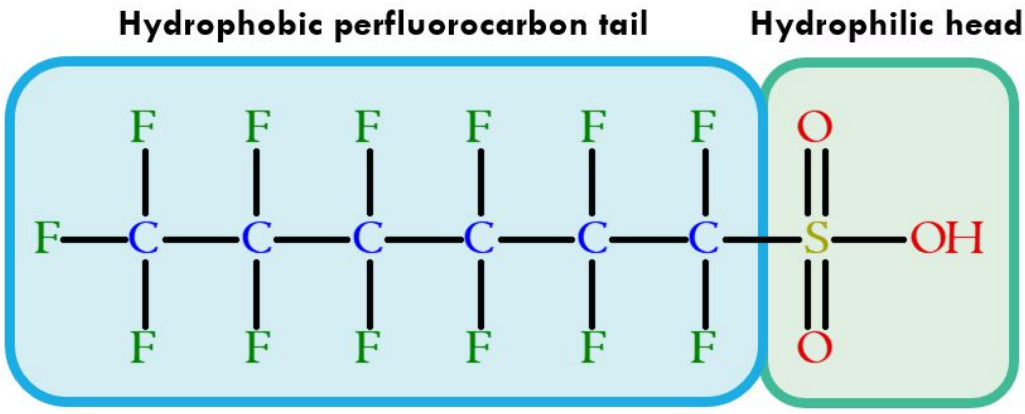

Figure 3. The chemical structure of PFHxS, which contains a six-carbon perfluorinated carbon chain (tail) and a sulfonic acid group (head). The substance is provided hydrophobic characteristics from its "tail" part and hydrophilic characteristics from its "head" part.

PFAS sorption is affected by site-specific properties such as organic carbon content, pH, clay content and ionic strength (Bolan et al., 2021). Among these, the soil's organic carbon content is often perceived as the dominant parameter controlling PFAS sorption to soils and sediments (Milinovic et al., 2015; Du et al., 2014; Higgins & Luthy, 2006). Still, while PFAS sorption usually increase with an increasing fraction of organic carbon, soil organic matter (SOM) is complex, and the effects separate SOM components may have on PFAS sorption is not fully understood (Mahinroosta & Senevirathna, 2020). However, the amphoteric charges in soil and other materials may further explain the pH and ionic strength dependence of PFAS sorption.

In general, soil pH is inversely correlated with PFAS sorption (Bolan et al., 2021; Mahinroosta & Senevirathna, 2020; Campos-Pereira et al., 2018). A decrease in pH leads to a dominance of protons (H^+) on solid surfaces, which anionic PFASs may attract and bind to, while an increase in pH causes surfaces to become more negatively charged, resulting in anionic substances being more electrostatically repelled (Du et al., 2014). The ionic strength can also affect the surface charges and lead to increased sorption through electrostatic interactions (Oliver et al., 2019). For instance, divalent cations such as Ca^{2+} and Mg^{2+} might form bridges between negative surface charges and anionic PFAS (Du et al., 2014; Higgins & Luthy, 2006). Inorganic anions, on the other hand, may compete with anionic PFASs for binding sites (Du et al., 2014). Altogether, a collection of factors affects PFAS sorption, and these should be considered when investigating new remediation strategies.

1.5 Potential of waste-based materials for remediation of PFAS contamination

Among the limited technologies for *in situ* (on-site) remediation of PFAS contaminated soil, the immobilization method is already widely used and have potential for being an efficient and economically viable treatment option (Mahinroosta & Senevirathna, 2020). This method first and foremost relies on the ability of soil amendments (sorbents) to efficiently bind a pollutant. The idea is that by adding suitable sorbents to a PFAS-contaminated area, the PFASs will be immobilized and prevented from leaching out to surrounding areas. Although introducing sorbents to contaminated sites does not destroy the present PFASs compounds, confining the contaminants within an already affected zone reduces their potential damage to surrounding communities (Darlington et al., 2018). A simplified and idealized scheme of the immobilization method for PFAS-contaminated soil is given in Figure 4.

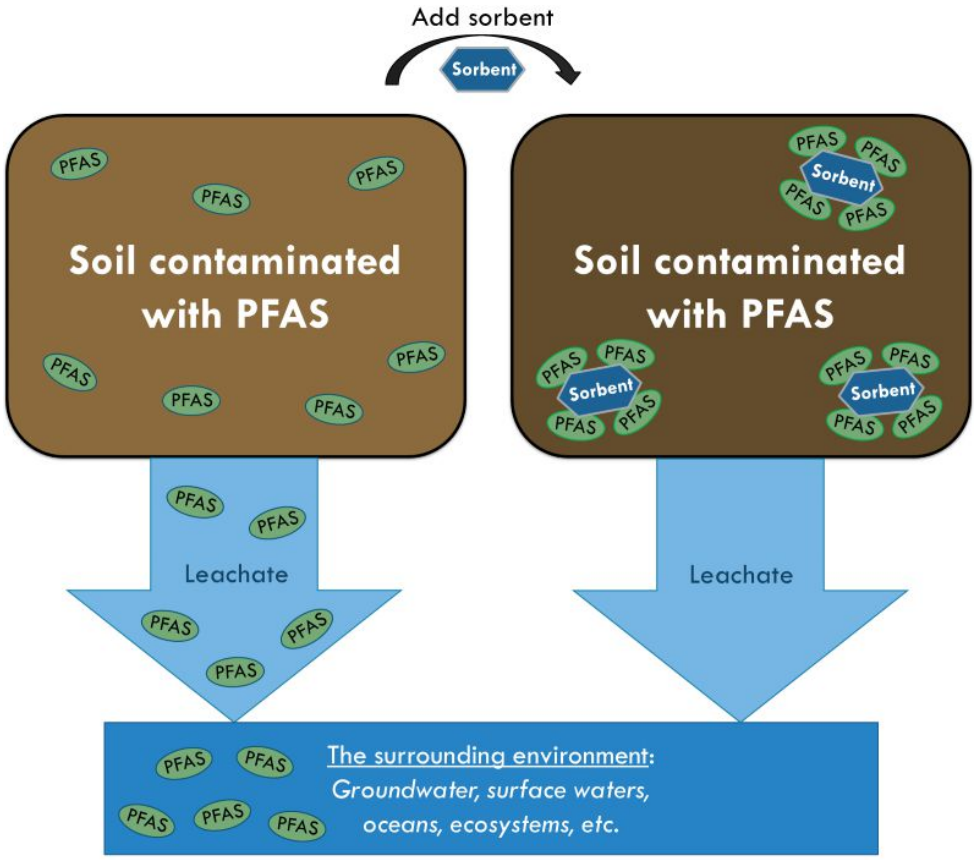

Figure 4. Schematic presentation of the immobilization (sorption and stabilization) method. The leaching of PFAS from contaminated soil is prevented by mixing a suitable sorbent into the soil, thus protecting the surrounding environment from PFAS contamination. In this idealized case, the sorbent particles bind all PFASs—independent of PFAS-type, soil characteristics and environmental conditions (Mahinroosta & Senevirathna, 2020).

While conventional sorbents, like activated carbon (AC), usually are fossil-based (Joseph et al., 2020), numerous waste-based materials have potential as efficient, sustainable sorbents. However, the literature on waste-based sorbents for PFAS remediation is very limited, and only a few waste materials have been tested for this purpose so far. Among these are woody residues (Sørmo et al., 2021), construction and demolition waste (Li & Zhang, 2014), and both organic and inorganic waste products (Sörengård et al., 2020). Especially biochars made from waste timber have been demonstrated to be effective sorbents for PFAS in soil, with performances comparable to commercial alternatives like AC (Sørmo et al., 2021; Silvani et al., 2019). Besides, using wood residues as a feedstock for sorbent production is considered a more climate-friendly alternative to fossil materials (Hagemann et al., 2020). Altogether, while data on waste-based sorbents is scarce, the use of such materials itself could bring forth both economic and environmental advantages.

Waste materials are generally cheaper and readily available in larger quantities than their commercial alternatives. Hence, waste-based sorbents that perform well in removing PFASs might overcome a large obstacle in the immobilization method: economic costs. If a large volume of sorbent is needed to reach a satisfactory PFAS removal, the capital costs can become significantly high, dependent on the sorbent material's price (Mahinroosta & Senevirathna, 2020). Sorbents based on waste materials—particularly from waste fractions that would otherwise end up in landfills—could thereby be an economical option for PFAS remediation and possibly also increase remediation efforts with it becoming more affordable. For instance, the use of biochar as a sorbent has already been proposed as low-cost option to AC (Zhi & Liu, 2018). Finding suitable waste-based sorbents could also valorise the waste materials in question and promote the transition to a more circular economy (Sørmo et al., 2021)—a system where all resources are re-used and recycled as much and long as possible, thus the creation of waste is minimized (Nilsen, 2021). Still, before any waste-based sorbents can be employed, they first need to provide an adequate PFAS-binding performance.

Whether a waste material is a suitable PFAS-sorbent depends on both the material's ability to immobilize PFASs and its possible content of substances that are harmful to health and the environment. A sorbent that contains large concentrations of hazardous substances, such as the heavy metals cadmium (Cd) and lead (Pb), cannot be used. A material's ability to function as a sorbent can be assessed by quantifying the material's sorption capacity in PFAS-contaminated soil. Examining a potential sorbent's ability to bind PFASs in "real-world" contaminated soils, which contain a cocktail of PFASs, is advantageous as it more closely represents what effect the sorbent could have in the field (Hale et al., 2017).

Sorption highly depends on both environmental factors and the PFASs' properties, and the former development of sorbents has mainly focused on long-chain PFASs as well (Li et al., 2020). Sorbents that work well on PFOS and PFOA might, however, not be appropriate sorbents for other PFASs. Thus, to validate a sorbent's immobilization effect, its sorption of numerous different PFASs should be examined. Since much is unknown about many waste-based sorbents' affinities for PFASs altogether, investigating the materials' binding effect on an array of PFASs could reveal some specific binding capabilities for certain PFAS types. Some previously untested waste materials might even be accustomed to sorb PFASs that conventional sorbents fail to bind.

1.5.1 Biochar from biological waste

Biochar is a soil amendment produced from biomass through pyrolysis. The material can be made from a large variety of biomass feedstocks, is highly porous and consists of carbon resistant to biodegradation (Hofstad, 2020), though the latter depends on the pyrolysis temperature which must be above 400–600 ºC for degradation-resistant structures to be formed (Zimmerman & Gao, 2013). Great PFAS sorption capacities have been shown for both commercial biochar (Zhi & Liu, 2018) and biochar made from waste products (Sørmo et al., 2021; Silvani et al., 2019). Thus, biochar could be valuable in a PFAS remediation context.

The biochars sorption ability can also further be enhanced through physical activation (Sørmo et al., 2021)—a process where oxidizing gases, like steam (H_2O) or carbon dioxide (CO_2), are used to create nanopores in the biochar surface at high temperatures above 800 ºC. While the materials' surface area and sorption capabilities are increased through activation (Hagemann et al., 2018), the process also comes at a trade-off with biochar yield. Hence, the degree of activation should be considered with regard to the specific remediation undertaking (Sørmo et al., 2021). Since activated biochars made from waste timber can be equally suitable PFAS sorbents as their commercial alternatives (Sørmo et al., 2021; Silvani et al., 2019), other biomass waste fractions might be suitable biochar feedstocks as well.

Each year, large amounts of biomass waste is generated. In Norway alone, 815 000 tonnes of wood waste, 187 000 tonnes of park- and gardening waste, and 639 000 tonnes of wet organic waste was generated in 2019. Respectively, the majority of these waste fractions were either incinerated, composted or sent to material recovery (Statistics Norway, 2021). Converting these wastes into biochar, or another high value resource, could be considered a sustainable way to produce sorbents.

1.5.2 Meat and seafood waste

Removing PFASs by using sorbents high in protein is a novel, yet promising, remediation method. PFASs are known to have a high binding affinity to human serum albumin (Li et al., 2021), and a higher protein content in soil is favourable for PFAS sorption onto soil (Li et al., 2019). A former study also found that proteins from *Cannabis Sativa* L. (hemp) could remove > 98 % of PFOS and PFHxS in contaminated groundwater (Turner et al., 2019). However, a drawback of biomaterials is that they degrade over time (Darlington et al., 2018), which may cause a desorption of their bound PFASs and odour challenges. Nevertheless, the ability of high-protein wastes to sorb PFAS might still be of use in future remediation endeavours.

Bonemeal, which is already used as a fertilizing soil amendment, is a potential sorbent candidate for PFAS remediation. The meat waste product is created by steam cooking animal bones in an autoclave and grinding them (Bjørnå, 2021). Bonemeal usually contains 45–55 % raw protein, and around 160 000 tonnes is produced in Norway each year (Harstad, 2021).

Chitosan is another organic waste with potential as a sorbent material. Crosslinked chitosan beads have been shown to efficiently sorb PFOS in water (Zhang et al., 2011), and chitosan alone also have PFAS-sorption capabilities (Sörengård et al., 2020). Chitosan is produced through deacetylation of chitin, which is an important component of crustacean shells, and shrimp shells are a good source of chitosan (Rasweefali et al., 2021). Each year, an estimated 450 000 tonnes of shrimp are fished from the North Atlantic Ocean (Johnsen, 2018). Shrimp shell waste accounts for approximately half of the total shrimp weight, thus utilizing this waste can reduce the negative environmental impacts of simply discarding it (Rasweefali et al., 2021).

1.5.3 Industrial and inorganic waste

Most industrial wastes like slag, dust, ashes, concrete and bricks end up in landfills (Statistics Norway, 2021), and finding good alternative uses for these masses could significantly reduce the amount of landfilling. While few studies have been conducted on these materials' ability to function as PFAS sorbents, they do have potential. For instance, a by-product from the metal processing industry (a low-cost industrial waste material) have earlier been shown to give a significant retention effect for PFOS in contaminated soil (Sævarsson et al., 2018). Both this material and many other industrial wastes contain high amounts of metal oxides. As a positive correlation between iron oxide and PFOS sorption has already been demonstrated (Wei et al., 2017), such sorbents could thereby be of interest in a remediation context.

2 Research aim and objectives

2.1 Purpose of study

The overall aim of this study is to find cost-efficient and environmentally benign sorbents for remediation of PFAS-contaminated soil. This aim is pursued by examining the ability of different waste-based materials to bind PFASs in contaminated soil. A related purpose is to find a possible application for waste streams that would otherwise end up in landfills, waste incineration plants or other suboptimal waste disposal forms.

In a broader sense, this work could contribute to our understanding and knowledge of treating contaminated soil with sorbents—supporting future work to prevent leakage of harmful PFAS compounds.

2.2 Research objectives and hypotheses

The PFAS sorption capacity will be tested for seven waste-based sorbents in total. The origins of these sorbents include organic waste (bonemeal and chitosan), industrial waste (slag, filter dust and ashes), construction waste (LECA) and waste timber (activated biochar). Several of these sorbents have never or scarcely been tested as PFAS sorbents. Accordingly, both the materials' sorption of different PFAS groups and their effect of various leaching conditions (including pH, electrical conductivity and dissolved organic carbon) will be investigated.

Based on the information and identified knowledge gaps in section 1 *Introduction*, the following research objectives have been defined:

(I) Investigate PFAS leaching from (unamended) contaminated soil, evaluated with respect to the soil's history and characteristics.

(II) Assess the ability of seven different waste-based materials to sorb PFAS, thus reduce PFAS leaching from contaminated soil.

(III) Compare the influences of specific chemical and physical factors on PFAS leaching.

(IV) Evaluate the waste-based materials suitability as sustainable sorbents for PFAS remediation of contaminated soil.

To achieve these objectives, a set of analyses will be performed at PFAS-contaminated soil from a former firefighting training site. An overview of the methodology and the focus area of this thesis is given in Figure 5.

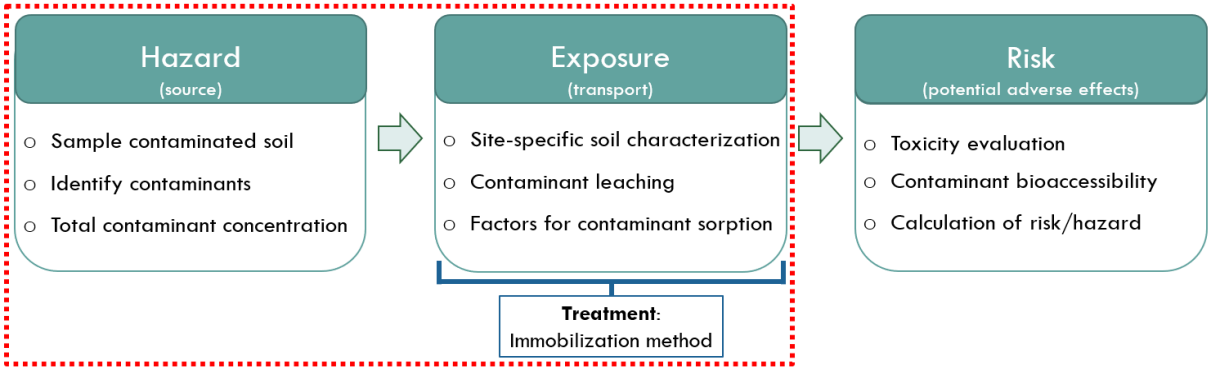

Figure 5. The connection between hazard, exposure and risk, adapted from Broomandi et al. (2020). The red box indicates the main focus of this thesis.

Along with the research objectives defined above, this thesis has the following hypotheses:

(i) Activated biochar will efficiently reduce PFAS leaching at low sorbent concentrations (< 1 % of soil dry weight) and cause reductions in dissolved organic carbon (DOC) and heavy metals

(ii) Relatively high sorbent concentrations of slag and filter dust (~ 10 % of soil dry weight) will be required to significantly reduce PFAS leaching

(iii) Bonemeal and chitosan will not reduce PFAS leaching as efficiently as biochar, but still significantly reduce leaching at 1–5 % (of soil dry weight) sorbent additions

(iv) Calcium content will help explain PFAS binding to sorbents

The hypotheses (i), (ii) and (iii) will be examined by performing batch tests on soil samples added different sorbent concentrations. Elemental analyses will also be performed on the leachates to investigate potential changes in dissolved elements, which connects to hypotheses (i) and (iv). Whether sorbent additions affect PFAS leaching will be assessed by determining the leachate PFAS concentrations. By measuring different PFAS types, information on which PFAS groups that are retained the most will also be achieved.

If successful, the main output of this work will be to provide knowledge that can bring *in situ* PFAS remediation technology one step closer to economically and environmental feasibility. Ultimately, the significant outcome would be to reduce the ecological impact of PFAS emitted from industry, AFFFs, waste infrastructure and consumer products.

3 Theory

3.1 Remediation of PFAS contamination

Due to the very limited reactivity of PFASs—caused by their strong C-F bonds—remediation strategies either strive to clean up or retain the pollutants at contaminated sites (Darlington et al., 2018). However, eliminating PFAS from soil masses is incredibly challenging. Several degradation and destruction technologies have been tested at a lab-scale, but their applicability is limited by the high energy required to break C-F bonds and the lacking field applications. Separation methods like soil washing, where PFASs are transferred from soil to liquid through washing, needs further development as well to reduce costs and energy demands (Mahinroosta & Senevirathna, 2020). While possible improvements for these methods are investigated, the immobilization method can be utilized to reduce PFAS leaching from already existing contamination hotspots. An overview of the PFAS sorption patterns and main challenges regarding the immobilization method will be given in this section.

3.1.1 Considerations for sorbent selection

Whereas the ideal sorbent for PFAS remediation has both a high sorption affinity and sorption capacity for PFASs, numerous factors affect the sorption process. Sorption affinity (which relates to the strength of the attractive forces between sorbate and sorbent) is highly influenced by the sorbent's surface chemistry, which again is subject to environmental factors like pH (Zhi & Liu, 2018). Sorption capacity, on the other hand, connects to a sorbents' potential for sorbing contaminants and increases with surface area. For instance, activated carbon has a very large sorption capacity due to its high surface area (Hale et al., 2017). The characteristics of the sorbent, the PFASs and the media in which the sorption happens should be considered when deciding on a treatment strategy.

The sorption behaviour of PFASs can be quantified by determining their partitioning coefficients, such as K_d or K_{oc} (described in section 4.4.2 *Partitioning coefficients for describing PFAS sorption*), and these coefficient values vary with the environmental factors, the chemicals' properties and choice of methodology (Bolan et al., 2021; Zareitalabad et al., 2013). In general, the higher the value of K_d is, the greater affinity the sorbate has for the surface. An overview of factors that influence PFAS partitioning (i.e., K_d) is given in Figure 6.

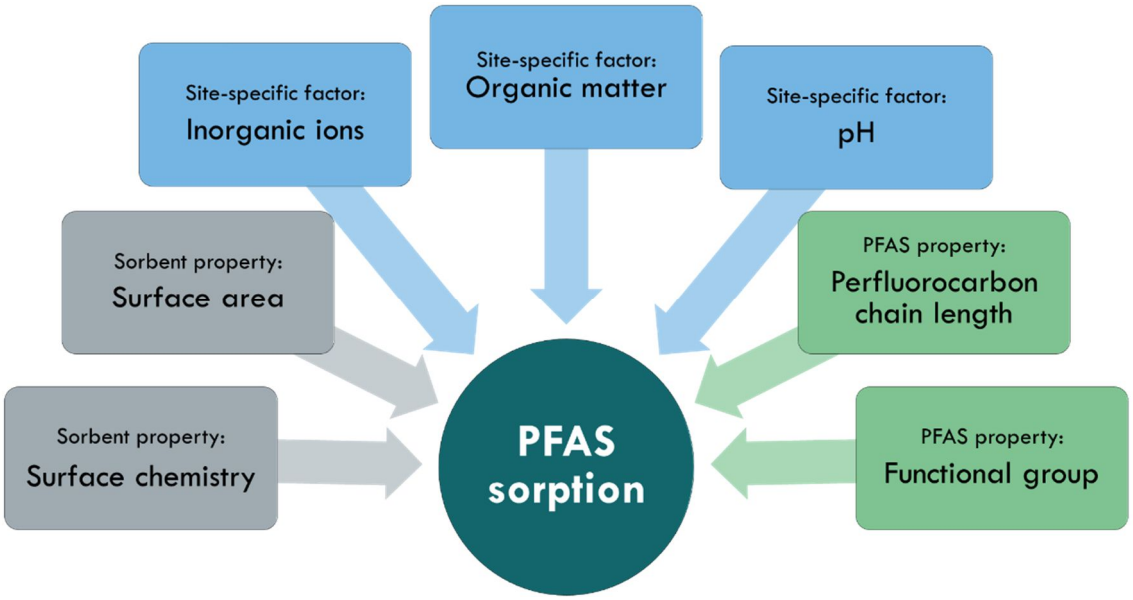

Figure 6. A summary of some factors that can affect the sorption efficiency of PFAS to solid phases (Bolan et al., 2021).

Organic matter content is among the most influential factors that affect PFAS sorption. In soils, anionic PFAS mainly bind to organic content through van der Waals hydrophobic interactions—a force that is often strong enough to overcome the electrostatic repulsion from negatively charged surfaces (Du et al., 2014). Furthermore, the total organic carbon (TOC) of a soil has been shown to influence PFAS leaching through significantly higher K_d values obtained for high-TOC soils compared to low-TOC soils (Sørmo et al., 2021; Silvani et al., 2019). During remediation efforts where sorbents are used, however, a higher TOC content can lessen the sorption effectivity of binding materials such as AC. These efficiency reductions are likely due to the organic material causing competitive PFAS sorption and clogging of porous sorbent materials (Sørmo et al., 2021). Moreover, dissolved organic carbon (DOC) can reduce K_d through both retaining PFAS in the solution and by competing for sorption sites (Du et al., 2014). Other site-specific factors like pH and the inorganic ion content are also important to consider in a remediation context.

As PFCAs and PFSAs generally have low pK_a-values, the substances are present as dissociated anions at environmentally relevant pH values (Vierke et al., 2013). Electrostatic interactions may thereby form between the anionic PFASs and positively charged functional groups on solid surfaces (Du et al., 2014), making pH an important factor as it controls the charges of amphoteric surfaces. Especially the sorption of long-chain PFAS seem to increase together with a lower pH, which has been demonstrated by how the partition coefficients (K_d and K_{oc}) decrease more per unit pH increase for long-chain PFASs than short-chain PFASs (Nguyen et

al., 2020; Campos-Pereira et al., 2018). PFAS sorption have also been reported to increase with increasing solution pH in the presence of divalent cations like Ca^{2+} and Mg^{2+}. For more basic sorbent surfaces, the cations could enhance sorption through cation bridging (Du et al., 2014). Various inorganic ions can also produce other phenomena in a PFAS sorption context.

In addition to cation bridging, the complex effects of inorganic ions on PFAS sorption can include salting out, competitive adsorption and compression of electrical double-layer. At high enough ionic strength, the water solubility of PFASs can be reduced so that sorption increases (Munoz et al., 2017; Du et al., 2014). Oppositely to this salting out effect, increased ionic strength may also compress the electrical double layer of sorbents—causing less PFAS to be sorbed instead (Wang & Shih, 2011). Moreover, inorganic anions like chloride (Cl^-) and sulphate (SO_4^{2-}) can compete with anionic PFASs for sorption sites and also cause reductions in PFAS sorption (Li et al., 2020; Du et al., 2014). Altogether, the influence of ions on PFAS sorption is intricate and depend on both concentration and ion types.

The PFAS types themselves also influence sorption, with perfluorocarbon chain length and functional group being among the most important factors. In sorption experiments, log K_d has been found to increase by 0.22 log units per CF_2 moiety in long-chain PFASs (Sörengård et al., 2020)—indicating that hydrophobic interactions played a major role in the sorption mechanism. In general, PFSAs have larger K_d values and are more easily sorbed compared to corresponding PFCAs (Sörengård et al., 2019; Du et al., 2014; Higgins & Luthy, 2006). This could be due to PFSAs being slightly more hydrophobic or having stronger electrostatic interactions than the PFCAs (Higgins & Luthy, 2006). On the whole, many factors are in play during PFAS immobilization efforts, and selecting remediation strategies based on individual contamination situations might provide the best results.

3.1.2 Advantages and weaknesses of different sorbents

As PFASs are neither removed nor destroyed in the stabilization technique, the permanence of the stabilization should be well understood (Ross et al., 2018). Knowledge is lacking on the long-term stability of different sorbents, but while biomaterials are more likely to biodegrade over time (Ahmed et al., 2020; Darlington et al., 2018), carbonaceous materials like coal and biochar are relatively resistant to degradation (Hofstad, 2020; Manum et al., 2020).

Apart from its stability, activated carbon (AC) is also quite cost-efficient and has a high PFAS sorption capacity compared to other commercial sorbents. However, safe disposal of these sorbents is necessary due to the challenge of regenerating the material (Du et al., 2014). In other words, removing sorbed PFASs from saturated sorbents to enable reuse of the materials is difficult (Gagliano et al., 2020). The sustainability issues related to AC being made from fossil sources is another disadvantage, though activated biochars can be suitable alternatives (Sørmo et al., 2021). Biochars can be made from an abundance of biomass feedstocks, including many waste fractions, and may be activated for enhanced sorption capabilities (Sørmo et al., 2021). However, as hydrophobic interaction is the dominating binding mechanism of carbonaceous sorbents, the materials are usually less efficient for binding short-chain PFASs—which depend more on electrostatic interaction than long-chain PFASs (Kah et al., 2021; Sørmo et al., 2021).

While short-chain PFASs with their relatively weak hydrophobicity are less efficiently removed by carbonaceous materials, sorbent materials based on ion-exchange mechanisms have showed more promise (Kah et al., 2021; Gagliano et al., 2020). Ion exchange resins consist of a hydrophobic backbone with positively charged co-polymers, which allows for multiple adsorption mechanisms. Ion exchange is likely the main binding mechanism of PFAS to ion resins, though its exact contribution is unclear (Kah et al., 2021). Resins are, however, costly compared to other options (Darlington et al., 2018), and the feasibility of restoring them through regeneration is uncertain (Gagliano et al., 2020).

Though ACs and ion exchange resins are the most studied sorbent types, other materials have PFAS sorption potential as well. Organoclays, silica and iron oxides are among the mineral materials that have been used to remove contaminants, and the materials' PFAS sorption ability could be enhanced through modifications (Darlington et al., 2018). The hydroxyl groups (-OH) of metal oxides are hypothesized to be exchangeable with PFASs—i.e., the contaminants may bind through ligand exchange (Du et al., 2014). Biomaterials and molecular imprinted polymers also have promise as sorbents for PFAS remediation (Darlington et al., 2018; Du et al., 2014). Altogether, as many sorption technologies are in their infancy, further validation is needed to determine their practical suitability as PFAS sorbents.

3.2 Batch leaching test

To determine the leaching potential of pollutants from a waste material or a soil, batch leaching tests are commonly used. This laboratory test typically involves preparing both a leaching solution and a contaminated sample before mixing them together until equilibrium conditions are reached (Townsend et al., 2003). A simplified scheme of a batch leaching procedure is given in Figure 7.

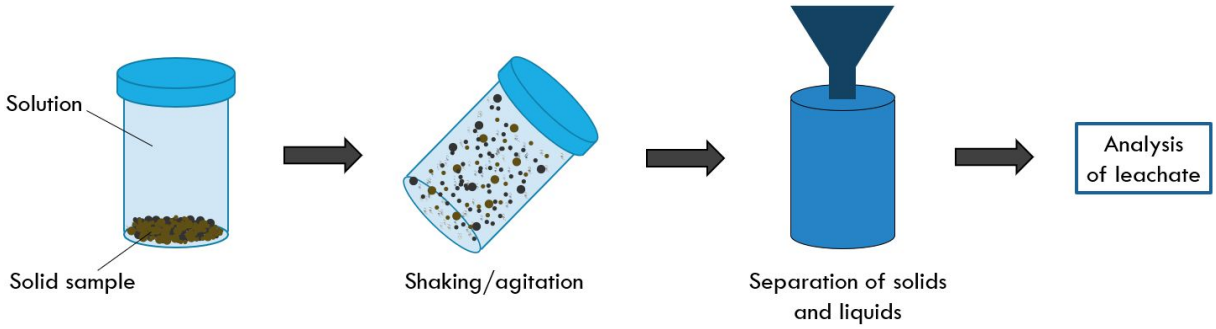

Figure 7. Simplified scheme of a batch leaching test, adapted from Król and Mizerna (2016). Among the previously used methods for separating the solid and aqueous fractions are filtration (Sørmo et al., 2021) and centrifugation (Sörengård et al., 2020).

The equilibrium times used in batch tests to study PFAS behaviour have varied widely between different studies. The time of agitation needed to reach equilibrium depend on the investigated PFASs types, and especially long-chain PFASs require more time achieve a sorption equilibrium (Kah et al., 2021). To avoid over- or underestimating K_d, a long enough experiment time is essential. In studies of PFAS-contaminated soil, 14 days have been suggested as an appropriate agitation time (Sørmo et al., 2021; Kupryianchyk et al., 2015).

During the agitation of the samples (which can be carried out with a shaking table), the soil is heavily flushed with water. Hence, the batch test can be considered an exhaustive procedure that represents a "worst-case scenario" for the soil in question (Sørmo et al., 2021). The batch leaching test may further reflect the theoretical maximum of PFAS leaching—on account of the large amount of water used relative to expected field conditions. Batch tests can therefore provide information on PFAS equilibrium concentrations (Hale et al., 2017), which may enable various soil amendments (sorbents) to be compared.

3.3 Considerations for working with PFAS

When handling PFAS-contaminated matrices, considerations should be taken to avoid contamination of the samples, heterogeneity and loss of analyte. The choice of equipment materials is principal in this matter, and materials that may contain or adsorb fluorinated compounds must be avoided during both sampling and handling. Recommended material types for equipment that is to be in direct contact with a PFAS-contaminated sample includes stainless steel, polypropylene (PP) and glass. These materials should still be cleaned prior to use to minimize the contamination risk. Polar solvents like methanol are recommended as washing solutions since they can extract potential fluorinated contaminants (Ahrens, 2010).

In addition to the choice of materials and equipment cleansing, incorrect handling of the samples can also cause error. For soil and sediment samples, homogenization is important to avoid heterogenous subsamples during experiments. The samples should also be dried (for instance, by air-, oven- or freeze-drying) and stored in closed containers between analyses. To reduce possible precursor transformation, the temperature of storing should be low and handling time at higher temperatures should be minimized (Ahrens, 2010).

4 Materials and methods

Sampled PFAS-contaminated soil was characterized though a series of soil analyses. Afterwards, soil samples were used in batch experiments with and without different waste-based sorbents to test how the materials affected PFAS-leaching. The analyses were performed at the Faculty of Environmental Sciences and Natural Resource Management (MINA) at the Norwegian University of Life Sciences (NMBU), unless otherwise stated. An overview of the methods is given in Figure 8.

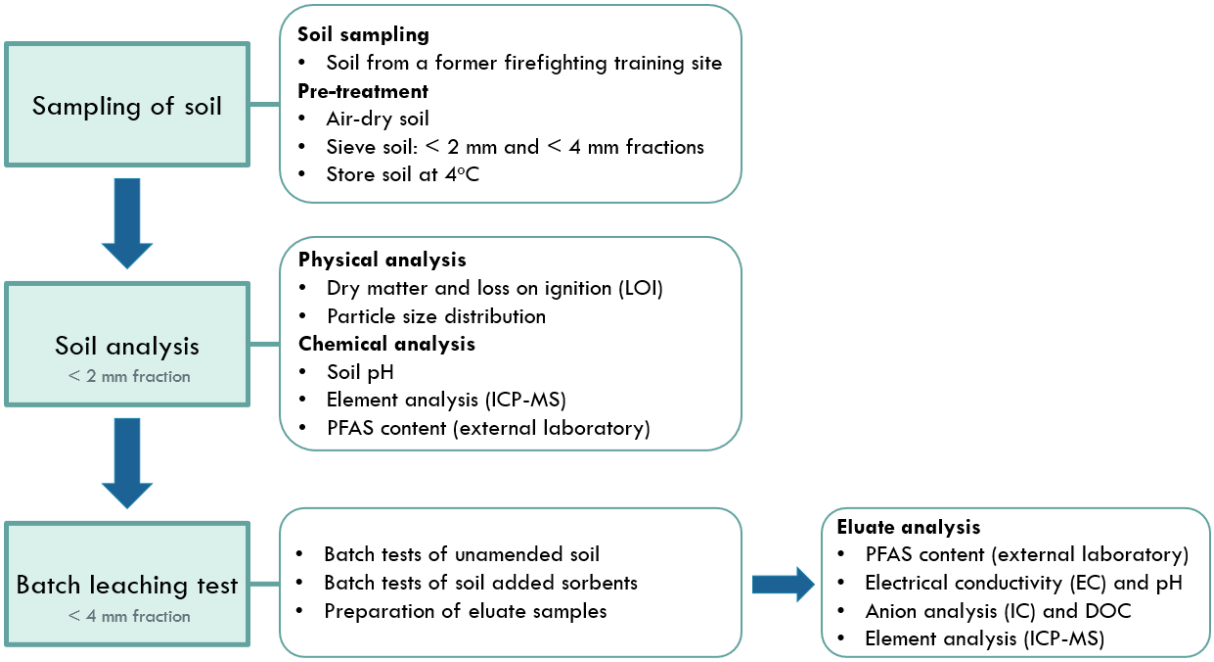

Figure 8. Flowchart that gives a summary of this thesis' materials and methods.

4.1 Sampling, storage and pre-treatment of soil

PFAS-contaminated soil was sampled, dried, stored and sieved into < 2 mm and < 4 mm fractions to be used in soil analyses and batch leaching tests, respectively. To avoid potential contamination during the handling of the PFAS-contaminated soil, the materials of the equipment used had to neither contain nor adsorb fluorinated compounds. Therefore, only prewashed equipment made of recommended materials such as polypropylene (PP) and stainless steel (Ahrens, 2010) were put in direct contact with the soil samples.

4.1.1 Sampling of soil

Soil (~ 30 cm depth) was sampled in October 2020 at a fire training facility associated with an airport in Eastern Norway. The area from which the soil was collected mainly consisted of glaciofluvial deposits. To avoid the grounds most affected by soil movements and washing, the excavation was carried out between two fire training platforms. The soil itself was homogenized by an excavator and transferred to polypropylene (PP) buckets. The containers were thereafter placed in a fume cupboard to airdry at room temperature for approximately 90 days. This was in order to let the soil's dryness reach equilibrium with the moisture content of the surrounding atmosphere, which is the definition of air-dry soil (Weil & Brady, 2017).

The sampling site was known to be highly contaminated with PFAS due to historical use of PFAS-containing AFFFs. While the usage of PFOS was phased out in 2001, the use of all PFAS-containing firefighting foams was first banned at the site in 2011. A mapping of the area in 2016 uncovered still high PFAS-concentrations in the ground, and a later published study found PFOS to account for 96 % of the measured PFASs (n=12). In the study, the soil was also characterized as sandy soil with an organic carbon content < 1 %, and the K_d values for PFOS were estimated to be 4.0–5.1 L/kg and 1.9–2.5 L/kg in soils with high and low AFFF impact, respectively (Høisæter et al., 2019). These sorption coefficients and soil characteristics might reflect values to be expected for the soil samples in this work.

In addition to the soil sampled in this study (Soil A), another previously sampled soil (Soil B) was initially analysed as well. This other soil had previously been collected at the outskirts of a different fire training facility in Eastern Norway and was believed to have been a former fill material. While both Soil A and Soil B were characterized through soil analyses and batch leaching tests of unamended soil, only Soil A was (for practical reasons) followed in the further analysis of the results. The reasoning for this is given in the results.

4.1.2 Sieving of the soil

The airdry soil samples were sieved through a 4-mm RETCH sieve (DIN 4188, stainless stell) to remove bigger stones and pieces of plant material. In addition, a fraction of the airdried soil was also sieved though a 2-mm Endecotts laboratory test sieve (ISO 3310-1, stainless steel) in preparation for the soil analyses. After the sieving and preceding the analyses, the soil was kept in a cold storage room at approximately 4 ºC. All the sieved soil was stored in PP-buckets that were placed back in the cold storage room between analyses.

4.2 Soil analyses

The soil was characterized by analysing its dry matter content, loss on ignition (LOI), particle size distribution, pH and metal content. Measurements of the soil's PFAS concentrations, total organic carbon (TOC), total inorganic carbon (TIC) and total carbon (TC) were also carried out. The soil was manually homogenized before each measurement, and all soil analyses were performed in triplicates. Information on the procedures, materials and equipment used for the soil analyses is given in this section.

4.2.1 Dry matter and loss on ignition

The soil's dry matter content was an important parameter to determine so that later analytical results could be based on the samples' amount of dry soil. Loss on ignition (LOI), which can provide a crude estimate of the soil's organic content, was also estimated based on the dry matter content.

To determine the soil's dry matter, (< 2 mm) soil was transferred to pre-weighed crucibles and dried in a drying cabinet at 105 ± 5 ºC for more than 6 hours. To thereafter determine LOI, the crucibles with the dried soil was calcinated for more than 3 hours at 550 ± 25 ºC in a calcinating oven (Eurotherm ESF 3 Carbolite Sheffield). The calcinated samples were cooled for a few minutes before they were weighed a final time. These analyses on dry matter and loss on ignition were in accordance with Krogstad et al. (2018), and the formulas for both parameters are given in Appendix A.

4.2.2 Particle size distribution

The particle size distribution refers to the soil's relative amounts of various soil texture classes (clay, silt and sand) and is usually expressed as weight percentages (Weil & Brady, 2017). Based on its particle size distribution, a soil can be named and classified into a texture class as described by Greve et al. (1999). These texture classes apply to soils with grain sizes less than 2 mm.

To determine the particle size distribution, a modified version of the method described by Rygalska (2019) was used. Approximately 10 grams of (< 2 mm) homogenized soil were weighed into a 1-litre glass beaker. To start decomposing the soil's organic material, the beaker was added 10 mL 33 % H_2O_2 and 20 mL deionized water. The beaker was thereafter covered

with a glass lid and left alone for 30 minutes. Another 10 mL 33 % H_2O_2 was then added before the beaker was heated to approximately 90 ºC on a heating plate. When the H_2O_2 had evaporated and visible reactions in the solution were not observed anymore, the sample was added 10 mL 2M HCl to prevent aggregates from forming. The beaker was thereafter filled with deionized water to its 1-litre mark and added a few drops of magnesium chloride ($MgCl_2$) to increase the sedimentation speed, making the dissolved particles settle faster. The following day, the clear water was removed with a suction hose, and the beaker was filled with deionized water and added some $MgCl_2$ once more. After again removing the water the third day, the sample was added 50 mL 0.05 M sodium pyrophosphate decahydrate ($Na_4P_2O_7 \cdot 10H_2O$) to prevent floc formations from charged particles. Potentially present clumps were dissolved by sonicating the samples in a Sonics UltraCell. Afterwards, the particles were mixed in the solution using a magnetic stirrer so that representative samples could be taken out and finally analysed for particle size with a LS 13 320 Particle Size Analyzer (Beckman Coulter).

4.2.3 Soil pH

10 mL soil was suspended in 25 mL deionized water, mixed and left to sedimentate before pH was measured using a PHM210 Standard pH meter (Radiometer, MeterLab®) with a glass electrode (Thermo Scientific™ Orion™ 8172BNWP ROSS™ Sure-Flow™). The pH meter was calibrated with buffer solutions of pH 4 and pH 7 (6.88). These soil pH measurements were performed in accordance with (Krogstad et al., 2018).

4.2.4 Element analysis of soil samples

An elemental analysis was performed to measure the soil's content of both heavy metals and other elements that might impact PFAS leaching. Approximately 3.5 g soil was grinded in a mortar grinder (Retsch RM 200) for about five minutes. Two sets of triplicates, where each sample consisted of ~ 0.25 grams of ground soil, were digested by microwave technique in a Milestone UltraCLAVE. One sample triplicate was digested with 5 mL nitric acid (HNO_3) and the other with both 5 mL HNO_3 and 1 mL hydrofluoric acid (HF). These acid mixes were used for separate sample digestions because the element recovery was expected to vary for different digestion mixes. The digestion procedure lasted 90 minutes and had a maximum temperature of 260 ºC. The digested samples were thereafter diluted to 50 mL with deionized water (18 megohm-cm) and analysed for 16 different elements using inductively coupled plasma

mass spectrometry (ICP-MS) with an Agilent 8800 Triple Quadrupole ICP-MS. Certified reference materials were digested and analysed as well to control the accuracy of the method. For the HNO_3-digestion, the materials *2709a* (NIST, 2009a) and *2710a* (NIST, 2009b) were utilized. Digestion with HNO_3 and HF was carried out with the reference material *NCS DC 73325* (China National Analysis Center for Iron and Steel, 2004).

The elements measured in the grinded soil were aluminium (Al), arsenic (As), calcium (Ca), cadmium (Cd), chromium (Cr), copper (Cu), iron (Fe), potassium (K), magnesium (Mg), manganese (Mn), sodium (Na), nickel (Ni), lead (Pb), antimony (Sb), selenium (Se) and zinc (Zn). The Norwegian Climate and Pollution Agency (2004) have defined normative values for some heavy metals in soil (Appendix B), and the soil's pollution status for these elements could thereby be evaluated as well.

The choice of using both HNO_3 and HF for digestion of the samples were due to the differential behaviour of the elements in question. Since soil samples usually contain both organic and inorganic materials, digestion has been recommended to include a mix of the oxidative acid HNO_3 and HF to get a full decomposition (Bye, 2019). Especially silicate matrices are efficiently decomposed in the presence of HF. Simultaneously, some alkaline earth metals have very low solubility in HF (Müller et al., 2014) and might be better recovered when digested with HNO_3 alone.

4.2.5 PFAS content and other soil analyses

The soil's content of different PFASs, dry matter, total organic carbon (TOC), total inorganic carbon (TIC) and total carbon (TC) was analysed in triplicates at an accredited laboratory (Eurofins). The PFAS analysis of the soil, which included Σ30 PFAS variants, was executed in accordance with method DIN 38414-14 mod. based on acetonitrile extraction and analysis by liquid chromatography coupled with mass spectrometry (LC-MS/MS). The PFASs analysed for were 4:2 FTS, 6:2 FTS, 8:2 FTS, HPFHpA, PF-3,7-DMOA, PFDeA, PFBA, PFBS, PFDoA, PFTrA, PFDS, PFHpA, PFHpS, PFHxA, PFHxDA, PFHxS, PFNA, PFOA, PFOS, PFOSA, PFPeA, PFTA, PFUnA, EtFOSA, EtFOSAA, EtFOSE, MeFOSAA, MeFOSE, MeFOSA and FOSAA. Soil dry matter was analysed using method SS-EN 12880:2000, and the soil's TOC, TIC and TC values were determined using method SS-EN 15936:2012 metodappl. A/SS-EN 13137:2001 m.

4.3 Batch tests and eluate treatment

Batch leaching tests were performed on PFAS-contaminated (< 4 mm) soil samples with and without sorbent additions to investigate the sorbents' effect on PFAS mobility and leaching. The PFAS leaching from control samples of both Soil A and Soil B was investigated, but Soil B was not analysed any further. Consequently, the sorbents' ability to reduce PFAS leaching was only assessed for Soil A, meaning that a larger number of sorbents could be investigated (table 2). The triplicate batch leachates for each sorbent mix were analysed for Σ33 PFASs, in addition to other chemical parameters like electrical conductivity (EC), pH, dissolved organic carbon (DOC), inorganic anions and trace elements.

4.3.1 Batch test

The PFAS leaching was determined by carrying out one-step batch shaking tests with liquid-to-solid ratios (L/S) of 10 L/kg, in accordance with standard EN 12457-2 (2003) with some modifications. After mixing 40 g soil (dry weight) with certain sorbent amounts and 400 mL deionized water (18 megohm-cm) in methanol-washed PP-bottles, the samples were shaken at room temperature for 14 ± 0.5 days on a tabletop shaker (Universal shaker SM 30, Edmund Bühler) (100 rpm). A 14-day duration of the agitation step was chosen to ensure that equilibrium conditions were reached. Following the shaking procedure, the suspended solids were allowed to settle overnight.

The batch tests were performed on triplicates of blank samples (deionized water), control samples (unamended soil) and soil mixed with sorbents at three different concentrations. An overview of the sorbents and the concentrations added to the soil samples is given in Table 2.

Table 2. A summary of the seven sorbents used as soil amendments to reduce PFAS leaching from soil. The choice of sorbent concentrations was based on assumptions about the required sorbent amounts for reducing PFAS leaching in the batch samples.

Sorbent name	**Concentration (% soil dw)**		
	Lowest	Middle	Highest
Activated biochar	0.1 %	0.5 %	1.0 %
Ash	1 %	2 %	5 %
Bonemeal	1 %	2 %	5 %
Chitosan	1 %	2 %	5 %
Filter dust	2 %	5 %	10 %
LECA	1 %	2 %	5 %
Slag	2 %	5 %	10 %

The biochar had been activated at 900 ºC using steam (H_2O) as the activation agent. Since a 1.00 molar ratio of activation agent to feedstock carbon had been utilized, the sorbent was said to be 100 % activated. The activated biochar in question had also previously been shown to efficiently bind PFASs at low doses in low-TOC soils (Sørmo et al., 2021).

The industrial waste materials, slag and filter dust, were both high in metal oxides. To keep these strongly alkaline sorbents from increasing the pH levels in the batch leachates, iron sulphate monohydrate ($FeSO_4 \cdot H_2O$) was used to adjust pH. Initial testing indicated that mixing $FeSO_4 \cdot H_2O$ with slag and filter dust in ratios of 1:5 and 3:5, respectively, gave the smallest changes in pH values relative to the batch control samples (Appendix C).

According to the providing company (Norsk Protein, n.d.), the bonemeal had a high organic content (65–75 %) and contained 8.7 ± 0.7 % nitrogen and 9.5 ± 1.5 % calcium. Based on the Kjeldahl method which usually employs a conversion factor of 6.25 (Hayes, 2020), the nitrogen content translates to a protein content of approximately (8.7 ± 0.7 %) * 6.25 = 54 ± 4.4 %. The chitosan was assumed to have a low protein content due to the deproteination step involved with synthesizing it from chitin (Davis, 2011, pp. 19-20).

4.3.2 PFAS analysis of batch leachates

The eluate volume required for each PFAS analysis (200 mL) was transferred to four (methanol-washed) 50-mL PP-centrifuge tubes which were centrifuged for 10 minutes at 3000 rpm, using a VWR Mega Star 1.6 Benchtop Centrifuge. The supernatants were thereafter carefully poured into designated PFAS bottles (provided by Eurofins), which were packaged and sent by a postal service the same day. The eluate samples were analysed for Σ33 PFASs according to method DIN38407-42 mod. by an accredited laboratory (Eurofins).

4.3.3 Electrical conductivity and pH

The electrical conductivity (EC) of each leachate was measured with a 712 Conductometer (Metrohm). Subsequent to the EC determinations, the pH was measured using a PHM210 Standard pH meter (Radiometer, MeterLab®) with a glass electrode (Thermo Scientific™ Orion™ 8172BNWP ROSS™ Sure-Flow™), in accordance with Krogstad et al. (2018).

4.3.4 Dissolved organic carbon (DOC) and inorganic anion content

For the DOC and anion analyses, 25 ± 5 mL eluate was filtered through 0.45 µm syringe filters (Whatman® 0.45 µm PES, Cytiva™) and stored at 4 °C until analysis. The DOC analyses were performed on a Total Organic Carbon Analyzer (TOC-V CPN, Shimadzu). In addition to the leachate samples, a certified reference material (*SANGAMON-03*) was analysed for quality control of the analysis.

The leachates' contents of sulphate (SO_4^{2-}), nitrate (NO_3^-) and chloride (Cl^-) was measured with an IC5000 Ion Chromatograph (Lachat, Zellweger analytics). The accuracy of this anion analysis was controlled by measuring both a certified reference material (*ION-96.4*) and an in-house standard.

4.3.5 Element analysis of batch leachates

In preparation of the element analysis, 9 mL of each leachate was filtered through 0.45 µm syringe filters (Whatman® 0.45 µm PES, Cytiva™) and conserved with 10 % u.p. HNO_3. The filtered samples were stored at 4 °C until analysis, which was performed with an Agilent 8800 ICP-MS in He-KED and Oxygen mode. The samples were analysed for the same elements as the soil samples (Al, As, Ca, Cd, Cr, Cu, Fe, K, Mg, Mn, Na, Ni, Pb, Sb, Se and Zn). In addition, all leachates were measured for phosphorous (P) to get an indication of their phosphate content. The limit of detection (LOD) and limit of quantification (LOQ) for each element were determined as described in Appendix D.

4.3.6 Quality control and assurance

All batch tests were performed in triplicate. To reduce the risk of sample contamination, the equipment used prior to the leachate's PFAS analyses was always washed with methanol (≥ 99.8 %, HiPerSolv CHROMANORM®, VWR Chemicals) and dried in a drying cabinet. This methanol-washed equipment included measuring tools and containers for the mixing soil, water and sorbents in the batch experiments.

It was also taken care to only use recommended materials—such as glass, PP and stainless steel—when handling the PFAS samples. The control samples, which consisted of unamended soil, were used as a reference to assess the different sorbents impact on both PFAS leaching

and various physiochemical properties. For each sample set, a blank sample consisting of 400 mL deionized water (18 megohm-cm) was also prepared and put through the same batch test procedure as the soil samples.

4.4 Data analysis

4.4.1 Calculation of PFAS leaching

After performing the batch tests, the leaching of the PFASs ($c_{leachable}$, [µg kg^{-1} of dry matter]) was quantified by using the equation

$$c_{leachable} = c_w * \left(\frac{V_w}{M_D} + \frac{MC}{100}\right) \quad (1)$$

where c_w [µg L^{-1}] is the leachate's PFAS concentration, V_w [L] is the volume of liquid used, MC [%] is moisture content and M_D [kg] is the dry mass of the test portion (EN 12457-2, 2003).

The soil's moisture content, MC, is the ratio between the mass of water contained in the soil and the soil's corresponding dry mass. MC was thereby calculated on basis of the soil's dry matter determination (see section 4.2.1 *Dry matter and loss on ignition*) as

$$MC = \frac{(M_W - M_D)}{M_D} * 100 \quad (2)$$

where M_W [kg] is the undried test potion's mass and M_D [kg] is the dried test portion's mass.

The leachable fraction of PFAS ($F_{leachable}$, [%]) was determined by dividing the leached fraction, $c_{leachable}$ [µg kg^{-1}] (calculated from eq. 1), with the initial soil concentration, $c_{soil,i}$ [µg kg^{-1}]. As the batch test is a highly rigorous procedure, the $F_{leachable}$ can represent the total leachable amount of PFAS in the soil (Sørmo et al., 2021).

$$F_{leachable} = \frac{c_{leachable}}{c_{soil,i}} \quad (3)$$

4.4.2 Partitioning coefficients for describing PFAS sorption

The sorption behaviour of the PFASs was quantified by determining their partitioning between the solid and water phase. The solid-water partitioning coefficient (K_d, [L/kg]) is a measure of a contaminant's relative distribution between the solid phase (c_s [µg kg^{-1}]) and the aqueous phase (c_w [µg L^{-1}]) at equilibrium. The partitioning coefficient, K_d, was calculated as

$$K_d = \frac{c_s}{c_w} \tag{4}$$

To determine the solid phase concentration (c_s) at equilibrium, the leachable concentration was subtracted from the initial soil concentration. To also include the soil's moisture content in the estimation, the solid phase was estimated as

$$c_s = c_{soil,i} - c_{leachable} \tag{5}$$

where $c_{soil,i}$ [µg kg^{-1} dry weight] is the initial soil concentration and $c_{leachable}$ [µg kg^{-1} dry weight] is the quantity of a constituent leached from the soil (Sørmo et al., 2021; Sörengård et al., 2020). The latter, $c_{leachable}$, was calculated from eq. (1).

The carbon content-normalized partitioning coefficients (K_{oc}, [L/kg]) were calculated as

$$K_{oc} = \frac{K_d}{f_{oc}} \tag{6}$$

where K_d is the solid-water partitioning coefficient (defined in eq. 4) and f_{oc} is the dimensionless fraction of organic carbon in the solid phase.

4.4.3 Statistical data treatment

Averages and standard deviations were calculated from three replicate values (triplicates) as defined in Appendix E. Blank values were subtracted from measured eluate concentrations, and half of the analytical limit of quantification (LOQ) were used in cases where the measured values were < LOQ. For certain soil parameters, a coverage factor of k=2 was used to increase the confidence of the measured value.

One-way analysis of variance (ANOVA) was used to compare the PFAS concentrations between different sorbents and between different sorbent concentrations. The assumption that the PFAS concentrations were normally distributed in each group was also investigated. Stepwise regression was thereafter performed on a subset of the sorption data where PFOS gradually changed with increasing sorbent dose. Minimum BIC (Bayes Information Criterion) was used as the stopping rule, and the analysis was performed in the backwards direction for the set of selected explanatory variables. The variables selected through this procedure were used to make a fitted model explaining PFOS leaching. The correlations between the individual variables and the leached PFOS were also investigated. These statistical analyses were all conducted using JPM® version 16.1 (SAS Institute, 2021).

5 Results

5.1 Soil analyses and characterization

The resulting characterization for the soil sampled in this study (Soil A) is given in this section, and supporting information can be found in Appendix F–H.

5.1.1 Soil chemistry

A summary of the soil's measured properties is given in Table 3. Through particle size distribution analysis, the soil was found to contain 4.6 ± 1.7 % clay, 23 ± 9.0 % silt and 70 ± 11 % sand. Based on these values, the soil could be classified as *silty sand* according to the texture classes described by Greve et al. (1999). A graph displaying the cumulative particle size is given in Appendix F.

Table 3. An overview of the sampled soil's pH, loss on ignition (LOI), total carbon (TC), total organic carbon (TOC) and total inorganic carbon (TIC) values. The soil's LOI was calculated by using eq. (A2) in Appendix A. Each value represents an average of triplicate measurements with uncertainties stated as standard deviations with coverage factor k=2.

	pH	**Loss on ignition**	**TC***	**TOC***	**TIC**
Soil value	6.17 ± 0.034	2.3 ± 0.11 %	0.50 ± 0.050 %	0.40 ± 0.060 %	< 0.1 %

* When standard deviations were equal to zero, the stated measurement uncertainties of the analysis (10 % for TC and 15 % for TOC) were used instead (Appendix H). These uncertainties also had a coverage factor k=2.

Both LOI and TOC give indications of the soil's organic matter content. As seen in Table 3, the average LOI value (2.3 ± 0.11 %) was more than five times higher than the average TOC value (0.40 ± 0.060 %).

5.1.2 Element analysis of soil

Soil samples were both digested with HNO_3 alone and with a mix of HNO_3 and HF. For most of the measured metals, a linear relationship was observed between the two digestion methods (fig. 9). Only the elements Mg and Al were measured at substantially higher concentrations after HNO_3-digestion compared to when digested with a mix of HNO_3 and HF. On the other hand, Na and Sb were clearly measured at their highest concentrations following HF-digestion. The full results from the soil element analysis are given in Appendix G.

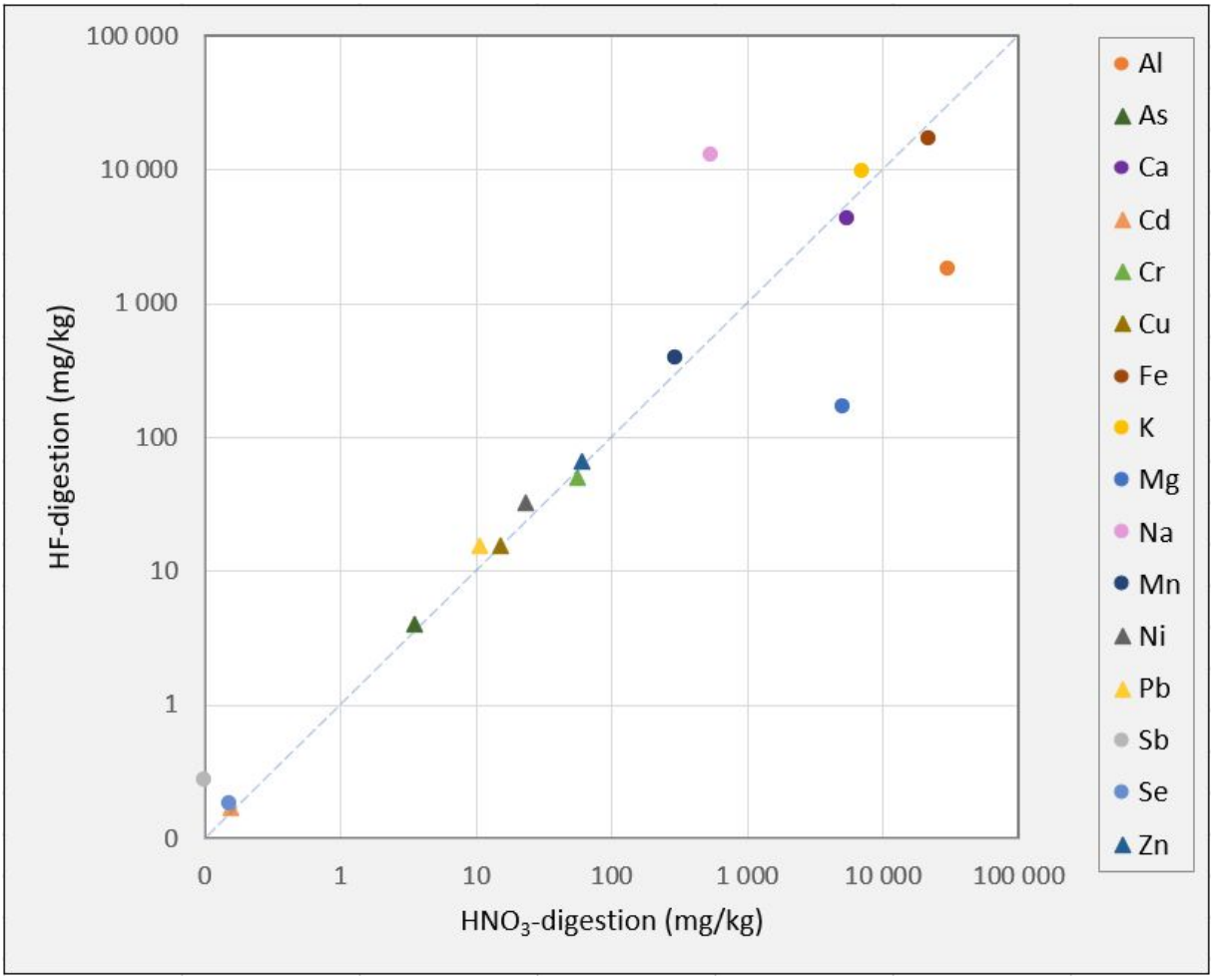

Figure 9. Measured element concentrations (n=16) from triplicate soil samples digested with both HNO_3 and HNO_3+HF. The heavy metals that possess soil normative values defined in the Norwegian Pollution Control Act (Norwegian Climate and Pollution Agency, 2004) have triangle-shaped markers.

5.1.3 PFAS concentration in soil

The PFAS analysis of the soil samples (n=3) resulted in the quantification of 20 PFASs (Appendix H). The measured concentrations ranged from 0.28 ± 0.010 to 1600 ± 170 µg/kg (dw soil) for PFBS and PFOS, respectively. PFOS accounted for approximately 94 % of the quantified PFASs, and perfluorooctane sulfonamide (PFOSA) accounted for 3 %. The remaining PFASs each represented < 0.61 % of the total PFAS concentration.

The measured PFOS concentration in the soil greatly exceeds the normative value of 100 µg/kg soil defined by the Norwegian Climate and Pollution Agency (2004).

5.2 Batch tests

Batch leaching tests were performed on control samples (unamended soil) and soil added different doses of various waste-based sorbents. Additional information about the analysis results can be found in Appendix I–S.

As described in section 4.1.1 *Sampling of soil*, two soils from different firefighting training sites were initially analysed through batch leaching tests (Appendix I). The PFAS distributions in the leachates of these two soils are shown in Figure 10. Only the soil sampled in this study (Soil A) was investigated further.

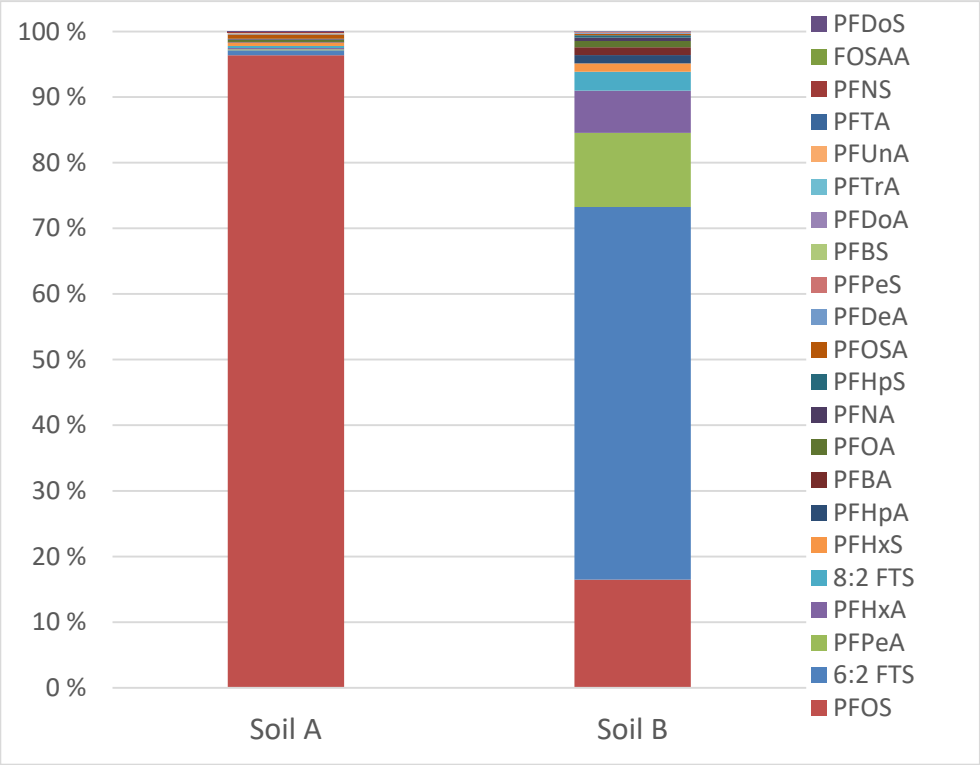

Figure 10. The distribution of different PFASs in leachates of the soil sampled in this work (Soil A) and a previously sampled soil (Soil B). The two soils were from separate firefighting training sites, and their PFAS distributions are given in percentages of their respective total PFAS concentrations.

As seen in Figure 10, the distribution of the measured PFASs varied between the soils. While PFOS represented > 95 % of the measured PFASs in Soil A, the largest component of Soil B was 6:2 FTS (which corresponded to 57 % of the measured PFASs). Soil B was not investigated further as its high complexity would complicate the comparison of the sorbents' effect on leaching with Soil A. In addition, information was lacking on the sampling of Soil B (including sampling date and depth), while Soil A had been sampled in relation to this study. In the continuing result section, all measurements will refer to Soil A.

5.2.1 PFAS leaching in unamended soil

Overall, 19 of the 31 screened PFASs were quantified in all triplicates of the batch control samples (Soil A). In descending order of concentration, the quantified PFASs were PFOS, 6:2 FTS, PFOSA, PFHxS, PFOA, 8:2 FTS, PFHxA, PFPeA PFNS, PFDaE, PFNA, PFHpS, PFUnA, FOSAA, PFHpA, PFBA, PFPeS and PFDoS. See Appendix J for more information on the individual compounds.

The leaching from the soil was dominated by PFOS, which accounted for 96 % of the total PFAS measured. This substance is therefore focused on in the following results and discussion sections, although the sorbents' impact on other PFASs will also be discussed. The estimated K_d and K_{oc} values for the PFASs that were quantified in both the soil sample and the batch control leachates are given in Table 4.

Table 4. The estimated concentrations of 16 PFASs in soil (c_s) and control leachate (c_w), including their solid-water partitioning coefficients (K_d) and their carbon content-normalized partitioning coefficients (K_{oc}). To estimate K_{oc}, an organic carbon fraction value (f_{oc}) of 0.0004 was used, which was based on the measured TOC value of 0.4 % (table 3). The table is arranged in descending order of c_w values.

PFAS	Perfluorocarbon chain length	c_s (µg kg^{-1} dw)	c_w (µg L^{-1})	$F_{leachable}$ (%)	K_d (L kg^{-1})	Log K_d	K_{oc} (L/kg^{-1})	Log K_{oc}
PFOS	8 (long-chain)	400 ± 170	*110 ± 0*	73	3.63	0.56	907	2.96
6:2 FTS	6 (long-chain)	1.3 ± 0.53	*0.84 ± 0.044*	86	1.58	0.20	395	2.60
PFOSA	8 (long-chain)	40 ± 2.6	*0.74 ± 0.047*	16	53.39	1.73	13346	4.13
PFHxS	6 (long-chain)	2.1 ± 0.53	*0.60 ± 0.026*	74	3.49	0.54	873	2.94
PFOA	7 (long-chain)	0.3 ± 0.25	*0.39 ± 0.010*	94	0.68	-0.17	169	2.23
8:2 FTS	8 (long-chain)	4.8 ± 0.57	*0.35 ± 0.017*	42	13.84	1.14	3460	3.54
PFHxA*	5 (short-chain)	-	*0.22 ± 0.017*	108	-	-	-	-
PFPeA*	4 (short-chain)	-	*0.183 ± 0.0056*	110	-	-	-	-
PFDeA	9 (long-chain)	0.6 ± 0.11	*0.113 ± 0.0058*	67	4.99	0.70	1248	3.10
PFNA	8 (long-chain)	0.0 ± 0.11	*0.100 ± 0.0096*	97	0.36	-0.44	90	1.96
PFHpS	7 (long-chain)	0.33 ± 0.068	*0.074 ± 0.0036*	69	4.41	0.64	1102	3.04
PFUnA	10 (long-chain)	2.3 ± 0.22	*0.07 ± 0.010*	24	32.05	1.51	8012	3.90
FOSAA	8 (long-chain)	0.3 ± 0.30	*0.070 ± 0.0097*	71	4.07	0.61	1017	3.01
PFHpA	6 (short-chain)	0.02 ± 0.054	*0.058 ± 0.0035*	97	0.34	-0.47	84	1.93
PFBA*	3 (short-chain)	-	*0.054 ± 0.0065*	122	-	-	-	-
PFBS	4 (short-chain)	0.07 ± 0.015	*0.021 ± 0.0012*	74	3.54	0.55	885	2.95

* Larger PFAS eluate concentrations than initial soil concentrations ($F_{leachable}$ > 100 %) caused c_s to be negative.

As seen in Table 4, K_d was estimated for all the long-chain PFASs and ranged from 0.34 L/kg to 53.39 L/kg. Greater than 100 % leaching ($F_{leachable}$) was observed for most of the short-chain PFASs, and proper K_d values could therefore not be produced for these substances.

5.2.2 PFAS leaching in soil amended with waste-based sorbents

The batch leachate concentrations of PFOS (which represented 96 % of the measured PFASs in the control sample) from different mixes of soil and sorbents are shown in Figure 11.

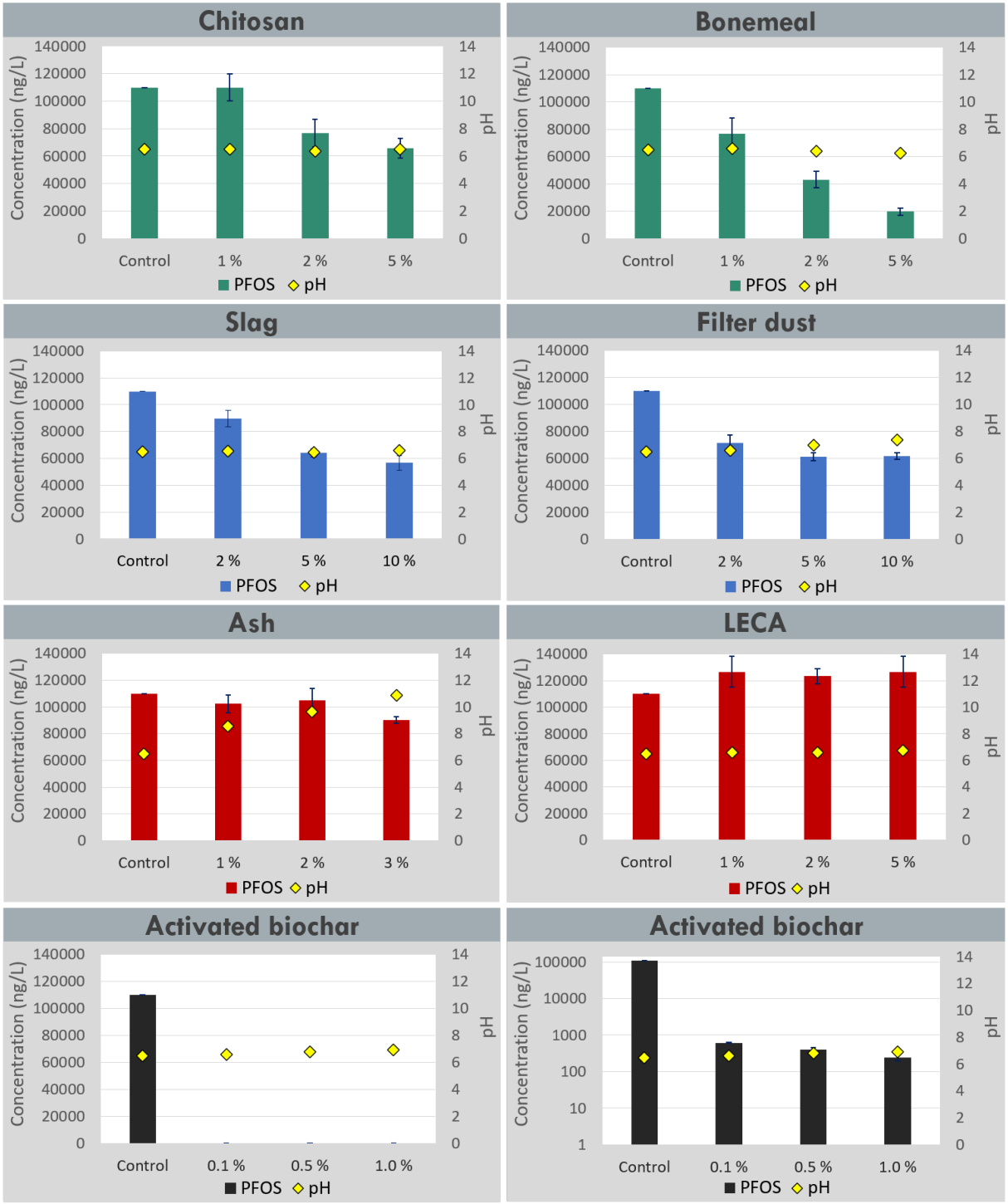

Figure 11. PFOS leachate concentrations (ng/L) and pH values for soil samples mixed with sorbents at different concentrations (% of soil dw). The sorbents used were bonemeal and chitosan (green), slag and filter dust (blue), ash and LECA (red) and activated biochar (black). Error bars based on the standard deviations of the PFOS concentration averages (n=3) are given for each column. Note that the PFOS concentrations of the biochar samples are presented with both arithmetic and logarithmic scales.

As seen in Figure 11, the leached PFOS concentrations gradually decreased with increasing sorbent amounts of both the organic sorbents (chitosan and bonemeal) and the industrial wastes (filter dust and slag). In the samples with 5 % (soil dw) chitosan and bonemeal, the PFOS leaching was reduced by ~ 40 % and ~ 82 %, respectively. The leached PFOS concentration was reduced by 44–48 % in the samples with 10 % (soil dw) slag and filter dust, while little to no PFOS reductions were seen in the ash and LECA samples. The activated biochar gave the largest declines in PFOS concentration (> 99 % reduction already at 0.1 % (soil dw) biochar). The measured leachate concentrations of all PFASs in each of the sorbent samples are given in Appendix K.

After PFOS, the remaining 19 quantified PFASs made up ~ 4 % of the PFASs in the control soil leachate. Each individual PFAS represented < 0.8 % of the total PFAS concentration (ΣPFAS). The different sorbents' influence on the leaching of these PFASs was still of interest, and the materials differed in their sorption abilities. In the following overview, a *significant* reduction denotes a > 50 % decrease in leachate concentration.

- **Activated biochar** was a highly efficient sorbent for all the quantified PFASs, and most PFAS concentrations were reduced to < LOQ in the samples with ≥ 0.5 (soil dw) biochar. All biochar doses reduced the ΣPFAS concentration by > 99 %.
- **Ash** did not significantly reduce the leachate concentrations of any of the PFASs and led to concentration increases for several of them instead.
- **Bonemeal** reduced the leachate concentrations of all long-chain PFASs by 63–99 %, except PFOA and PFHpS. The sorbent did not significantly sorb short-chain PFASs. Still, 5 % (soil dw) bonemeal reduced the ΣPFAS concentration by ~ 80 %.
- **Chitosan** only significantly reduced the concentrations of three long-chain PFASs: FOSAA, PFUnA and PFNS. In the sample with 5 % (soil dw) chitosan, the ΣPFAS concentration was reduced by ~ 37 %.
- **Filter dust** only significantly reduced the leachate concentrations of FOSAA, PFUnA, PFNS and PFDeA. In the sample with 10 % (soil dw) filter dust, the ΣPFAS concentration was reduced by ~ 42 %.
- **LECA** did not notably reduce the concentrations of any of the quantified PFASs.
- **Slag** only significantly reduced the leachate concentrations of FOSAA, PFNS and PFDeA. In the sample with 10 % (soil dw) slag, the ΣPFAS concentration was reduced by ~ 45 %.

The leaching of PFOSA

While both activated biochar and the highest bonemeal addition efficiently reduced the PFOSA leachate concentrations, the ash and filter dust caused increases in the leached PFOSA instead (fig. 12). The measured pH values were > 7.3 for all leachates that saw sharp increases in the PFOSA concentration.

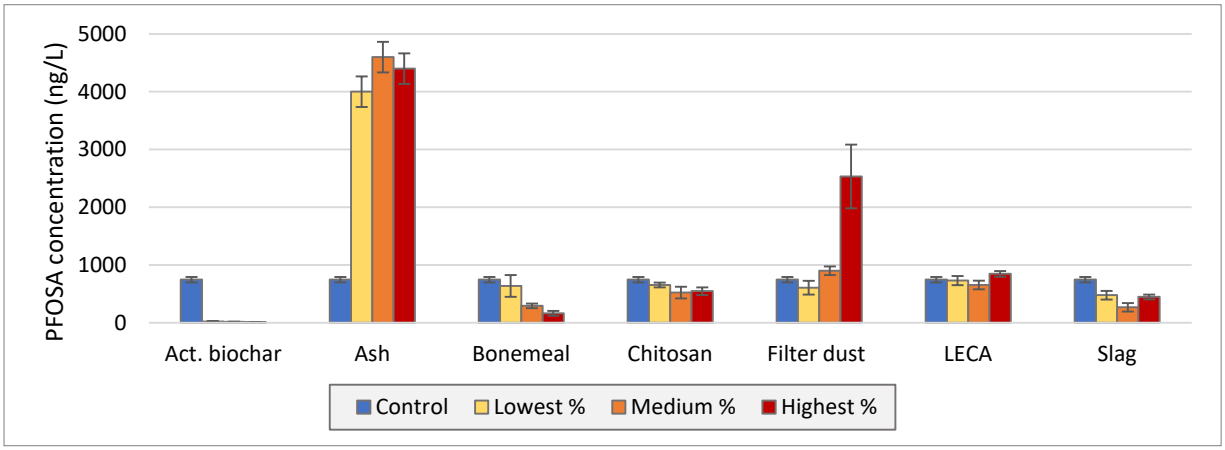

Figure 12. The average batch leachate concentrations of PFOSA (ng/L) for different sorbents and sorbent doses. The ash, bonemeal, chitosan and LECA materials had been added as 1, 2 and 5 % (soil dw). Filter dust and slag were added as 2, 5 and 10 % (soil dw), while the activated biochar was added as 0.1, 0.5 and 1.0 % (soil dw). The error bars represent the standard deviations of the averages (n=3).

The effect of perfluorocarbon chain length

The different chain lengths of the measured PFSAs and PFCAs affected sorption to the sorbents, as seen through their changes in log K_d values compared to the control soil values (Appendix L). Using bonemeal as an soil additive caused log K_d values to increase for many of the long-chain PFASs (fig. 13). The strongest increases in log K_d relative to the control soil (i.e., 0 % bonemeal) were observed for the PFCAs; elevated log K_d values occurred for all PFCAs added 2 % and 5 % bonemeal.

For the PFSAs, the bonemeal additions had the largest impact on the substance with eigth perfluorocarbons (PFOS). The log K_d of this eight-carbon PFSA gradually increased with each increase in bonemeal dose. The only short-chain PFSA displayed in the graph (four perfluorocarbons) was not increasingly sorbed by increasing % bonemeal.

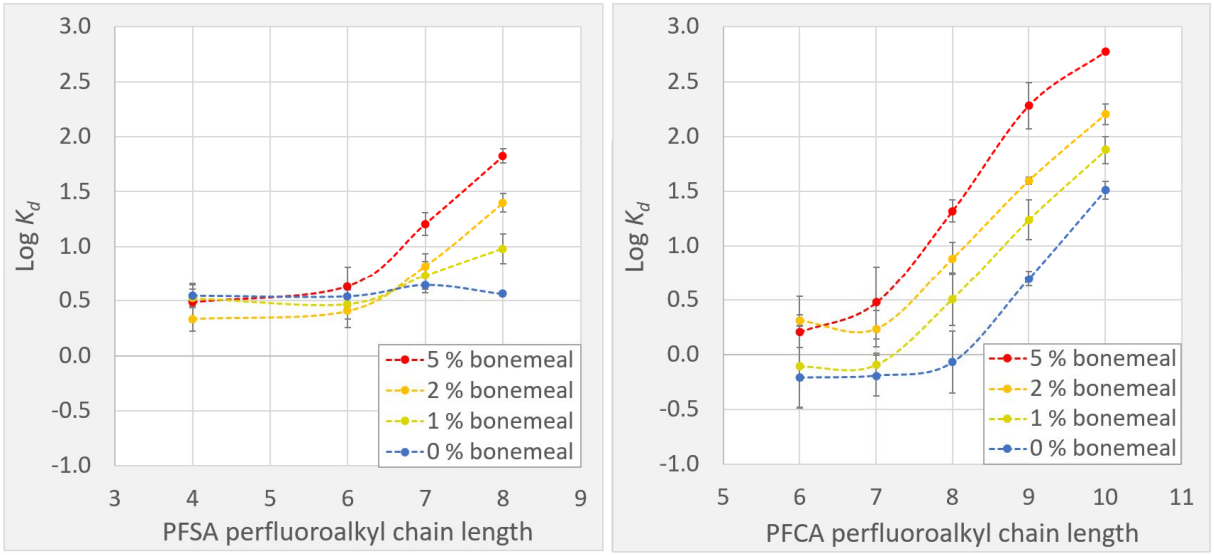

Figure 13. The log K_d values for PFAAs of various chain lengths subjected to different bonemeal doses (1 %, 2 % and 5 % of soil dw). The graphs for PFSAs (left) and PFCAs (right) show the log K_d values for both the different bonemeal additions and the control samples without bonemeal (blue graphs). The error bars represent the standard deviations of the mean log K_d values (n=3).

The effect of different perfluorocarbon chain lengths was less pronounced in the sorption of PFAAs to activated biochar (fig. 14). Relative to the control sample (0 % biochar), the log K_d values estimated were substantially higher for all PFAAs at all biochar amendment doses.

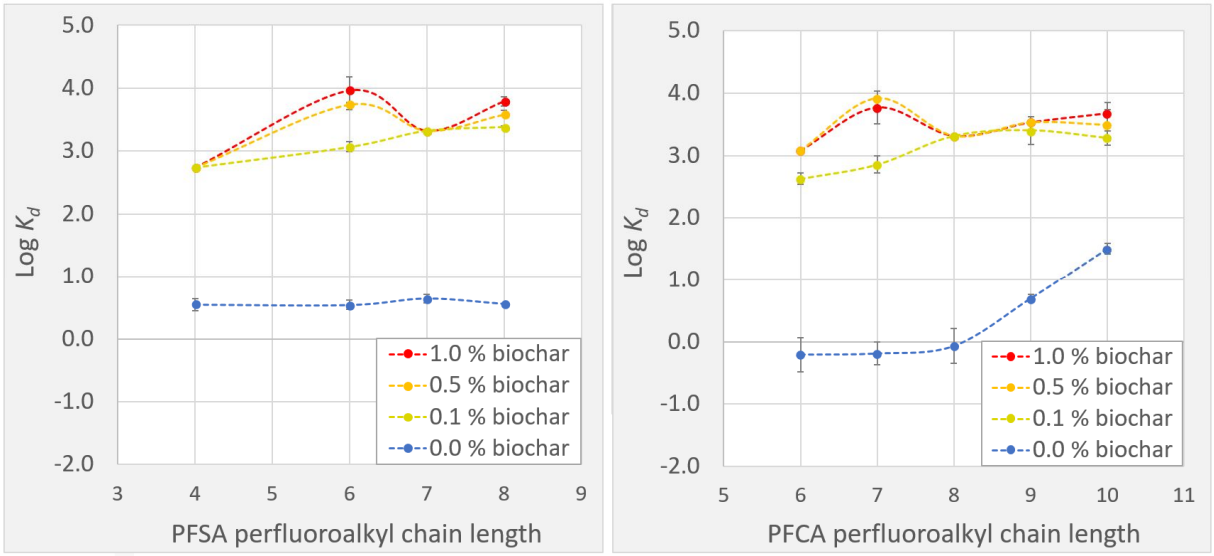

Figure 14. The log K_d values for PFAAs of different perfluorocarbon chain lengths at different biochar doses (0.1 %, 0.5 % and 1.0 % of soil dw), in addition to the log K_d values of the control samples without biochar (blue graphs). Error bars representing the standard deviation of log K_d (n=3) are also displayed.

5.2.3 Electrical conductivity and pH

As seen in Figure 11, pH increased with increasing sorbent dose in both the ash and filter dust samples. The pH of the ash samples increased from 8.57 ± 0.095 (1 % ash) to 10.86 ± 0.037 (5 % ash). A smaller pH increase was observed in the filter dust samples, which went from 6.60 ± 0.036 (2 % filter dust) to 7.35 ± 0.040 (10 % filter dust). The pH levels of the remaining batch leachates were all close to the control sample pH of 6.5 ± 0.10. The full set of pH and EC measurements can be found in Appendix M.

The electrical conductivity (EC) clearly increased in leachates from the ash, bonemeal, filter dust and slag samples as a consequence of increasing the sorbent additions (fig. 15). Conversely, the effect of increasing mixtures of LECA, chitosan and activated biochar negligably affected the EC in the batch leachates.

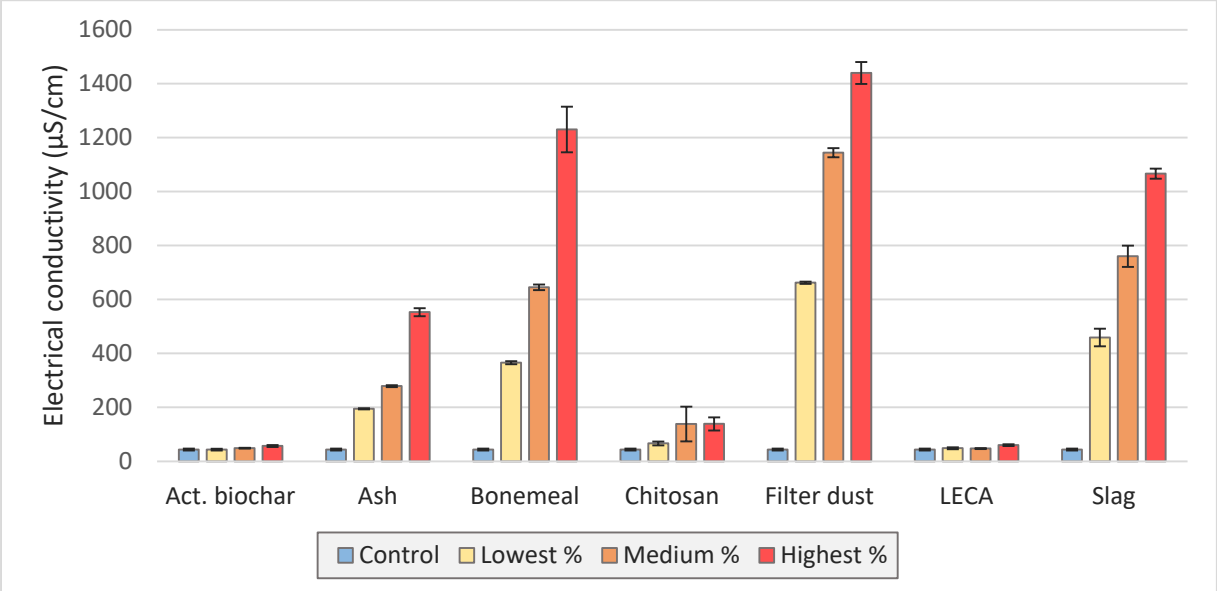

Figure 15. The measured EC (µS/cm) for batch leachates of soil added different sorbent concentrations. The lowest, medium and highest sorbent doses were 1 %, 2 % and 5 % (soil dw) for ash, LECA, bonemeal and chitosan. Biochar was added at 0.1 %, 0.5 % and 1 % (soil dw), while slag and filter dust were added at 2 %, 5 % and 10 % (soil dw). Error bars are displayed as standard deviations (n=3).

5.2.4 Dissolved organic carbon (DOC) and leached inorganic anions

The batch leachates' DOC concentrations increased most for the samples which had been added bonemeal (fig. 16). The changes in DOC were more modest for the other sorbent types, and 1 % (soil dw) activated biochar decreased DOC by ~ 80 % relative to the control sample. All the measured DOC concentrations and their uncertainties can be found in Appendix N.

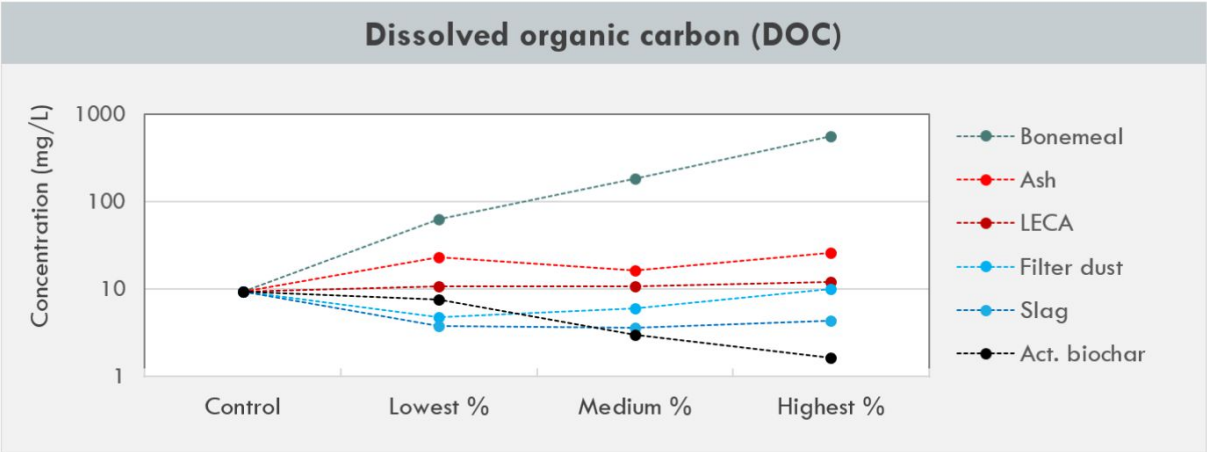

Figure 16. The average DOC concentrations (n=3) in the batch leachates of soil mixed with sorbents. The ash, bonemeal and LECA materials had been added as 1, 2 and 5 % (soil dw). Filter dust and slag were added as 2, 5 and 10 % (soil dw), and the activated biochar was added as 0.1, 0.5 and 1.0 % (soil dw). Due to very high measurement uncertainties, the chitosan samples' DOC concentrations were not included in the graph. Note that concentrations are presented on logarithmic scales.

While only low concentrations of nitrate (NO_3^-) were determined in the batch leachates (Appendix O), the sulphate (SO_4^{2-}) concentrations clearly increased in the leachates of soil amended with ash, slag and filter dust (fig. 17). Chitosan, however, reduced the sulphate concentrations with increasing admixtures. Lastly, leached chloride (Cl^-, mg/L) increased considerably in response to all sorbent mixtures, except the ones with slag and LECA.

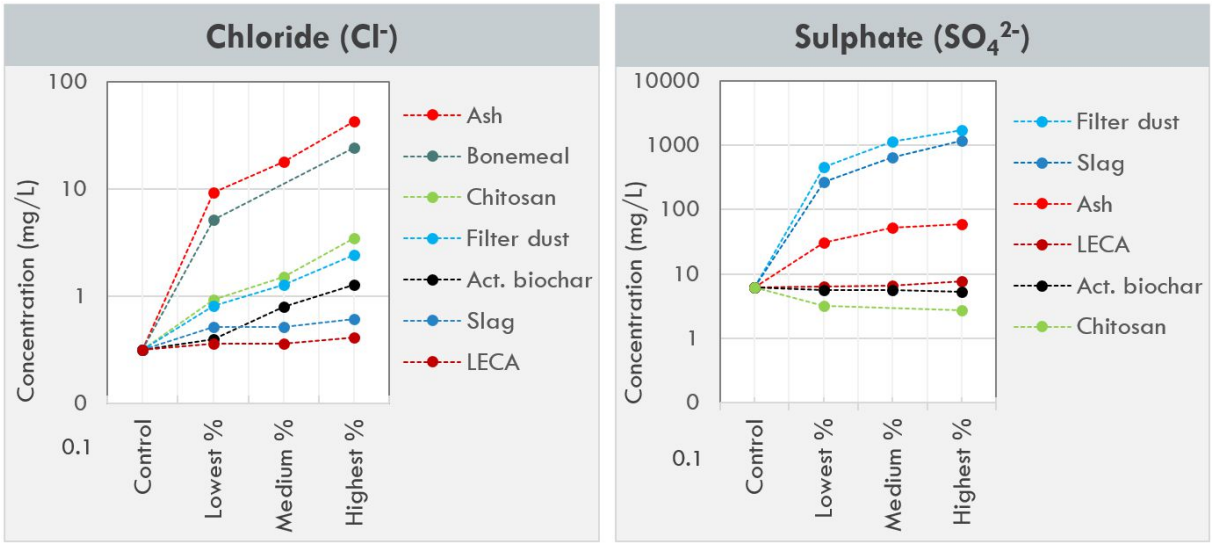

Figure 17. The estimated average (n=3) concentrations of chloride (left) and sulphate (right) in the leachates from soil mixed with different sorbents. The ash, bonemeal, chitosan and LECA materials had been added as 1, 2 and 5 % (soil dw). Filter dust and slag were added as 2, 5 and 10 % (soil dw), and the activated biochar was added as 0.1, 0.5 and 1.0 % (soil dw). The anions were not measurable in the 2 % (medium %) bonemeal admixture, and the sulphate concentrations of the 2 % (medium %) chitosan and all bonemeal admixtures were not included due to very high uncertainties (Appendix O). Note that concentrations are presented on logarithmic scales.

5.2.5 Leached element concentrations

The batch leachates of the control soil contained 7 ± 1.7 mg/L Ca and 0.380 ± 0.0074 mg/L Mg (Appendix P). The calcium concentrations gradually increased in the leachates of ash, bonemeal, filter dust and slag with increasing sorbent admixtures (fig. 18).

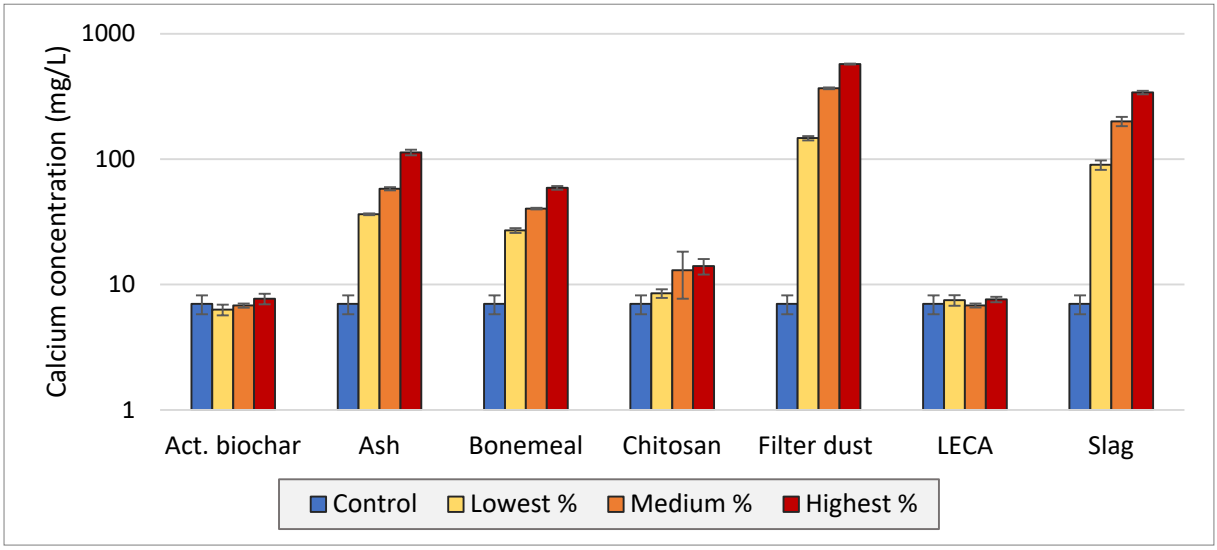

Figure 18. The average Ca concentrations (mg/L) in the leachates of the different sorbent mixtures. The ash, bonemeal, chitosan and LECA materials had been added as 1, 2 and 5 % (soil dw). Filter dust and slag were added as 2, 5 and 10 % (soil dw), while the activated biochar was added as 0.1, 0.5 and 1.0 % (soil dw). Error bars are given as the standard deviations of each average (n=3). Note that the concentrations are shown on a logarithmic scale.

The magnesium concentrations followed a pattern similar to the calcium concentrations. Thus, the amounts of dissolved Mg gradually increased with increasing sorbent admixtures, and the largest concentrations could be observed in the leachates of filter dust (24 ± 2 mg/L) and slag (10 ± 1.7 mg/L), while the concentration increases where smaller for bonemeal (5.97 ± 0.058 mg/L) and chitosan (1.4 ± 0.12 mg/L). The ash, however, caused the Mg concentration to decrease in the leachates (by ~ 96 % at the highest ash dose).

Leached heavy metal concentrations

The batch leachates of the control samples possessed low enough concentrations of As, Cr, Cu, Pb, Ni and Zn for the water to be classified as "good" according to the Norwegian quality standards for metals in fresh water (table B2 in Appendix B). An overview of the leachate concentrations of these metals in the different sorbent samples are given in Figure 19.

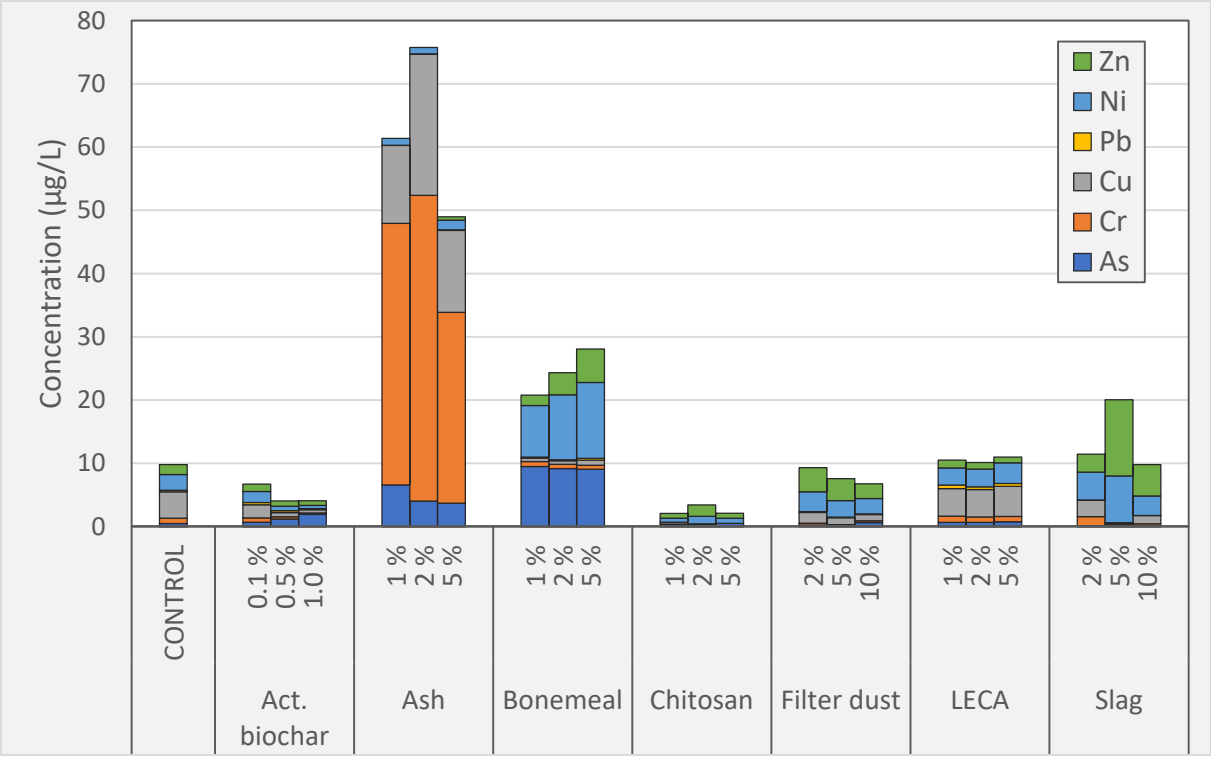

Figure 19. The average concentrations of As, Cr, Cu, Pb, Ni and Zn (µg/L) in the leachates of the control soil and the different sorbent mixes (% of soil dw). All metals are covered by the Norwegian quality standards (Norwegian Environment Agency, 2020). The concentration values and their associated uncertainties are given in Appendix P.

Increasing the activated biochar doses from 0.1 % to 1.0 % (soil dw) reduced the leachate concentrations of Cu, Ni, Cr and Zn by 53–88 % (relative to the control sample). Simultaneously, the As concentration increased with increasing biochar admixtures (fig. 19). If considering the Norwegian quality standards for fresh water, the Zn would change the classification from "good" to "background" classification, and As would change from "good" to "moderate" (Norwegian Environment Agency, 2020). The biochar still reduced the heavy metal sum (n=6) from 9.8 ± 0.71 µg/L (control) to 4.1 ± 0.12 µg/L (1.0 % soil dw biochar).

The bonemeal treatment also changed the leachates' composition of the metals covered by the Norwegian Environment Agency (2020). For all bonemeal doses, the Ni and As concentrations were increased enough to change the solutions' classifications from "good" (control soil) to "moderate" and "bad", respectively. The bonemeal also sharply reduced the Cu leachate concentration. Chitosan, on the other hand, caused substantial reductions in Cu, Pb, Cr and Ni.

The largest increase in the leachate concentrations of heavy metals occurred for the ash sampels. Relative to the control, Cr increased by > 3500 % in the leachates of all ash admixtures (fig. 19). The ash also caused the Cu and As concentrations to substantially increase.

5.2.6 Statistical data treatment

ANOVA analysis

A plot of the total PFAS concentration by sorbent type (fig. 20) was created by performing a one-way ANOVA test. The p-value of the test was < 0.001, meaning that at least one concentration reduction was significant. Additional information from the ANOVA test, including another ANOVA test performed on the sorbent types alone, is given in Appendix Q.

The clearest reductions in the leached PFAS concentration, relative to the control sample, were observed for the activated biochar and bonemeal samples (fig. 20). While the reductions were high in leachates from all the biochar-treated soils, the PFAS concentration reductions were less effective (but still clearly controlled by) the increasing bonemeal additions. All LECA amendmends increased the sum PFAS concentrations relative to the control samples, whereas significant reductions in leached total PFAS were not observed for the ash amendment. Overall, visible reductions in PFAS concentrations were only seen for activated biochar, bonemeal, chitosan, filter dust and slag.

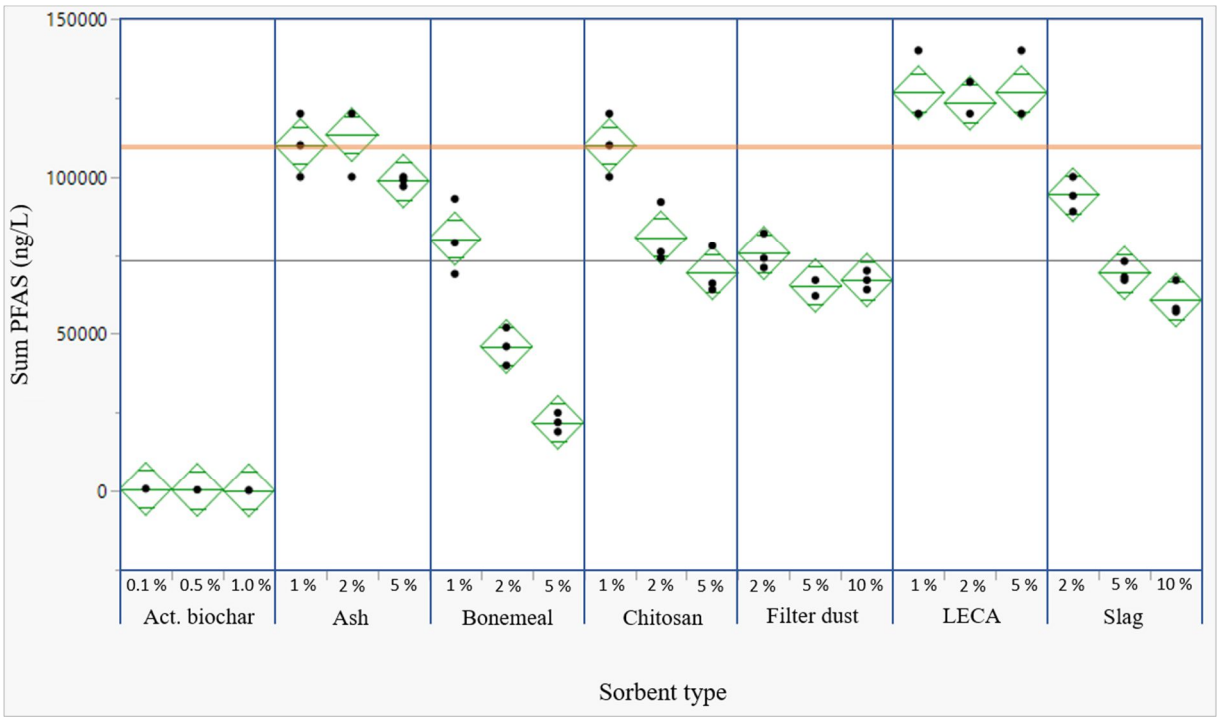

Figure 20. Plot of Σ33-PFAS leachate concentrations by sorbent type at different doses (% soil dw). The sum PFAS concentration of the control samples is shown by the orange line. The confidence intervals (95 %) of the concentration averages are given as green rhombuses and were based on the pooled estimate of error variance.

Stepwise regression and correlations

Through stepwise regression, the relationships between the PFOS leaching and the measured leachate properties were assessed for a subset of the sorption data (Appendix R). The final variables chosen for inclusion in the stepwise regression were electrical conductivity (EC) and the leachate concentrations of dissolved organic carbon (DOC), phosphorous (P), magnesium (Mg), calcium (Ca) and iron (Fe). This selection of variables was based on scientific grounds, which are described in section 3.1 *Remediation of PFAS contamination*.

The parameters included in the stepwise regression were all assumed to potentially influence PFOS leaching and sorption. Previously, PFAS concentrations have been found to correlate with EC (Knutsen et al., 2019), and DOC may increase the PFOS desorption from soil and sediment (Tang et al., 2017). Ca and Mg were included as their divalent ions can promote PFAS sorption (Du et al., 2014). Moreover, P (indicating phosphate) and Fe participate in compounds that may impede or promote PFAS sorption, respectively (Campos-Pereira et al., 2020). The majority of the other measured substances either possessed very low concentrations or were believed to be of little significance to the PFOS leachate concentrations in this study.

When excluding the highly sorbing activated biochar, EC and the leached Ca concentration appeared to be most significant for the leached PFOS concentration, resulting in an R^2 of 0.73 (EC alone had an R^2 of 0.57). Fitting a model to explain PFOS concentration by these two explanatory variables resulted in eq. (7). The parameter estimates both had low variance inflation factors (VIF) and p-values (see Table R1 in Appendix R).

$$\text{PFOS (ng/L)} = 112\,476 - 91\ \text{EC (µS/cm)} + 137\ \text{Ca}_{\text{leached}}\ \text{(mg/L)} \tag{7}$$

Nonparametric correlations

Due to the non-normality of EC and leached Ca concentration, even after applied normalization (logarithmic transformation), a Spearman's rank correlation test was performed (table 5). Both EC and the leached Ca concentration showed a negative correlation with the leached PFOS concentration. In addition, a high positive correlation was observed between EC and Ca.

Table 5. The Spearman's rank-order correlations between the EC, the leached PFOS concentration and the leached Ca concentrations. The Spearman's correlation coefficient (ρ) measures the strength and direction of association between the variables.

Variable	by Variable	Spearman ρ	Prob>|ρ|	-8 -4 0 4 8
EC (µS/cm)	PFOS (ng/L)	-0.8192	<.0001*	
Ca (mg/L)	PFOS (ng/L)	-0.6415	<.0001*	
Ca (mg/L)	EC (µS/cm)	0.9238	<.0001*	

6 Discussion

The results obtained from the soil analyses and batch leaching tests are discussed in this section—with respect to this thesis' research aim and objectives. Firstly, the soil analyses and characterisation are evaluated. The second part deals with the batch test results and includes discussions on the soil samples both with and without sorbent amendments. The seven sorbents' influence on PFAS leaching and other measured leachate parameters are also assessed. In the end, the waste-based materials suitability as PFAS sorbents in contaminated soil is evaluated.

6.1 Soil analyses and characterization

6.1.1 Chemical and physical soil analyses

The sampled soil was characterized as silty sand with a TOC content of 0.40 ± 0.060 %. PFOS represented 94 % of the Σ20 quantified PFASs in the soil, which was heavily contaminated since the measured PFOS concentration (1600 ± 170 µg/kg dw) was far above the current soil normative value of 100 µg/kg dw (Norwegian Climate and Pollution Agency, 2004). These findings corresponded with a previous analysis, which described soil from the same area as sandy soil with a predominance of PFOS and a TOC content of < 1 % (Høisæter et al., 2019).

Since PFASs are especially susceptible to leach out of sandy soils, which have a low PFAS sorption capacity (Bolan et al., 2021), the studied soil's K_d values were expected to be relatively modest. With the soil's low organic content, competitive sorption and clogging of sorbent pores by organic matter would likely not impede the sorbents' sorption capacity considerably. The activated biochar, which previously had worked well as a PFAS sorbent in low-TOC soil (Sørmo et al., 2021), was thereby further anticipated to greatly decrease PFAS leaching from the contaminated soil. In the first hypothesis of this thesis, activated biochar was predicted to also reduce the heavy metal leaching. That part was challenging to verify here as the soil's heavy metal content was rather low.

Among the heavy metals covered by the Norwegian legislations, which included As, Cd, Cr, Cu, Ni, Pb and Zn (Appendix B), only Cr at 56 ± 3.1 mg/kg slightly exceeded its normative value of 50 mg/kg (following HNO_3-digestion) (Norwegian Climate and Pollution Agency, 2004). As the Cr concentration in the soil sample was close to the normative value limit, the soil was not considered substantially contaminated with the heavy metals in question.

6.1.2 Other considerations on the soil analyses

As seen in Table 3, the measured TOC (0.40 ± 0.060 %) was much lower than the estimated LOI (2.3 ± 0.11 %). While both these values are measures of the soil's organic content, LOI analyses are often affected by various losses—e.g., the lattice water of clay. Even with the soil's low clay content (4.6 ± 1.7 %), the measurement can have been influenced by the loss of volatile salts, inorganic carbon and sulphide oxidation (Santisteban et al., 2004; Veres, 2002). LOI is generally considered to be roughly twice the total organic carbon content (Veres, 2002), and a conversion factor of 1.72 is regularly used to estimate TOC from LOI (DelVecchia et al., 2014). LOI has still been found to repeatedly overestimate soil TOC at calcination temperatures above 500 ºC (Bojko & Kabala, 2014; Frangipane et al., 2009). Frequent overestimations have also been demonstrated at LOI values below 8 % (Bojko & Kabala, 2014). The calcination temperature of 550 ºC and the relatively low LOI of the soil used in this study could partly explain why the LOI/TOC ratio was > 4. Altogether, the measured TOC was deemed a more accurate estimate for soil organic carbon than LOI and was used for estimating K_{oc} (table 4).

The element measurements slightly differed between the two digestion methods preceding the ICP-MS analysis (fig. 9). The highest recoveries of Al and Mg were achieved when just HNO_3 was used in the digestion, but Na and Sb were most recovered when both HF and HNO_3 were used. That more Mg was measured after HNO_3-digestion was expected since alkaline earth metals generally have low solubility in HF (Müller et al., 2014). A higher yield of Sb following the HNO_3:HF digestion was also consistent with former studies (Okkenhaug et al., 2015).

6.2 Batch tests – the leaching behaviour of PFAS

6.2.1 PFAS leaching from unamended soil

In accord with the soil PFAS analysis, the PFAS leaching from the unamended soil was also dominated by PFOS, which represented 96 % of the Σ20 quantified PFASs in the leachate. Compared to the initial soil concentration, approximately 73 % of the PFOS was estimated to have leached out of the soil (table 4). The leachable fraction of PFOS was thereby very high, but still not unreasonable as it resulted from a harsh batch test procedure. Moreover, the measured fraction of leached PFOS fit well with a previous study where 71 % of the PFOS leached from a low-TOC soil (Sørmo et al., 2021). As the soil used in this study was a silty sand with a low TOC content, the obtained results were considered plausible.

The log K_d of PFOS was calculated to 0.56 L/kg (table 4) and fit fairly well with the results of Sørmo et al. (2021) and Silvani et al. (2019), which had PFOS log K_d values (low-TOC soil) of 0.6 and 0.67 L/kg, respectively. However, K_d values can vary a great deal between different soil types. For instance, Zareitalabad et al. (2013) reported PFOS log K_d values that ranged from < 1 to 35.3 L/kg in different soils and sediments. Adjusting the partitioning coefficients for the soil's organic carbon content, which is a highly important factor for the PFAS sorption patterns in soil (Milinovic et al., 2015), can reduce the spread of the coefficient values. Zareitalabad et al. (2013) further presented an average PFOS log K_{oc} value of 3.0 L/kg (coefficient of variation 21 %). The PFOS log K_{oc} value estimated in this work was 2.96 L/kg (table 4), thus also within this average value. Altogether, these findings show that while log K_d values highly fluctuate, experimental log K_{oc} values can be very similar between different soils and sediments.

Several of the leached PFASs were found to account for > 100 % leaching (table 4). These paradoxical results are likely connected to flaws of the analytical methods. For instance, the analyte extraction of the soil analysis was probably less effective than that of the batch leaching test, causing an underestimation of the soil's PFAS concentrations. As the leachable PFAS fraction ($F_{leachable}$) was calculated by dividing the leached fraction with the initial soil concentration (eq. 3), such underestimations would cause elevated $F_{leachable}$ estimations. The high leaching observed could also connect to the PFASs' perfluorocarbon chain lengths.

The > 100 % leached PFASs—PFHxA, PFPeA and PFBA—are all short-chain PFASs, which generally bind more weakly to soil and are more liable to leach than long-chain PFASs. Hydrophobic interaction has earlier been proposed to be the main binding mechanism in soil (Ross et al., 2018). The long-chain PFASs' higher hydrophobicity, provided by their longer perfluoroalkyl chains (fig. 3), is thereby likely the reason that they bind more strongly to soil compared to their short-chain analogues. Moreover, compared to the long-chain PFASs, the short-chain PFASs might also undergo more electrostatic repulsion from the soil's negatively charged surfaces and organic matter.

The initial concentrations of the three > 100 % leached short-chain PFASs were also relatively low (< 2.1 µg/kg dw soil, as seen in Appendix H). Based on a former PFAS analysis of an AFFF assumed to represent the foams used at the firefighting training site (Høisæter et al., 2019), the soil sampled in this study has presumably been exposed to substantial amounts of different short-chain PFASs. Most of these very mobile short-chain substances have likely

leached away over time (for instance, following precipitation events), causing the studied soil to contain fairly low amounts of short-chain PFAS. Moreover, when the PFAS concentrations approach the quantification limits, measurements are often progressively more uncertain. The K_d estimations of PFBA, which had a leachate concentration of 0.054 ± 0.0065 µg/L (table 4) and an LOQ of 0.010 µg/L, could thereby be expected to be quite uncertain.

Another possible explanation for the > 100 % PFAS leaching is the occurrence of precursor transformations during the leaching test period of 14 days. Precursors can be defined as polyfluoroalkyl compounds with the potential to transform into stable PFAAs through natural processes (Houtz & Sedlak, 2012). The presence and conversion of such substances could thus have elevated the final leachate concentrations of their degradation products (PFAAs), and the $F_{leachable}$ values of the stable PFAAs would increase. Since only a small portion of the > 6000 existing PFASs were analysed for, the studied soil could contain many different precursors. Still, > 100 % PFAS leaching has been observed in previous research (Hale et al., 2017), and using similar methodical approaches still enables results like K_d values to be compared between studies.

6.2.2 PFAS leaching from sorbent-amended soil

Effect of sorbents on the leaching of PFOS

Since PFOS represented the vast majority of the PFASs measured in both the soil and the control sample leachates (table 4), changes in PFOS concentration would largely affect the total PFAS concentration. Hence, the sorbents' ability to reduce PFOS leaching was important, and this ability varied between the different materials and the concentration they were added in.

As seen in Figure 11, the material that most efficiently removed PFOS was biochar, which caused > 99 % reduction in the leachate PFOS concentrations already at the lowest biochar dose (0.1 % soil dw). The leached PFOS concentrations of all the biochar samples were low enough to change the leachate water's classification from "bad" or "very bad" to the lower range of the "moderate" class (table 1). As the biochar surface is negatively charged (Sørmo et al., 2021), some electrostatic repulsion would occur for PFOS and other anionic PFASs that have negatively charged functional groups. Since most of the PFOS was still sorbed, the hydrophobic forces between the PFOS's fluorinated chain and the sorbent surface have presumably been strong enough to overcome the repulsive effects.

The bonemeal also clearly removed PFOS from the leachate, although 5 % (soil dw) bonemeal was needed to obtain a PFOS concentration reduction of ~ 82 % (fig. 11). The final PFOS concentration after using 5 % bonemeal was 20000 ± 2500 ng/L, which was low enough to make the leachate water change its classification from "bad" or "very bad" to "moderate" (table 1). PFOS is "proteinophilic" (Conder et al., 2008), and the bonemeal's high protein content (estimated to 54 ± 4.4 %) might explain the rather efficient PFOS removal. The large DOC concentrations in the bonemeal leachates can simultaneously have mobilized PFOS (Tang et al., 2017) and reduced the bonemeal's sorption effect. Nonetheless, bonemeal is a novel sorbent and its sorption of PFASs has not been studied earlier (as far as is known). The exact PFOS removal mechanisms are therefore uncertain, but hydrophobic interactions between the perfluorocarbon chains and the hydrophobic sites of proteins is suggested to be a dominant PFAS removal mechanism of other high-protein sorbents (Turner et al., 2019). Interaction between the PFOS' negatively charged functional group and the positively charged groups (i.e., amides) of the proteins can also have contributed to the sorption (Sheng et al., 2014).

In the samples with 5 % (soil dw) chitosan, the PFOS concentration was only reduced by ~ 40 % compared to the control samples. The resulting leachate, which had a final PFOS concentration of 66000 ± 7400 ng/L, would thereby still have been classified as "bad" or "very bad" (table 1). As chitosan polymer surfaces are typically positively charged and relatively hydrophilic (Ye et al., 2014), electrostatic interaction possibly played a role in the sorption that occurred. Still, PFOS might rely more on hydrophobic interactions than electrostatic interactions for binding to surfaces (Sörengård et al., 2020), and the sorption can have been limited by a lack of hydrophobic sites.

The industrial wastes, which consisted of iron sulphate and slag in a 1:5 ratio and iron sulphate and filter dust in a 5:3 ratio, also caused rather modest (< 50 %) reductions in the PFOS concentrations (fig. 11). The materials' content of positively charged metal oxides (such as Fe oxides) were assumed to provide possible PFAS sorption sites. When close to a neutral pH, below the iron oxides' point of zero charge (PZC), electrostatic interactions would dominate PFOS sorption to the oxides (Ferrey et al., 2012). Rather high sorbent concentrations were still required to reach a substantial PFOS retention. In a previous study, 20 % of a similar industrial waste was needed to achieve ~ 70 % retention of PFOS in a contaminated soil (Sævarsson et al., 2018). Hence, the industrial wastes in question might have low sorption capacities or affinities for PFOS. The limited dependence of PFOS sorption on electrostatic interactions could partly explain the low concentration reductions observed in this study.

The least efficient PFOS sorbents of the materials investigated were ash and LECA, and the latter actually increased the leached PFOS concentration by ~ 15 % (fig. 11). These increases in PFOS concentration did not correlate with increasing LECA doses. Since the LECA did not cause any obvious changes in the other geochemical factors measured (such as pH, DOC or element concentrations), the reasons for the increased PFOS concentrations remain uncertain. The ash treatment decreased the PFOS concentration by < 20 % and is not considered a good sorbent either. The gradual pH increases with increasing ash admixture (fig. 11) could partly explain the material's sorption inefficiency, since more alkaline conditions would cause deprotonation of both sorbent and soil surfaces. Nonetheless, a much larger PFOS concentration reduction would be required for the sorbents to be regarded as suitable for remediation.

Effect of sorbents on the leaching of other PFASs

The binding capacity and binding affinity of the activated biochar were large enough for both long- and short-chain PFASs to be efficiently sorbed. Due to the low hydrophobicity of the short-chain PFASs, they had a limited potential for (van der Waals) hydrophobic interaction. The short-chain PFASs were therefore expected to be more affected by electrostatic repulsion from the negatively charged biochar surface than the long-chain PFASs. That biochar efficiently removed all the quantified PFASs, independent of chain length, can thereby indicate that the hydrophobic interactions overcame the electrostatic repulsion for all these PFASs in the binding to biochar.

That the bonemeal caused sorption of most long-chain PFASs, but was inefficient for short-chain PFASs, can give some clues about the binding mechanisms at play. The hydrophobicity of a PFAS increase with increasing perfluoroalkyl chain length (Li et al., 2020). Since the bonemeal only sorbed long-chain PFASs, hydrophobic interactions likely played the dominant role in sorption. Furthermore, the sorption of short-chain PFASs probably depends on electrostatic interactions (Li et al., 2020; Sörengård et al., 2020), and the bonemeal might lack strong enough positive charges to attract the short-chain substances. Another possible explanation for why merely long-chain PFASs were sorbed is that they occupy all sorption sites and outcompete the less hydrophobic short-chain PFASs. Such competing effects between PFASs of different molecular sizes have been suggested previously (Xiao et al., 2017). The bonemeal also vastly increased the DOC content (fig. 16), and some PFASs may have been retained in the solution as a consequence—causing a reduction in the sorption of these PFASs.

Because of the typically positive surface charges of chitosan (Ye et al., 2014), electrostatic interaction with anionic PFASs could be a possible binding mechanism for the sorbent. That chitosan only significantly reduced the concentration of three long-chain PFASs (FOSAA, PFNS and PFUnA) may, to the contrary, imply that hydrophobic interactions was the dominating factor for binding. In other words, there is little indication that electrostatic interactions played a large part in the PFAS sorption. Still, chitosan did also cause reductions in the leachate concentrations of sulphate (fig. 17) and Ni, Cu and Cr (fig. 19). The sulphates might be crosslinked with protonated amino groups of the sorbent (Weißpflog et al., 2020), and the metal ions are possibly sorbed through ion exchange and surface complexation (Pivarčiová et al., 2014). The chitosan could have a greater sorption affinity for sulphate and certain metals than for the measured PFASs. In that case, potential sorption sites might have been saturated with such substances and made unavailable for the PFASs.

Electrostatic interactions were also expected to contribute to the PFAS sorption to the filter dust and slag, due to the materials' content of metal oxides. Especially iron oxides have previously been linked to the sorption of PFASs (Darlington et al., 2018; Wei et al., 2017). Whereas the exact composition of the filter dust and slag was unknown, both materials were known to contain metal oxides which could provide sorption sites for PFASs (Du et al., 2014). However, both materials only caused significant concentration reductions (> 50 % compared to the control sample) for a few long-chain PFASs. Like chitosan, the PFAS sorption to these materials thereby did not appear to be dominated by electrostatic interactions. The few PFASs that the materials sorbed were also initially present in relatively low amounts. Slight concentration fluctuations would largely influence the estimated leachate concentration declines. Whether the sorbents in question would cause similar concentration reductions for higher concentrations of these long-chain PFASs is uncertain.

The irregular leaching of PFOSA

As observed in Figure 12, the PFOSA concentrations sharply increased in the ash samples and the sample with the highest filter dust dose (5 % soil dw). These were also the only samples with pH values > 7.3 (fig. 11). Substantial increases in the leached PFOSA concentrations did not occur in any of the other samples, which all had relatively stable pH values ≤ 7. Hence, the large PFOSA releases might have been caused by the changes in the environmental conditions that these pH increases produced.

PFOSA had a very high estimated log K_d value and a leachable fraction ($F_{leachable}$) of only 16 % in the control samples (table 4), meaning that most of the substance was strongly bound to the soil. Moreover, PFOSA was the second most abundant PFAS in the soil, which was not surprising as the chemical is among the most common PFASs found at firefighting training sites (van Hees, 2017). With a relatively large amount of PFOSA bound to the soil, profound releases could be triggered by changes in factors that control PFAS sorption. An increase in pH cause soil particles to become more negatively charged (Oliver et al., 2019), which likely weakens the attractive forces between PFOSA and the soil. Since the sharp PFOSA concentration increases only were observed in samples with pH values > 7.3, a critical point for PFOSA release might lie somewhere around this pH. When pH was raised above this value, most of the chemicals were likely electrostatically repelled. Electrostatic forces have also earlier been suggested to represent a dominant factor for sorption in low-TOC soils (Liu et al., 2020). Likewise, the surface electrostatic interactions can have controlled the PFOSA binding to the soil used in this study.

6.2.3 Factors affecting PFAS sorption in sorbent-amended soil

Effect of chain length and functional group

As earlier discussed, PFASs with long perfluorocarbon chain lengths tend to sorb more than PFASs with short chains, and sorption is also affected by the PFASs' functional groups. The sorption patterns of PFCAs (carboxylic acids) and PFSAs (sulfonic acids) to biochar and bonemeal will be the focus of the discussion below.

For the samples mixed with bonemeal, different sorption patterns were observed between the PFCAs and PFSAs of different lengths. As seen in Figure 13, the log K_d of long-chain PFCAs (≥ 7 perfluorocarbons) in the bonemeal samples clearly increased together with the perfluoroalkyl chain length. The long-chain PFSAs (≥ 6 perfluorocarbons) did not follow the same increasing patterns, but instead mainly showed elevated log K_d values for the PFSA with 8 perfluorocarbons (i.e., PFOS). These sorption trends are in accordance with Sörengård et al. (2020), which found a significant trend of increasing sorption for long-chain PFCAs to different sorbents, but no similar pattern for long-chain PFSAs.

That PFAS sorption increases with chain length is likely due to the increased hydrophobicity that accompanies each additional CF_2 moiety (fig. 3), which strengthens their binding to hydrophobic surfaces (Nguyen et al., 2020). Long-chain PFASs might also adhere to surfaces

through multiple contact points due to their larger molecular size (Zhao et al., 2014), which could explain that the largest log K_d increases are observed for the long-chain PFASs. Still, log K_d values were only obtained for one short-chain PFSA (4 perfluorocarbons) and one short-chain PFCA (6 perfluorocarbons). Compared to the control sample, the bonemeal did not cause any log K_d increase for the short-chain PFSA, but some increase was seen for the short-chain PFCA (fig. 13). Whether the bonemeal would similarly influence the partition coefficients of other short-chain PFCAs and PFSAs is uncertain. Yet, the sorption of the PFAAs was affected by more than just the substances' sizes. By comparing the log K_d values of PFCAs and PFSAs with the same perfluorocarbon chain lengths, the functional groups themselves were also found to influence sorption (fig. 20).

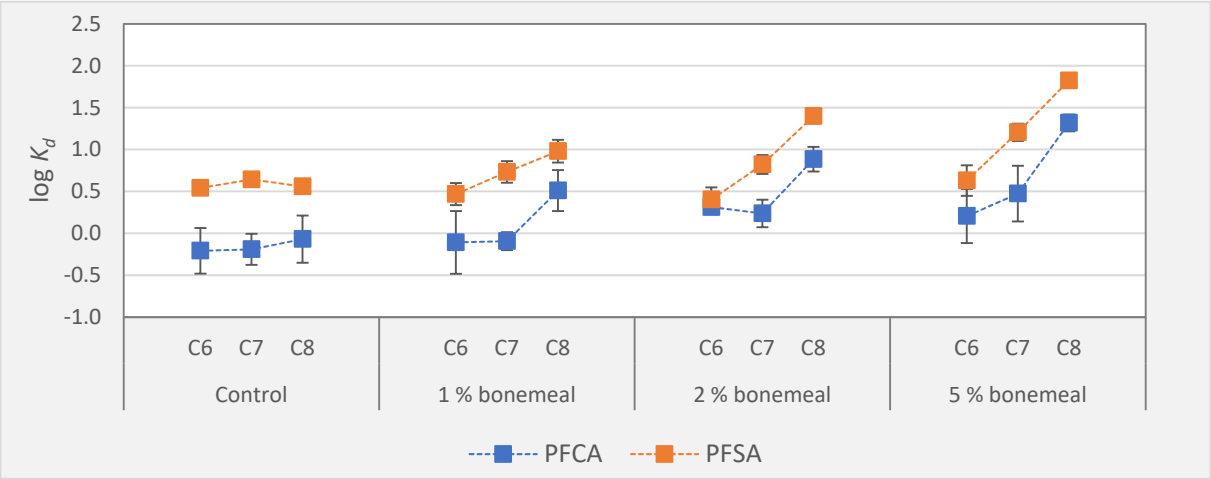

Figure 20. The average log K_d values (n=3) of different PFAAs (PFCAs and PFSAs) with perfluorocarbon chain lengths of C6–C8, following batch leaching tests with control soil and soil mixed with 1 %, 2 % and 5 % (soil dw) bonemeal. The error bars represent the averages' standard deviations.

As displayed in Figure 20 (based on the values of Figure 13), the PFSAs had higher log K_d values than the PFCAs of the same perfluoroalkyl chain length. This tendency of PFSAs to sorb more than their PFCA counterparts agrees with numerous former studies, including investigations of PFAS binding to soil (Campos-Pereira et al., 2018), sediments (Zhao et al., 2012; Higgins & Luthy, 2006) and various sorbent materials (Sørmo et al., 2021; Sörengård et al., 2020). The higher sorption of PFSAs compared to PFCAs can relate to the higher hydrophobicity or larger size of the sulfonate group compared to the carboxylate group (Higgins & Luthy, 2006). Since hydrophobic interactions are thought to be the driving force for PFAS sorption to bonemeal, increases in both an PFAS' hydrophobicity and molecular size (more contact points) could favour sorption. Hydrophobicity is likely also important for PFAS sorption to biochar, which was found to increase the log K_d values more than bonemeal.

The activated biochar greatly increased the log K_d of all PFAAs in question (fig. 14). Several of the substances were even reduced to concentrations below their respective LOQs (Appendix K), causing "maximum" log K_d values to occur. Such maximums were obtained for the PFCA with 8 perfluorocarbons and the PFSAs with 4 and 7 perfluorocarbons at all biochar doses (0.1, 0.5 or 1.0 % soil dw). In Figure 14, the points of each biochar dose assembled at the same log K_d values for these three PFAAs. Compared to the bonemeal sorbent (fig. 13), the sorption of PFAAs to biochar was not largely influenced by the perfluorocarbon chain lengths. This could be due to the biochar not being fully saturated, thus causing minimal competition between the sorbates. A potential chain length dependency would therefore only have been evident at lower biochar doses than the ones used in this study. Since both PFCAs and PFSAs were effectively sorbed by biochar, differences between these two groups are not perceptible either. Yet, observations so far supports the assumption of hydrophobic interaction being the main sorption mechanism for this sorbent as well.

Carbonaceous materials (such as biochar) are among the most well-studied sorbents for PFASs, and the materials' strong hydrophobic surfaces are often used to explain how PFASs can sorb on these otherwise negatively charged materials (Deng et al., 2012). As the PFCAs and PFSAs investigated are assumed to be anionic at the close-to-neutral pH values that occurred in this study, some repulsing forces have likely been present. These forces were still not strong enough to cause any clear distinctions between the different perfluorocarbon chain lengths observed in Figure 14. With only negligible changes in pH (fig. 11) and EC (fig. 15) with increasing biochar admixtures, these factors have likely not affected sorption in the biochar samples. Altogether, the biochar's large surface area (thus sorption capacity) and affinity for anionic PFASs is believed to have made the material the most efficient sorbent for PFASs in this study.

Effect of dissolved components on PFAS leaching

From the statistical analysis, it was made clear that the sorbents differed in their PFAS sorption capabilities. Through one-way ANOVA (fig. 20), significant differences were uncovered between separate sorbent doses (and the different sorbent types also differed, as seen in Figure Q2 in Appendix Q). In the later stepwise regression analysis, a model containing electrical conductivity (EC) and leached Ca concentration was found to explain 73 % of the variance in leached PFOS concentrations. Even though the variance inflation factors (VIF) were low for the resulting parameter estimates, indicating no multicollinearity issues between the two variables, a high positive correlation between leached Ca and EC also existed (table 5).

The EC and the leached Ca concentrations significantly correlated with both each other and the leached PFOS concentration (table 5). With a Spearman's correlation coefficient (ρ) of 0.92, a very strong positive association occurred between the EC and the Ca concentration. The leached PFOS concentration was, on the other hand, negatively associated with both the EC (ρ of -0.82) and the Ca concentration (ρ of -0.64). Increased Ca concentrations have previously been linked to reductions in PFOS leaching (Chen et al., 2012; Higgins & Luthy, 2006), and the negative association between the leached Ca and PFOS concentrations fit well with these findings. In other words, Ca appear to enhance PFOS sorption—possibly due to a Ca bridging effect between anionic PFASs and negatively charge surfaces. The positive parameter estimate seen for the Ca concentration in the final regression model (eq. 7) was therefore unexpected.

Following the backwards stepwise regression, the model's estimated parameters were negative for EC (-90.6) and positive for the Ca content (+136.8). Still, based on both the Spearman correlations (table 5) and earlier studies, the Ca parameter should have had a negative value. The regression model's positive parameter estimate for Ca is therefore believed to be the result of a statistical suppressor effect, which can cause the sign of an estimate parameter to change in the presence of highly correlated variables (Friedman & Wall, 2005). Nonetheless, while the regression model with an R^2 of 0.73 could explain 73 % of the variation seen in the leached PFOS concentrations, EC was simultaneously found to explain 57 % of the variation by itself.

Altogether, the statistical analyses performed indicate that EC was an important parameter for explaining the leached PFOS concentration, thus EC may also describe the sorption of PFOS. As EC is a measure of the total ion concentration in a solution (Jacobsen, 2021), a close relationship between EC and Ca might still have influenced the model though suppression. While not completely certain, Ca still appears to be an important variable among the measured ions for explaining PFOS sorption.

6.2.4 Other considerations regarding the batch leachate analysis

While the Norwegian quality standards for fresh water (Norwegian Environment Agency, 2020) is a useful tool for assessing the contamination status of water bodies, the guidelines were not designed for evaluating batch leachates. The water classifications defined earlier in both the results and discussion sections are therefore merely helpful to illustrate the concentration changes. Both the contaminant leaching and the sorbents' sorption abilities in the environment would most likely be comparatively different from the results presented in this thesis.

The batch leaching procedure used in this study do not simulate natural conditions for several reasons. The L/S ratio of 10 was much greater than what would occur on-site, causing the chemical equilibrium to differ as a consequence. Only a finite amount of water was used in each test as well, possibly causing the leached substances to upconcentrate during the 14-day agitation step. There was also a large potential for contact between the sorbents and the leached contaminants during the rigorous agitation. Hence, in a typical *in situ* immobilization procedure where sorbents are mixed into topsoil, lower sorption than that of the leaching tests might be observed. Altogether, the work performed in this study is simply of an explanatory nature to see the different waste-based materials potential as sorbents.

Soil is a heterogenous and complex mixture, and the sorbent materials are likely to possess some heterogeneity as well. Despite the efforts to homogenise the soil and sorbent materials prior to use, some heterogeneity can still have influenced the measurements. For instance, the large SO_4^{2-} fluctuations that rendered the bonemeal values unusable (fig. 17) could be due to variations in the material. It cannot be ruled out that the > 100 % leaching observed for some short-chain PFASs in the control samples (table 4) is a result of soil heterogeneity either.

6.3 The waste-based materials' suitability as PFAS sorbents

The PFAS sorption ability of the waste-based materials was tested in a single soil, thus only for a single set of conditions. As seen in Figure 10, the distributions of PFAS types can vary substantially between locations, depending on the contamination sources. The materials' suitability as PFAS sorbents thereby depends on both the remediation goal and the contamination situation in question. Since chemical and physical conditions also affect a remediation procedure, more research would be needed to say something about the sorbents' overall eligibility for PFAS remediation. The PFAS sorption patterns identified can still be used to evaluate the different materials' suitability as sorbents in systems similar to that of this work.

6.3.1 Activated biochar

The activated biochar efficiently reduced the PFAS leaching (> 99 % PFAS reduction at all biochar doses). Since the material sorbed different types and lengths of PFASs alike, the biochar is a suitable sorbent for remediation of PFAS contamination in the soil type used in this work. The biochar also reduced the leachates' DOC and heavy metal concentrations, indicating that

it possessed satisfactory sorption capacity to sorb all these compounds simultaneously. Whereas the heavy metals Cu, Ni, Cr and Zn were reduced by the biochar, the As concentration increased somewhat. This As concentration increase could be due to former pressure impregnation of the wood waste feedstock, which earlier was a common application for As compounds (Pedersen, 2021). The ability of a biochar to sorb different metals can also vary based on feedstock and pyrolysis conditions (Li et al., 2017), and several biochars have previously been rather inefficient at sorbing As (Agrafioti et al., 2014; Beesley & Marmiroli, 2011). The overall ability of the biochar to reduce the heavy metal concentrations was still considered good. Furthermore, with the material's known resistance to biodegradation (Hofstad, 2020), the activated biochar was deemed the best sorbent for PFASs in contaminated soil of the materials tested.

6.3.2 Bonemeal

The bonemeal was the second most efficient material for PFAS sorption, and it caused a sharp decrease in the leachate concentrations of PFOS and most of the other long-chain PFASs. That bonemeal can sorb PFASs this well has, as far as is known, not been documented previously. However, the sorbent did not efficiently remove short-chain PFASs and caused increases in the leachates' EC, DOC and heavy metal content—which could affect the conditions of different soil systems. Given that bonemeal degrade relatively quickly, its applicability for long-term immobilization of PFAS in soil is low. However, with its clear PFAS sorption capabilities, bonemeal could still have potential for PFAS remediation in other scenarios—for instance in a filtering system where the PFAS-contaminated media and the sorbent only are in contact for a limited time. Still, further investigations of the material's content of potentially harmful substances would be required for it to be used as a sorbent.

6.3.3 Ash. chitosan, filter dust, LECA and slag

Due to their either non-existing or relatively limited PFAS sorption capabilities, the remaining sorbents were not regarded as suitable sorbent materials in this work. Still, the PFAS sorption of chitosan, slag and filter dust materials could be enhanced through modifications. For instance, efficient PFOS removal from water has previously been obtained with crosslinked chitosan beads (Zhang et al., 2011) and filters using low-cost industrial waste materials high in metal oxides (Sævarsson et al., 2018). The particularly high increases in heavy metals produced by the ash sorbent (fig. 19) likely renders it unusable as a sorbent overall.

7 Conclusion and recommendations

This study aimed to identify efficient waste-based sorbents for the remediation of PFAS-contaminated soil, and the study's design provided both sufficient and insufficient data to verify the hypotheses defined in section 2.2 *Research objectives and hypotheses*.

The activated biochar efficiently reduced the PFASs in the batch leachates, and the sorbent also caused additional reductions in DOC and heavy metals—thus hypothesis (i) was verified. Relative to the control sample, 0.1 % (soil dw) biochar was enough to reduce the total PFAS concentration by > 99 %. However, hypothesis (ii) was falsified since the samples with 10 % (soil dw) slag and filter dust only reduced the total PFAS concentrations by ~ 45 % and ~ 42 %, respectively. A more substantial PFAS sorption would likely require higher doses than 10 % (soil dw) of these sorbents. Hypothesis (iii) was partially verified as 5 % (soil dw) bonemeal reduced the total PFAS concentration by ~ 80 %, while 5 % (soil dw) chitosan only caused a ~ 37 % reduction. These two organic sorbents thus possess very different sorption abilities.

Whether the calcium content contribute to explaining the PFAS binding to the sorbents, as suggested in hypothesis (iv), could not be fully determined. While a model with leached Ca concentration and EC as explanatory variables could explain 73 % of the variance in leached PFOS concentration, the high correlation between Ca and EC caused issues for the model's validity. A strong negative association was still identified between the leached concentrations of Ca and PFOS, in line with the expectation that Ca can enhance sorption of anionic PFASs.

This study shows that activated biochar was indeed the best sorbent among the tested materials, although bonemeal also showed great potential for sorbing long-chain PFASs. With its limited resistance to biodegradation, bonemeal is potentially more fit for other sorption technologies (like water filtering). While the remaining sorbents possessed inadequate PFAS sorption abilities, waste-based materials generally have many advantages as sorbents. The materials are often more economic and readily available in larger quantities compared to commercial sorbents. The sorption properties can also be enhanced through modification, which is an area that has a large potential for further studies. Since waste materials represent a potentially imminent remediation option for PFAS contamination, future research should focus on further investigating and improving such materials. Such efforts can eventually lead to the development of sustainable remediation options in line with a shift towards circular economy.

8 Literature

Agrafioti, E., Kalderis, D. & Diamadopoulos, E. (2014). Arsenic and chromium removal from water using biochars derived from rice husk, organic solid wastes and sewage sludge. *Journal of Environmental Management*, 133: 309-314. doi: https://doi.org/10.1016/j.jenvman.2013.12.007.

Ahmed, M. B., Johir, M. A. H., McLaughlan, R., Nguyen, L. N., Xu, B. & Nghiem, L. D. (2020). Per- and polyfluoroalkyl substances in soil and sediments: Occurrence, fate, remediation and future outlook. *Science of The Total Environment*, 748: 141251. doi: https://doi.org/10.1016/j.scitotenv.2020.141251.

Ahrens, L. H. (2010). *Determination of perfluoroalkyl compounds in water, sediment, and biota*. ICES techniques in marine environmental sciences (trykt utg.), vol. no. 48. Copenhagen: International Council for the Exploration of the Sea.

Ateia, M., Maroli, A., Tharayil, N. & Karanfil, T. (2019). The overlooked short- and ultrashort-chain poly- and perfluorinated substances: A review. *Chemosphere*, 220: 866-882. doi: https://doi.org/10.1016/j.chemosphere.2018.12.186.

Banzhaf, S., Filipovic, M., Lewis, J., Sparrenbom, C. J. & Barthel, R. (2017). A review of contamination of surface-, ground-, and drinking water in Sweden by perfluoroalkyl and polyfluoroalkyl substances (PFASs). *Ambio*, 46 (3): 335-346. doi: 10.1007/s13280-016-0848-8.

Beesley, L. & Marmiroli, M. (2011). The immobilisation and retention of soluble arsenic, cadmium and zinc by biochar. *Environmental Pollution*, 159 (2): 474-480. doi: https://doi.org/10.1016/j.envpol.2010.10.016.

Bjørnå, F. (2021). *Beinmel*. snl.no: Store Norske Leksikon. Available at: https://snl.no/beinmel (accessed: 16.06.2021).

Bojko, O. & Kabala, C. (2014). Loss-On-Ignition as an estimate of Total Organic Carbon in the mountain soils. *Polish Journal of Soil Science*, 47: 71-79.

Bolan, N., Sarkar, B., Yan, Y., Li, Q., Wijesekara, H., Kannan, K., Tsang, D. C. W., Schauerte, M., Bosch, J., Noll, H., et al. (2021). Remediation of poly- and perfluoroalkyl substances (PFAS) contaminated soils – To mobilize or to immobilize or to degrade? *Journal of Hazardous Materials*, 401: 123892. doi: https://doi.org/10.1016/j.jhazmat.2020.123892.

Broomandi, P., Guney, M., Kim, J. R. & Karaca, F. (2020). Soil Contamination in Areas Impacted by Military Activities: A Critical Review. *Sustainability*, 12 (21). doi: 10.3390/su12219002.

Buck, R. C., Franklin, J., Berger, U., Conder, J. M., Cousins, I. T., de Voogt, P., Jensen, A. A., Kannan, K., Mabury, S. A. & van Leeuwen, S. P. J. (2011). Perfluoroalkyl and polyfluoroalkyl substances in the environment: Terminology, classification, and origins. *Integrated Environmental Assessment and Management*, 7 (4): 513-541. doi: https://doi.org/10.1002/ieam.258.

Bye, R. (2019). *Viktige momenter ved dekomponering av prøvematerialer i analytisk kjemi*. Norges miljø- og biovitenskapelige universitet (NMBU).

Campos-Pereira, H., Ullberg, M., Kleja, D. B., Gustafsson, J. P. & Ahrens, L. (2018). Sorption of perfluoroalkyl substances (PFASs) to an organic soil horizon – Effect of cation composition and pH. *Chemosphere*, 207: 183-191. doi: https://doi.org/10.1016/j.chemosphere.2018.05.012.

Campos-Pereira, H., Kleja, D. B., Sjöstedt, C., Ahrens, L., Klysubun, W. & Gustafsson, J. P. (2020). The Adsorption of Per- and Polyfluoroalkyl Substances (PFASs) onto Ferrihydrite Is Governed by Surface Charge. *Environmental Science & Technology*, 54 (24): 15722-15730. doi: 10.1021/acs.est.0c01646.

Cappelen, P., Jartun, M., Reiten, S., Alling, V., Preus-Olsen, G. & Hartnik, T. (2016). *PFAS-forurensning i grunnen – Oppsummeringsrapport fra workshop 26. november 2015*.

Chen, H., Zhang, C., Yu, Y. & Han, J. (2012). Sorption of perfluorooctane sulfonate (PFOS) on marine sediments. *Mar Pollut Bull*, 64 (5): 902-906. doi: 10.1016/j.marpolbul.2012.03.012.

China National Analysis Center for Iron and Steel. (2004). *Certificate of Certified Reference Materials. NCS DC 73319–NCS DC 73326*. Beijing, China.

Conder, J. M., Hoke, R. A., Wolf, W. d., Russell, M. H. & Buck, R. C. (2008). Are PFCAs Bioaccumulative? A Critical Review and Comparison with Regulatory Criteria and Persistent Lipophilic Compounds. *Environmental Science & Technology*, 42 (4): 995-1003. doi: 10.1021/es070895g.

Cousins, I. T., DeWitt, J. C., Glüge, J., Goldenman, G., Herzke, D., Lohmann, R., Miller, M., Ng, C. A., Scheringer, M., Vierke, L., et al. (2020). Strategies for grouping per- and polyfluoroalkyl substances (PFAS) to protect human and environmental health. *Environmental Science: Processes & Impacts*, 22 (7): 1444-1460. doi: 10.1039/D0EM00147C.

Darlington, R., Barth, E. & McKernan, J. (2018). The Challenges of PFAS Remediation. *The Military engineer*, 110 (712): 58-60.

Davis, S. P. (2011). *Chitosan : manufacture, properties, and usage*. Hauppauge, N.Y.: Nova Science Publishers.

DelVecchia, A. G., Bruno, J. F., Benninger, L., Alperin, M., Banerjee, O. & de Dios Morales, J. (2014). Organic carbon inventories in natural and restored Ecuadorian mangrove forests. *PeerJ*, 2: e388. doi: 10.7717/peerj.388.

Deng, S., Zhang, Q., Nie, Y., Wei, H., Wang, B., Huang, J., Yu, G. & Xing, B. (2012). Sorption mechanisms of perfluorinated compounds on carbon nanotubes. *Environmental Pollution*, 168: 138-144. doi: https://doi.org/10.1016/j.envpol.2012.03.048.

Du, Z., Deng, S., Bei, Y., Huang, Q., Wang, B., Huang, J. & Yu, G. (2014). Adsorption behavior and mechanism of perfluorinated compounds on various adsorbents—A review. *Journal of Hazardous Materials*, 274: 443-454. doi: https://doi.org/10.1016/j.jhazmat.2014.04.038.

EN 12457-2. (2003). *Characterisation of waste - Leaching - Compliance test for leaching of granular waste materials and sludges - Part 2: One stage batch test at a liquid to solid ratio of 10 l/kg for materials with particle size below 4 mm (without or with size reduction)*. Brussels, Belgium: European Committee for Standardization.

European Commission. (2020a). *Commission Staff Working Document: Poly- and perfluoroalkyl substances (PFAS) (SWD/2020/249 final)*. EUR-Lex: Publications Office of the European Union. Available at: https://eur-lex.europa.eu/legal-content/EN/TXT/?uri=CELEX%3A52020SC0249&qid=1627373018359 (accessed: 26.07.2021).

European Commission. (2020b). *DIRECTIVE (EU) 2020/2184 OF THE EUROPEAN PARLIAMENT AND OF THE COUNCIL of 16 December 2020 on the quality of water intended for human consumption (recast) (Text with EEA relevance)*.

Farrance, I. & Frenkel, R. (2012). Uncertainty of Measurement: A Review of the Rules for Calculating Uncertainty Components through Functional Relationships. *The Clinical biochemist. Reviews*, 33 (2): 49-75.

Ferrey, M. L., Wilson, J. T., Adair, C., Su, C., Fine, D. D., Liu, X. & Washington, J. W. (2012). Behavior and Fate of PFOA and PFOS in Sandy Aquifer Sediment. *Groundwater Monit R*, 32 (4): 63-71. doi: 10.1111/j.1745-6592.2012.01395.x.

Filipovic, M., Woldegiorgis, A., Norström, K., Bibi, M., Lindberg, M. & Österås, A.-H. (2015). Historical usage of aqueous film forming foam: A case study of the widespread distribution of perfluoroalkyl acids from a military airport to groundwater, lakes, soils and fish. *Chemosphere*, 129: 39-45. doi: https://doi.org/10.1016/j.chemosphere.2014.09.005.

Frangipane, G., Pistolato, M., Molinaroli, E., Guerzoni, S. & Tagliapietra, D. (2009). Comparison of loss on ignition and thermal analysis stepwise methods for determination of sedimentary organic matter. *Aquatic Conserv: Mar. Freshw. Ecosyst*, 19 (1): 24-33. doi: 10.1002/aqc.970.

Friedman, L. & Wall, M. (2005). Graphical Views of Suppression and Multicollinearity in Multiple Linear Regression. *The American statistician*, 59 (2): 127-136. doi: 10.1198/000313005X41337.

Gagliano, E., Sgroi, M., Falciglia, P. P., Vagliasindi, F. G. A. & Roccaro, P. (2020). Removal of poly- and perfluoroalkyl substances (PFAS) from water by adsorption: Role of PFAS chain length, effect of organic matter and challenges in adsorbent regeneration. *Water Research*, 171: 115381. doi: https://doi.org/10.1016/j.watres.2019.115381.

Glüge, J., Scheringer, M., Cousins, I. T., DeWitt, J. C., Goldenman, G., Herzke, D., Lohmann, R., Ng, C. A., Trier, X. & Wang, Z. (2020). An overview of the uses of per- and polyfluoroalkyl substances (PFAS). *Environmental Science: Processes & Impacts*, 22 (12): 2345-2373. doi: 10.1039/D0EM00291G.

Greve, M. H., Sperstad, R. & Nyborg, Å. (1999). *Retningslinjer for beskrivelse av jordprofil : versjon 1.0*. NIJOS-rapport (trykt utg.), vol. 37/99. Ås: Norsk institutt for jord- og skogkartlegging.

Hagemann, N., Spokas, K., Schmidt, H.-P., Kägi, R., Böhler, M. A. & Bucheli, T. D. (2018). Activated Carbon, Biochar and Charcoal: Linkages and Synergies across Pyrogenic Carbon's ABCs. *Water*, 10 (2). doi: 10.3390/w10020182.

Hagemann, N., Schmidt, H.-P., Kägi, R., Böhler, M., Sigmund, G., Maccagnan, A., McArdell, C. S. & Bucheli, T. D. (2020). Wood-based activated biochar to eliminate organic micropollutants from biologically treated wastewater. *Science of The Total Environment*, 730: 138417. doi: https://doi.org/10.1016/j.scitotenv.2020.138417.

Hale, S. E., Arp, H. P. H., Slinde, G. A., Wade, E. J., Bjørseth, K., Breedveld, G. D., Straith, B. F., Moe, K. G., Jartun, M. & Høisæter, Å. (2017). Sorbent amendment as a remediation strategy to reduce PFAS mobility and leaching in a contaminated sandy soil from a Norwegian firefighting training facility. *Chemosphere*, 171: 9-18. doi: 10.1016/j.chemosphere.2016.12.057.

Hansen, H. J. & Danielsberg, A. (2009). *Tilstandsklasser for forurenset grunn (TA-2553/2009) [Classification of condition for contaminated sites]*: Norwegian Pollution Control Authority.

Harstad, O. M. (2021). *Kjøttbeinmel*. snl.no: Store Norske Leksikon. Available at: https://snl.no/kj%C3%B8ttbeinmel (accessed: 16.08.2021).

Hayes, M. (2020). Measuring Protein Content in Food: An Overview of Methods. *Foods (Basel, Switzerland)*, 9 (10): 1340. doi: 10.3390/foods9101340.

HEPA. (2018). *PFAS National Environmental Management Plan*: Heads of EPAs Australia and New Zealand (HEPA).

Higgins, C. P. & Luthy, R. G. (2006). Sorption of Perfluorinated Surfactants on Sediments. *Environmental Science & Technology*, 40 (23): 7251-7256. doi: 10.1021/es061000n.

Hofstad, K. (2020). *Biokull*. snl.no: Sto. Available at: https://snl.no/biokull (accessed: 06.09.2021).

Houtz, E. F. & Sedlak, D. L. (2012). Oxidative Conversion as a Means of Detecting Precursors to Perfluoroalkyl Acids in Urban Runoff. *Environmental Science & Technology*, 46 (17): 9342-9349. doi: 10.1021/es302274g.

Høisæter, Å., Pfaff, A. & Breedveld, G. D. (2019). Leaching and transport of PFAS from aqueous film-forming foam (AFFF) in the unsaturated soil at a firefighting training facility under cold climatic conditions. *Journal of Contaminant Hydrology*, 222: 112-122. doi: https://doi.org/10.1016/j.jconhyd.2019.02.010.

Jacobsen, E. (2021). *Konduktometri*. snl.no: Store Norske Leksikon. Available at: https://snl.no/konduktometri (accessed: 22.11.2021).

Johnsen, J. P. (2018). *Rekefiske*. snl.no: Store Norske Leksikon. Available at: https://snl.no/rekefiske (accessed: 16.08.2021).

Joseph, B., Kaetzl, K., Hensgen, F., Schäfer, B. & Wachendorf, M. (2020). Sustainability assessment of activated carbon from residual biomass used for micropollutant removal at a full-scale wastewater treatment plant. *Environ. Res. Lett*, 15 (6): 64023. doi: 10.1088/1748-9326/ab8330.

Kah, M., Oliver, D. & Kookana, R. (2021). Sequestration and potential release of PFAS from spent engineered sorbents. *Sci Total Environ*, 765: 142770-142770. doi: 10.1016/j.scitotenv.2020.142770.

Knutsen, H., Mæhlum, T., Haarstad, K., Slinde, G. A. & Arp, H. P. (2019). Leachate emissions of short- and long-chain perand polyfluoralkyl substances (PFASs) from various Norwegian landfills.

Krogstad, T., Børresen, T. & Almås, Å. R. (2018). *Field and laboratory methods for the analysis of soil*. Norwegian University of Life Sciences, Ås, Norway: Faculty of Environmental Sciences and Natural Resource Management.

Król, A. & Mizerna, K. (2016). Directions of development of research methods in the assessment of leaching of heavy metals from mineral waste. *E3S web of conferences*, 10: 50. doi: 10.1051/e3sconf/20161000050.

Kupryianchyk, D., Hale, S., Breedveld, G. & Cornelissen, G. (2015). Treatment of sites contaminated with perfluorinated compounds using biochar amendment. *Chemosphere*, 142. doi: 10.1016/j.chemosphere.2015.04.085.

Li, F., Fang, X., Zhou, Z., Liao, X., Zou, J., Yuan, B. & Sun, W. (2019). Adsorption of perfluorinated acids onto soils: Kinetics, isotherms, and influences of soil properties. *Science of The Total Environment*, 649: 504-514. doi: https://doi.org/10.1016/j.scitotenv.2018.08.209.

Li, F., Duan, J., Tian, S., Ji, H., Zhu, Y., Wei, Z. & Zhao, D. (2020). Short-chain per- and polyfluoroalkyl substances in aquatic systems: Occurrence, impacts and treatment. *Chemical Engineering Journal*, 380: 122506. doi: https://doi.org/10.1016/j.cej.2019.122506.

Li, H., Dong, X., da Silva, E. B., de Oliveira, L. M., Chen, Y. & Ma, L. Q. (2017). Mechanisms of metal sorption by biochars: Biochar characteristics and modifications. *Chemosphere*, 178: 466-478. doi: https://doi.org/10.1016/j.chemosphere.2017.03.072.

Li, W., Hu, Y. & Bischel, H. N. (2021). In-Vitro and In-Silico Assessment of Per- and Polyfluoroalkyl Substances (PFAS) in Aqueous Film-Forming Foam (AFFF) Binding to Human Serum Albumin. *Toxics*, 9 (3): 63. doi: 10.3390/toxics9030063.

Li, Y.-M. & Zhang, F.-S. (2014). Characterization of a cetyltrimethyl ammonium bromide-modified sorbent for removal of perfluorooctane sulphonate from water. *Environ Technol*, 35 (20): 2556-2568. doi: 10.1080/09593330.2014.912253.

Liu, Y., Qi, F., Fang, C., Naidu, R., Duan, L., Dharmarajan, R. & Annamalai, P. (2020). The effects of soil properties and co-contaminants on sorption of perfluorooctane sulfonate (PFOS) in contrasting soils. *Environmental Technology & Innovation*, 19: 100965. doi: https://doi.org/10.1016/j.eti.2020.100965.

Lindstrom, A. B., Strynar, M. J. & Libelo, E. L. (2011). Polyfluorinated Compounds: Past, Present, and Future. *Environmental Science & Technology*, 45 (19): 7954-7961. doi: 10.1021/es2011622.

Mahinroosta, R. & Senevirathna, L. (2020). A review of the emerging treatment technologies for PFAS contaminated soils. *J Environ Manage*, 255: 109896-109896. doi: 10.1016/j.jenvman.2019.109896.

Manum, S. B., Eide, C. H. & Rosvold, K. A. (2020). *Kull*. snl.no: Store Norske Leksikon. Available at: https://snl.no/kull (accessed: 17.11.2021).

Milinovic, J., Lacorte, S., Vidal, M. & Rigol, A. (2015). Sorption behaviour of perfluoroalkyl substances in soils. *Science of The Total Environment*, 511: 63-71. doi: https://doi.org/10.1016/j.scitotenv.2014.12.017.

Munoz, G., Budzinski, H. l. n. & Labadie, P. (2017). Influence of Environmental Factors on the Fate of Legacy and Emerging Per- and Polyfluoroalkyl Substances along the Salinity/Turbidity Gradient of a Macrotidal Estuary. *Environ. Sci. Technol*, 51 (21): 12347-12357. doi: 10.1021/acs.est.7b03626.

Müller, E. I., Mesko, M. F., Moraes, D. P., Korn, M. d. G. A. & Flores, É. M. M. (2014). Chapter 4 - Wet Digestion Using Microwave Heating. In Flores, É. M. d. M. (ed.) *Microwave-Assisted Sample Preparation for Trace Element Analysis*, pp. 99-142. Amsterdam: Elsevier.

Nguyen, T. M. H., Bräunig, J., Thompson, K., Thompson, J., Kabiri, S., Navarro, D. A., Kookana, R. S., Grimison, C., Barnes, C. M., Higgins, C. P., et al. (2020). Influences of Chemical Properties, Soil Properties, and Solution pH on Soil–Water Partitioning Coefficients of Per- and Polyfluoroalkyl Substances (PFASs). *Environmental Science & Technology*, 54 (24): 15883-15892. doi: 10.1021/acs.est.0c05705.

Nickerson, A., Maizel, A. C., Kulkarni, P. R., Adamson, D. T., Kornuc, J. J. & Higgins, C. P. (2020). Enhanced Extraction of AFFF-Associated PFASs from Source Zone Soils. *Environmental Science & Technology*, 54 (8): 4952-4962. doi: 10.1021/acs.est.0c00792.

Nilsen, H. R. (2021). *Sirkulær økonomi*. snl.no: Store norske leksikon. Available at: https://snl.no/sirkul%C3%A6r_%C3%B8konomi (accessed: 16.08.2021).

NIST. (2009a). *Certificate of Analyses. Standard Reference Material 2709a. San Joaquin Soil.*: National Institute of Standards & Technology.

NIST. (2009b). *Cetrificate of Analysis. Standard Reference Material 2710a. Montana I Soil.*: National Institute of Standards & Technology.

Norconsult. (2019). *Reporting for Part 1 and Part 2 of the Norwegian Environment Agency's orders: "Overall assessment of PFAS contamination at Avinor's airports"*. Avinor.no: Avinor. Available at: https://avinor.no/globalassets/_konsern/miljo-og-samfunn/pfos/rapporter/reporting-for-part-1-and-part-2_overall-assessment_including-appendices.pdf (accessed: 25.08.2021).

Norsk Protein. (n.d.). *Kjøttbeinmjøl. Organisk gjødsel og jordforbedringsmidler.* Hamar, Norway: Norsk Protein AS.

Norwegian Environment Agency. (2020). *Grenseverdier for klassifisering av vann, sediment og biota – revidert 30.10.2020 [Quality standards for water, sediment and biota – revised 2020.10.30]*. M-608: The Norwegian Environment Agency (Miljødirektoratet).

Norwegian Geotechnical Institute. (2020). *Proposal for new Normative Values for PFOS and PFOA in contaminated soil*

Norwegian Climate and Pollution Agency. (2004). *Forskrift om begrensning av forurensning (forurensningsforskriften): Del 1. Forurenset grunn og sedimenter*. Lovdata. Available at: https://lovdata.no/dokument/SF/forskrift/2004-06-01-931/KAPITTEL_1#KAPITTEL_1 (accessed: 22.10.2021).

Okkenhaug, G., Almås, Å., Morin, N., Hale, S. & Arp, H. P. (2015). The Presence and Leachability of Antimony in different Wastes and Waste Handling Facilities in Norway. *Environ. Sci.: Processes Impacts*, 17. doi: 10.1039/C5EM00210A.

Oliver, D., Li, Y., Orr, R., Nelson, P., Barnes, M., McLaughlin, M. & Kookana, R. (2019). The role of surface charge and pH changes in tropical soils on sorption behaviour of per- and polyfluoroalkyl substances (PFASs). *Science of The Total Environment*, 673. doi: 10.1016/j.scitotenv.2019.04.055.

Pedersen, B. (2021). *Arsen [Arsenic]*. snl.no: Store Norske Leksikon. Available at: https://snl.no/arsen (accessed: 10.12.2021).

Pivarčiová, L., Rosskopfova, O., Galamboš, M. & Rajec, P. (2014). Sorption of nickel on chitosan. *Journal of Radioanalytical and Nuclear Chemistry*, 300. doi: 10.1007/s10967-014-3007-3.

Rasweefali, M. K., Sabu, S., Sunooj, K. V., Sasidharan, A. & Xavier, K. A. M. (2021). Consequences of chemical deacetylation on physicochemical, structural and functional characteristics of chitosan extracted from deep-sea mud shrimp. *Carbohydrate Polymer Technologies and Applications*, 2: 100032. doi: https://doi.org/10.1016/j.carpta.2020.100032.

Ross, I., McDonough, J., Miles, J., Storch, P., Thelakkat Kochunarayanan, P., Kalve, E., Hurst, J., S. Dasgupta, S. & Burdick, J. (2018). A review of emerging technologies for remediation of PFASs. *Remediation Journal*, 28 (2): 101-126. doi: https://doi.org/10.1002/rem.21553.

Rygalska, M. (2019). *Coulter LS 13320 med Aqueous Liquid Module (ALM)*. Ås: Norwegian University of Life Sciences (NMBU).

Santisteban, J. I., Mediavilla, R., López-Pamo, E., Dabrio, C. J., Zapata, M. B. R., García, M. J. G., Castaño, S. & Martínez-Alfaro, P. E. (2004). Loss on ignition: a qualitative or quantitative method for organic matter and carbonate mineral content in sediments? *Journal of paleolimnology*, 32 (3): 287-299. doi: 10.1023/B:JOPL.0000042999.30131.5b.

SAS Institute. (2021). *JMP® Trial, version 16.1.0*. Cary, NC, USA: SAS Institute Inc.

Sheng, N., Li, J., Liu, H., Zhang, A. & Dai, J. (2014). Interaction of perfluoroalkyl acids with human liver fatty acid-binding protein. *Archives of toxicology*, 90. doi: 10.1007/s00204-014-1391-7.

Silvani, L., Cornelissen, G., Botnen Smebye, A., Zhang, Y., Okkenhaug, G., Zimmerman, A. R., Thune, G., Sævarsson, H. & Hale, S. E. (2019). Can biochar and designer biochar be used to remediate per- and polyfluorinated alkyl substances (PFAS) and lead and antimony contaminated soils? *Science of The Total Environment*, 694: 133693. doi: https://doi.org/10.1016/j.scitotenv.2019.133693.

Statistics Norway. (2021). *Avfallsregnskapet*. Available at: https://www.ssb.no/natur-og-miljo/avfall/statistikk/avfallsregnskapet (accessed: 04.08.2021).

Sunderland, E. M., Hu, X. C., Dassuncao, C., Tokranov, A. K., Wagner, C. C. & Allen, J. G. (2019). A review of the pathways of human exposure to poly- and perfluoroalkyl substances (PFASs) and present understanding of health effects. *Journal of Exposure Science & Environmental Epidemiology*, 29 (2): 131-147. doi: 10.1038/s41370-018-0094-1.

Sævarsson, H. T., Høiseter, Å., Thune, G. E., Smebye, A. B. & Okkenhaug, G. (2018, September). *Immobilization of PFAS contaminated sandy soil from a Norwegian firefighting training facility*. NORDROCS 2018 - crossing borders, Helsingör, Denmark, pp. 146-150.

Sörengård, M., Kleja, D. B. & Ahrens, L. (2019). Stabilization and solidification remediation of soil contaminated with poly- and perfluoroalkyl substances (PFASs). *Journal of Hazardous Materials*, 367: 639-646. doi: https://doi.org/10.1016/j.jhazmat.2019.01.005.

Sörengård, M., Östblom, E., Köhler, S. & Ahrens, L. (2020). Adsorption behavior of per- and polyfluoralkyl substances (PFASs) to 44 inorganic and organic sorbents and use of dyes as proxies for PFAS sorption. *Journal of Environmental Chemical Engineering*, 8 (3): 103744. doi: https://doi.org/10.1016/j.jece.2020.103744.

Sørmo, E., Silvani, L., Bjerkli, N., Hagemann, N., Zimmerman, A. R., Hale, S. E., Hansen, C. B., Hartnik, T. & Cornelissen, G. (2021). Stabilization of PFAS-contaminated soil with activated biochar. *Science of The Total Environment*, 763: 144034. doi: https://doi.org/10.1016/j.scitotenv.2020.144034.

Tan, K. H. (2011). *Principles of soil chemistry*. 4th ed. ed. Books in soils, plants, and the environment. Boca Raton, Fla: CRC Press.

Tang, J., Zhang, Y., Zha, Y., Li, X. & Fan, S. (2017). Oxalate Enhances Desorption of Perfluorooctane Sulfonate from Soils and Sediments. *Water, Air, & Soil Pollution*, 228 (12): 462. doi: 10.1007/s11270-017-3626-8.

Townsend, T., Jang, Y.-C. & Tolaymat, T. (2003). A Guide to the Use of Leaching Tests in Solid Waste Management Decision Making.

Turner, B. D., Sloan, S. W. & Currell, G. R. (2019). Novel remediation of per- and polyfluoroalkyl substances (PFASs) from contaminated groundwater using Cannabis Sativa L. (hemp) protein powder. *Chemosphere*, 229: 22-31. doi: https://doi.org/10.1016/j.chemosphere.2019.04.139.

U.S. EPA (United States Environmental Protection Agency). (2018). *Technical Fact Sheet: Draft Toxicity Assessments for GenX Chemicals and PFBS*. Available at: https://www.epa.gov/sites/default/files/2018-12/documents/tech_fact_sheet_genx_pfbs_draft_tox_assess_final_508.pdf (accessed: 29.08.2021).

U.S. EPA (United States Environmental Protection Agency). (2020). *PFAS Master List of PFAS Substances (Version 2)*. CompTox Chemicals Dashboard. Available at: https://comptox.epa.gov/dashboard/chemical_lists/pfasmaster (accessed: 13.04.2021).

UNEP. (2019). *The new POPs under the Stockholm Convention*. Available at: http://chm.pops.int/TheConvention/ThePOPs/TheNewPOPs/tabid/2511/Default.aspx (accessed: 25.08.2021).

van Hees, P. (2017). *Analysis of the unknown pool of PFAS: Total Oxidizable Precursors (TOP), PFOS Precursor (PreFOS) and Telomer Degradation*. Eurofins.

Veres, D. (2002). A Comparative Study Between Loss on Ignition and Total Carbon Analysis on Mineralogenic Sediments. *Studia Universitatis Babes-Bolyai, Geologia*, 47: 171-182. doi: 10.5038/1937-8602.47.1.13.

Vierke, L., Berger, U. & Cousins, I. T. (2013). Estimation of the Acid Dissociation Constant of Perfluoroalkyl Carboxylic Acids through an Experimental Investigation of their Water-to-Air Transport. *Environmental Science & Technology*, 47 (19): 11032-11039. doi: 10.1021/es402691z.

Wang, F. & Shih, K. (2011). Adsorption of perfluorooctanesulfonate (PFOS) and perfluorooctanoate (PFOA) on alumina: Influence of solution pH and cations. *Water Research*, 45 (9): 2925-2930. doi: https://doi.org/10.1016/j.watres.2011.03.007.

Wei, C., Song, X., Wang, Q. & Hu, Z. (2017). Sorption kinetics, isotherms and mechanisms of PFOS on soils with different physicochemical properties. *Ecotoxicology and Environmental Safety*, 142: 40-50. doi: https://doi.org/10.1016/j.ecoenv.2017.03.040.

Weil, R. R. & Brady, N. C. (2017). Glossary of Soil Science Terms. In *The Nature and Properties of Soils*, pp. 1057-1071. Harlow: Pearson.

Weißpflog, J., Boldt, R., Kohn, B., Scheler, U., Jehnichen, D., Tyrpekl, V. & Schwarz, S. (2020). Investigation of mechanisms for simultaneous adsorption of iron and sulfate ions onto chitosan with formation of orthorhombic structures. *Colloids and Surfaces A: Physicochemical and Engineering Aspects*, 592: 124575. doi: https://doi.org/10.1016/j.colsurfa.2020.124575.

Xiao, X., Ulrich, B. A., Chen, B. & Higgins, C. P. (2017). Sorption of Poly- and Perfluoroalkyl Substances (PFASs) Relevant to Aqueous Film-Forming Foam (AFFF)-Impacted Groundwater by Biochars and Activated Carbon. *Environmental Science & Technology*, 51 (11): 6342-6351. doi: 10.1021/acs.est.7b00970.

Ye, J.-R., Chen, L., Zhang, Y., Zhang, Q. & Shen, Q. (2014). Turning the chitosan surface from hydrophilic to hydrophobic by layer-by-layer electro-assembly. *RSC Advances*, 4: 58200-58203. doi: 10.1039/c4ra10327k.

Zareitalabad, P., Siemens, J., Hamer, M. & Amelung, W. (2013). Perfluorooctanoic acid (PFOA) and perfluorooctanesulfonic acid (PFOS) in surface waters, sediments, soils and wastewater - A review on concentrations and distribution coefficients. *Chemosphere*, 91 (6): 725-32. doi: 10.1016/j.chemosphere.2013.02.024.

Zhang, Q., Deng, S., Yu, G. & Huang, J. (2011). Removal of perfluorooctane sulfonate from aqueous solution by crosslinked chitosan beads: Sorption kinetics and uptake mechanism. *Bioresource Technology*, 102 (3): 2265-2271. doi: https://doi.org/10.1016/j.biortech.2010.10.040.

Zhao, L., Zhu, L., Yang, L., Liu, Z. & Zhang, Y. (2012). Distribution and desorption of perfluorinated compounds in fractionated sediments. *Chemosphere*, 88 (11): 1390-1397. doi: https://doi.org/10.1016/j.chemosphere.2012.05.062.

Zhao, L., Zhang, Y., Fang, S., Zhu, L. & Liu, Z. (2014). Comparative sorption and desorption behaviors of PFHxS and PFOS on sequentially extracted humic substances. *Journal of Environmental Sciences*, 26 (12): 2517-2525. doi: https://doi.org/10.1016/j.jes.2014.04.009.

Zhi, Y. & Liu, J. (2018). Sorption and desorption of anionic, cationic and zwitterionic polyfluoroalkyl substances by soil organic matter and pyrogenic carbonaceous materials. *Chemical Engineering Journal*, 346: 682-691. doi: https://doi.org/10.1016/j.cej.2018.04.042.

Zimmerman, A. & Gao, B. (2013). The Stability of Biochar in the Environment. In, pp. 1-40.

Zushi, Y., Hogarh, J. N. & Masunaga, S. (2012). Progress and perspective of perfluorinated compound risk assessment and management in various countries and institutes. *Clean Technologies and Environmental Policy*, 14 (1): 9-20. doi: 10.1007/s10098-011-0375-z.

Appendices

Appendix A Formulas for dry matter (DM) and loss on ignition (LOI)

To calculate the dry matter (DM) content of a soil, a sample of it must be weighed in a crucible before and after being dried at 105 ± 5 °C for at least 6 hours. The DM in percent is then calculated as

$$\% \, DM = \frac{\left(m_{dry_{tot}} - m_{crucible}\right)}{m_{undried}} * 100 \quad \text{(A1)}$$

where m_{dry_tot} is the weight of the crucible with the sample after drying, $m_{crucible}$ is the crucible weight and $m_{undried}$ is the weight of the undried sample.

Following calcination (at least 3 hours at 550 ± 25 °C), the loss on ignition (LOI) in percent is calculated as

$$\% \, LOI = \frac{\left(m_{dry_{tot}} - m_{calcinated_{tot}}\right)}{\left(m_{dry_{tot}} - m_{crucible}\right)} * 100 \quad \text{(A2)}$$

where m_{dry_tot} is the weight of the crucible with sample after drying, $m_{calcinated\_tot}$ is the weight of crucible and sample after calcination and $m_{crucible}$ is the crucible weight (Krogstad et al., 2018).

Appendix B Metal normative values and quality standards

The Norwegian normative values for heavy metals in soil are given in Table B1, while quality standards (limit values) for metals in fresh water are given in Table B2.

Table B1. Normative values for heavy metals in soil (Norwegian Climate and Pollution Agency, 2004).

Class	Normative value (mg/kg)
Arsenic (As)	8
Cadmium (Cd)	1.5
Copper (Cu)	100
Lead (Pb)	60
Nickel (Ni)	60
Chromium (Cr)	50 (tot)
Zinc (Zn)	200

Table B2. Quality standards for selected metals (µg/L) in fresh water (Norwegian Environment Agency, 2020).

Class Classification	**Class I Background**	**Class II Good**	**Class III Moderate**	**Class IV Bad**	**Class V Very bad**
Arsenic (As)	0 – 0.15	0.15 – 0.5	0.5 – 8.5	8.5 – 85	> 85
Chromium (Cr)	0 – 0.1	0.1 – 3.4			> 3.4
Copper (Cu)	0 – 0.3	0.3 – 7.8		7.8 – 15.6	> 15.6
Lead (Pb)	0 – 0.02	0.02 – 1.2	1.2 – 14	14 – 57	> 57
Nickel (Ni)	0 – 0.5	0.5 – 4	4 – 34	34 – 67	> 67
Zinc (Zn)	0 – 1.5	1.5 – 11		11 – 60	> 60

Appendix C Test ratios of the industrial wastes with iron (II) sulphate

Both the industrial wastes (slag and filter dust) were rich in metal oxides and strongly alkaline. To keep the pH values near the unamended soil's pH during the batch tests, the sorbents were mixed with iron sulphate ($FeSO_4$), an acidic by-product from the titanium industry. A set of pH tests were performed to find suitable ratios for $FeSO_4$ and the sorbents. The results of mixing slag with $FeSO_4$ are shown in Figure C1, while the results of mixing $FeSO_4$ and filter dust are displayed in Figure C2.

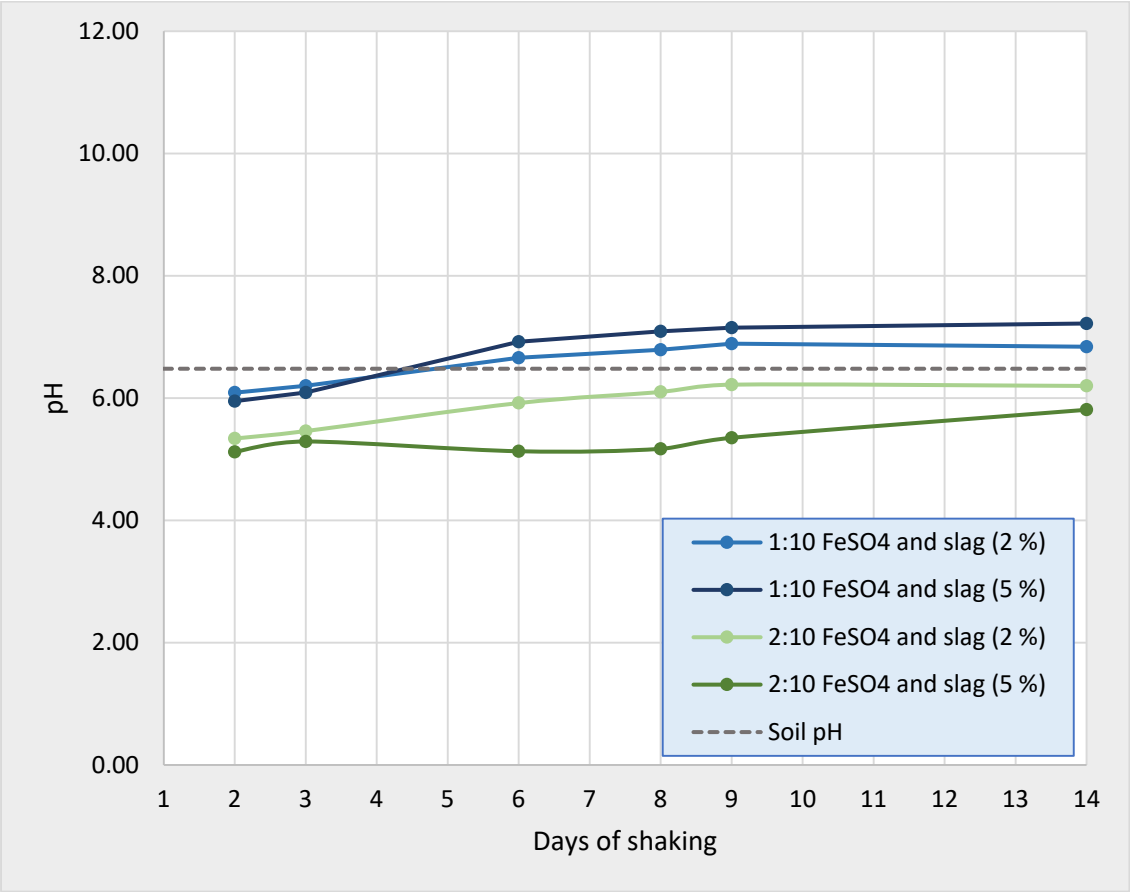

Figure C1. The pH levels of $FeSO_4$ and slag mixed in a 1: 10 ratio and a 2:10 ratio. The different sorbent ratios were added to soil at 2 % (soil dw) and 5 % (soil dw), diluted to an L/S ratio of 10 with deionized water and followed through 14 days of agitation at a tabletop shaker (100 rpm). The soil pH value (dotted line) was based on the pH measurements of batch test control samples.

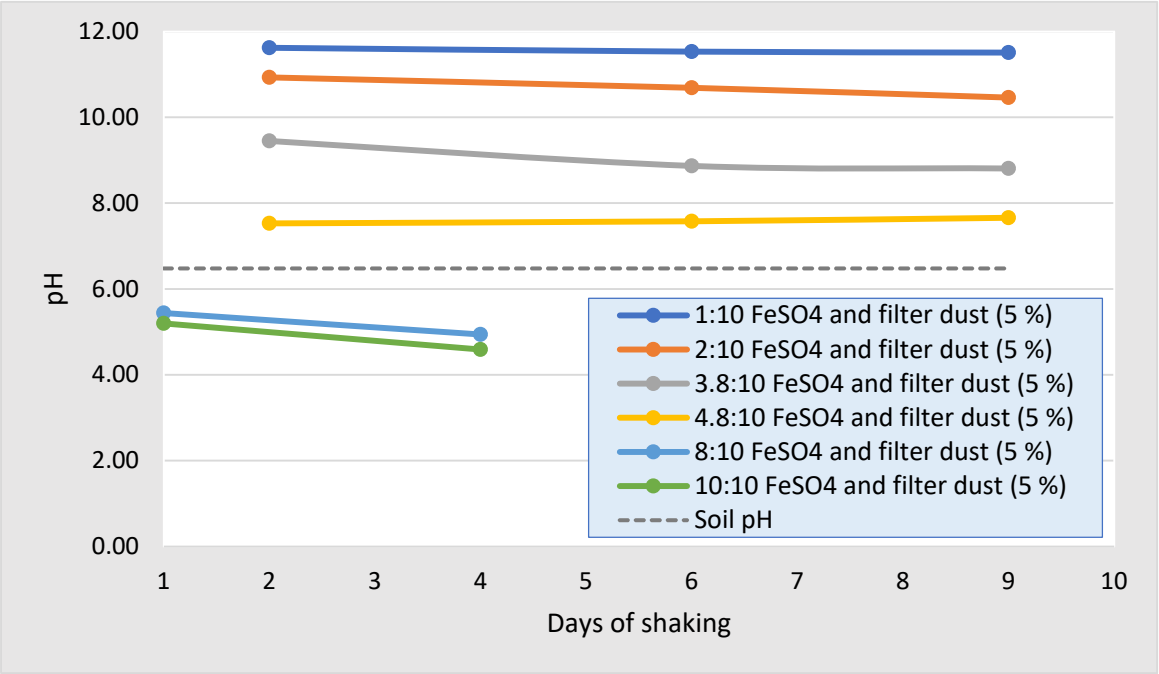

Figure C2. The pH levels of different $FeSO_4$ and filter dust ratios (followed for nine days). All mixes were added to the soil at 5 % (soil dw) and agitated at a tabletop shaker (100 rpm) in L/S ratios of 10 with deionized water. The soil pH value (dotted line) was based on the pH measurements of batch test control samples.

As both the $FeSO_4$-to-filter dust ratios of 4.8:10 and 8:10 were concluded to diverge too much from the soil pH (fig. C2), a ratio of 6:10 was predicted to be a better fit. However, between the $FeSO_4$ and slag ratios of 1:10 and the 2:10 (fig. C1), the latter was preferred as the pH values did not exceed the control sample pH.

Appendix D Limit of detection (LOD) and limit of quantification (LOQ)

The LOD and LOQ values were calculated according to the formulas below:

$$\text{LOD} = 3 * STDEV_{blank} \quad \text{(D1)}$$

$$\text{LOQ} = 10 * STDEV_{blank} \quad \text{(D2)}$$

A description of the standard deviation formula is given in in Appendix E.

Appendix E Standard deviation calculations

The standard deviation is a measure of the variation in a set of values and can be calculated as

$$STDEV = \sqrt{\frac{\sum(x - \bar{x})^2}{(n-1)}} \quad \text{(E1)}$$

where x is a value in the dataset, $\bar{x}$ is the average and n is the sample size.

During the estimations different parameters (for instance K_d), arithmetic calculations (table E1) were used to further estimate the uncertainty of these parameters.

Table E1. Rules for calculating the combined uncertainty of an estimate containing uncorrelated variables (Farrance & Frenkel, 2012). In this table, y is the quantity to be determined, x_n is the value of a given variable n and u is the standard uncertainty.

Type	**Function**	**Standard uncertainty (u)**
Addition	$y = x_1 + x_2$	$u^2(y) = u^2(x_1) + u^2(x_2)$ $u(y) = \sqrt{u^2(y)} = \sqrt{u^2(x_1) + u^2(x_2)}$
Subtraction	$y = x_1 - x_2$	$u^2(y) = u^2(x_1) + u^2(x_2)$ $u(y) = \sqrt{u^2(y)} = \sqrt{u^2(x_1) + u^2(x_2)}$
Multiplication	$y = x_1 * x_2$	$u^2(y) = \left[\frac{u^2(x_1)}{x_1}\right]^2 + \left[\frac{u^2(x_2)}{x_2}\right]^2$ $u(y) = \sqrt{u^2(y)} = \sqrt{\left[\frac{u^2(x_1)}{x_1}\right]^2 + \left[\frac{u^2(x_2)}{x_2}\right]^2}$
Division	$y = \frac{x_1}{x_2}$	$u^2(y) = \left[\frac{u^2(x_1)}{x_1}\right]^2 + \left[\frac{u^2(x_2)}{x_2}\right]^2$ $u(y) = \sqrt{u^2(y)} = \sqrt{\left[\frac{u^2(x_1)}{x_1}\right]^2 + \left[\frac{u^2(x_2)}{x_2}\right]^2}$

Appendix F Cumulative particle size analysis

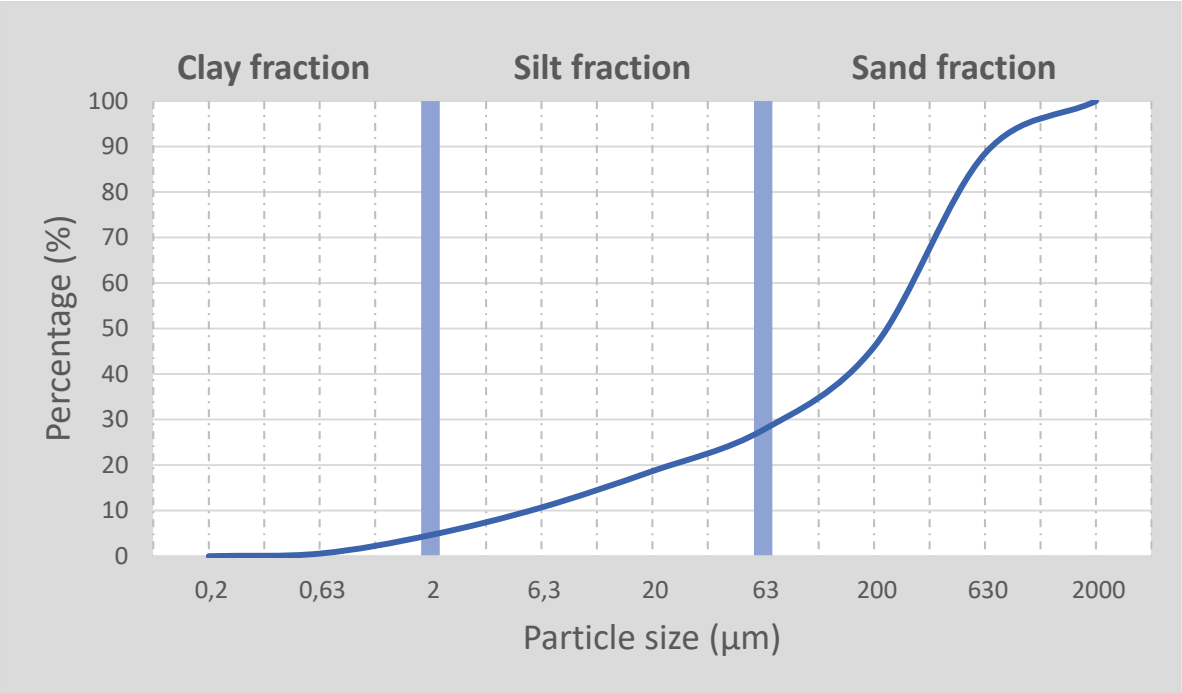

Figure F1. Cumulative particle size analysis curve for (< 2 mm) silty sand (Soil A) gathered at a former fire training facility. The particle size fractions are defined as < 2 µm for clay, 2–63 µm for silt and < 63 µm for sand. The distribution of different soil separates is given as weight percentages.

Appendix G Element analysis of soil

The element concentration in the soil sampled at a former firefighting training site is given in Table G1. Apart from chromium (Cr), which was measured to 56 ± 3.1 mg/kg using HNO_3-digestion, all metals were below the soil normative values defined by (Norwegian Climate and Pollution Agency, 2004). The normative value for Cr (tot) is 50 mg/kg (Appendix B), meaning that the soil's measured Cr concentration still considered "good" based on established soil contamination classifications (Hansen & Danielsberg, 2009).

Table G1. Soil concentrations of Σ16 elements measured by performing ICP-MS on Soil A digested with either HNO_3 or a mix of HF and HNO_3 (referred to as HF-digestion in the table). The standard deviations were estimated from three replicates. Antimony (Sb) could not be quantified following the HNO_3-digestion.

Element	Unit	HNO_3-digestion	HF-digestion
Al	g/kg	29.7 ± 0.58	1.8 ± 0.36
As	mg/kg	3.53 ± 0.058	4.0 ± 0.23
Ca	g/kg	5.4 ± 0.12	4.4 ± 0.15
Cd	mg/kg	0.157 ± 0.21	0.17 ± 0.010
Cr	mg/kg	56 ± 3.1	50 ± 1.2
Cu	mg/kg	15 ± 0	16 ± 1.2
Fe	g/kg	21.3 ± 0.58	17.3 ± 0.58
K	g/kg	6.9 ± 0.26	9.9 ± 0.99
Mg	g/kg	5 ± 0	0.17 ± 0.010
Mn	g/kg	0.29 ± 0.012	0.397 ± 0.0058
Na	g/kg	0.54 ± 0.015	13 ± 1.0
Ni	mg/kg	23 ± 1.0	33 ± 2.5
Pb	mg/kg	10.7 ± 0.58	15.3 ± 0.58
Sb	mg/kg	<LOD	0.28 ± 0.015
Se	mg/kg	0.15 ± 0.050	0.18 ± 0.059
Zn	g/kg	0.061 ± 0.0015	0.066 ± 0.0044

Appendix H PFAS analysis in soil from a firefighting training facility

Table H1. The measured PFAS concentrations, dry matter, total carbon (TC), total inorganic carbon (TIC) and total organic carbon (TOC) in triplicate samples of Soil A. The standard deviations for the averages were measured as shown in Appendix E. Each PFAS measurement had a stated measurement uncertainty of 23 % in the analysis report. The dry matter, TC, and TOC had measurement uncertainties of 5 %, 10 % and 15 %, respectively. All the measurement uncertainties had a coverage factor of k=2.

Analysis	Unit	Soil-1	Soil-2	Soil-3	Average	LOQ
Sum PFAS	µg/kg dw	1700	1700	1400	1600 ± 173	---
PFOS	µg/kg dw	1600	1600	1300	1500 ± 173	0.1
PFOSA	µg/kg dw	45	47	50	47 ± 2.5	0.1
6:2 FTS	µg/kg dw	9.4	9.8	10	9.7 ± 0.31	0.1
8:2 FTS	µg/kg dw	8.6	7.7	8.5	8.3 ± 0.49	0.1
PFHxS	µg/kg dw	8.5	8.2	7.6	8.1 ± 0.46	0.1
PFDS	µg/kg dw	4.7	3.8	4.3	4.3 ± 0.45	0.1
PFOA	µg/kg dw	3.9	4.3	4.3	4.2 ± 0.23	0.1
PFUnA	µg/kg dw	2.8	3.2	3.0	3.0 ± 0.20	0.1
PFHxA	µg/kg dw	2.0	2.1	2.0	2.03 ± 0.058	0.1
PFTrA	µg/kg dw	2.1	1.9	1.9	2.0 ± 0.12	0.1
PFDeA	µg/kg dw	1.6	1.7	1.8	1.7 ± 0.10	0.1
PFPeA	µg/kg dw	1.6	1.7	1.7	1.67 ± 0.058	0.1
PFHpS	µg/kg dw	1.1	1.1	1.0	1.07 ± 0.058	0.1
PFNA	µg/kg dw	1.0	1.1	1.0	1.03 ± 0.058	0.1
FOSAA	µg/kg dw	0.75	1.3	0.92	1.0 ± 0.28	0.1
MeFOSAA	µg/kg dw	0.52	0.77	0.69	0.7 ± 0.13	0.1
PFHpA	µg/kg dw	0.59	0.57	0.65	0.60 ± 0.042	0.1
PFBA	µg/kg dw	0.46	0.45	0.43	0.45 ± 0.015	0.1
PFDoA	µg/kg dw	0.38	0.32	0.40	0.37 ± 0.042	0.1
PFBS	µg/kg dw	0.27	0.29	0.28	0.28 ± 0.010	0.1
4:2 FTS	µg/kg dw	< 0.10	< 0.10	< 0.10	---	0.1
HPFHpA	µg/kg dw	< 0.10	< 0.10	< 0.10	---	0.1
PF-3,7-DMOA	µg/kg dw	< 0.50	< 0.50	< 0.50	---	0.5
PFHxDA	µg/kg dw	< 0.50	< 0.50	< 0.50	---	0.5
PFTA	µg/kg dw	< 0.10	< 0.10	< 0.10	---	0.1
EtFOSA	µg/kg dw	< 0.20	< 0.20	< 0.20	---	0.2
EtFOSAA	µg/kg dw	< 0.10	< 0.10	< 0.10	---	0.1
EtFOSE	µg/kg dw	< 0.10	< 0.10	< 0.10	---	0.1
MeFOSE	µg/kg dw	< 0.10	< 0.10	< 0.10	---	0.1
MeFOSA	µg/kg dw	< 0.20	< 0.20	< 0.20	---	0.2
Dry matter	%	99.40	99.50	99.30	99.4 ± 0.10	0.25
TC	%	0.50	0.50	0.50	0.50 ± 0	0.1
TIC	%	< 0.1	< 0.1	< 0.1	---	0.1
TOC	%	0.40	0.40	0.40	0.40 ± 0	0.2

Appendix I PFAS concentrations of control batch leachates

Table I1. An overview of the measured PFAS concentrations (ng/L) in the leachates from Soil A and Soil B following one-step batch leaching tests. The unamended soil samples were from separate firefighting training facilities and had different PFAS distributions (fig. 10). The standard deviations were calculated as shown in Appendix E. Due to the samples' high PFAS concentrations, the LOQ values were elevated to 10 ng/L for all PFASs except PF-3.7-DMOA (LOQ = 100 ng/L) and PFNS, PFDoS, PFDS, EtFOSA, MeFOSE and MeFOSA (LOQ = 20 ng/L).

	Soil A1	Soil A2	Soil A3	Average	Soil B1	Soil B2	Soil B3	Average
Sum PFAS	*110000*	*110000*	*110000*	*110000 ± 0*	*180000*	*180000*	*200000*	*190000 ± 11000*
PFOS	110000	110000	110000	110000 ± 0	29000	32000	31000	31000 ± 1500
6:2 FTS	820	810	890	840 ± 44	100000	97000	120000	110000 ± 13000
PFOSA	710	800	730	750 ± 47	350	430	460	410 ± 56
PFHxS	610	570	620	600 ± 26	2200	2500	2400	2400 ± 150
PFOA	400	390	380	390 ± 10	1600	1900	1800	1800 ± 150
8:2 FTS	330	330	380	350 ± 29	4600	5500	6000	5400 ± 710
PFHxA	230	230	200	220 ± 17	12000	12000	12000	12000 ± 0
PFPeA	190	180	180	183 ± 5.8	21000	21000	21000	21000 ± 0
PFNS	140	160	150	150 ± 10	<20	<20	<20	---
PFDeA	110	120	110	113 ± 5.8	270	320	300	300 ± 25
PFNA	91	98	110	99 ± 9.6	820	940	1100	1000 ± 140
PFHpS	78	71	73	74 ± 3.6	630	750	640	670 ± 66
PFUnA	83	63	68	70 ± 10	12	11	17	13 ± 3.2
FOSAA	62	81	68	70 ± 9.7	<10	<10	<10	---
PFHpA	62	58	55	58 ± 3.5	2300	2300	2400	2330 ± 57
PFBA	54	61	48	54 ± 6.5	2200	2200	2300	2230 ± 57
PFPeS	35	33	36	34 ± 1.5	200	180	190	190 ± 10
PFDoS	22	<20	<20	14 ± 6.9	<20	<20	<20	---
PFBS	20	20	22	21 ± 1.1	130	110	130	120 ± 12
PFTA	19	17	18	18 ± 1.0	13	13	12	12.7 ± 0.58
PFTrA	5	5	16	8 ± 6.3	18	<10	<10	9 ± 7.5
4:2 FTS	<10	<10	<10	---	<10	<10	<10	---
HPFHpA	<10	<10	<10	---	<10	<10	<10	---
PF-3,7-DMOA	<100	<100	<100	---	<100	<100	<100	---
PFDoA	<10	<10	<10	---	18	27	23	22 ± 4.5
PFDS	<20	<20	<20	---	<20	<20	<20	---
PFHxDA	<10	<10	<10	---	<10	<10	<10	---
EtFOSA	<20	<20	<20	---	<20	<20	<20	---
EtFOSAA	<10	<10	<10	---	<10	<10	<10	---
EtFOSE	<10	<10	<10	---	<10	<10	<10	---
MeFOSAA	<10	<10	<10	---	<10	<10	<10	---
MeFOSE	<20	<20	<20	---	<20	<20	<20	---
MeFOSA	<20	<20	<20	---	<20	<20	<20	---

Appendix J Overview of some PFASs and their properties

Table J1. Overview of selected PFASs with information on PFAS type, fluorocarbon (FC) chain length, CAS-number and molecular formula. The different PFAS groups are colour coded: blue for perfluoroalkyl carboxylic acids (PFCA), orange for perfluoroalkyl sulfonic acids (PFSA), pink for fluorotelomer sulfonic acids (FTSA) and yellow for perfluorooctane sulfonamido substances (preFOS). The preFOS are known precursors to PFOS.

PFAS	Type / chain length	CAS-number	Molecular formula
Perfluorooctane sulfonate (PFOS)	PFSA, 8FC	1763-23-1	C_8F_{11}-SO_3H
6:2 fluorotelomer sulfonate (6:2 FTS)	FTSA, 6FC	27619-97-2	C_6F_{13}-$CH_2CH_2SO_3$
Perfluorooctane sulfonamide (PFOSA)	preFOS, 8FC	754-91-6	C_8F_{17}-SO_2NH_2
Perfluorohexane sulfonate (PFHxS)	PFSA, 6FC	355-46-4	C_6F_{13}-SO_3H
Perfluorooctanate (PFOA)	PFCA, 7FC	335-67-1	C_7F_{15}-COOH
8:2 fluorotelomer sulfonate (8:2 FTS)	FTSA, 8FC	39108-34-4	C_8F_{17}-$CH_2CH_2SO_3$
Perfluorohexanate (PFHxA)	PFCA, 5FC	307-24-4	C_5F_{11}-COOH
Perfluoropentanoic acid (PFPeA)	PFCA, 4FC	2706-90-3	C_4F_9-COOH
Perfluorononanesulfonic acid (PFNS)	PFSA, 9FC	68259-12-1	C_9F_{19}-SO_3H
Perfluorodecanoic acid (PFDeA)	PFCA, 9FC	335-76-2	C_9F_{19}-COOH
Perfluorononanate (PFNA)	PFCA, 8FC	375-95-1	C_8F_{17}-COOH
Perfluoroheptanesulfonic acid (PFHpS)	PFSA, 7FC	375-92-8	$C_7F_{15}SO_3H$
Perfluoroundecanoic acid (PFUNA)	PFCA, 10FC	2058-94-8	$C_{10}F_{21}$-COOH
Perfluorooctanesulfonamidoacetic acid (FOSAA)	preFOS, 8FC	2806-24-8	C_8F_{17}-SO_2NH-CH_2COOH
Perfluoroheptanate (PFHpA)	PFCA, 6FC	375-85-9	C_6F_{13}-COOH
Perfluorobutanoic acid (PFBA)	PFCA, 3FC	375-22-4	C_3F_7-COOH
Perfluoropentane sulfonic acid (PFPeS)	PFSA, 5FC	2706-91-4	C_5F_{11}-SO_3H
Perfluorobutane sulfonate (PFBS)	PFSA, 4FC	375-73-5	C_4F_9-SO_3H
Perfluorotetradecanoic acid (PFTA)	PFCA, 13FC	376-06-7	$C_{13}F_{27}$-COOH

Appendix K PFAS concentrations of batch tests with sorbents

Table K1. Concentrations (ng/L) of the Σ33 PFASs measured in the one-step batch test leachates of PFAS-contaminated soil (Soil A) added different concentrations of sorbent materials (in % of soil dw). Each batch test was performed in triplicate. Due to high PFAS concentrations in the leachate solutions, LOQ values were elevated for all sorbents except activated biochar.

	0.1 % activated biochar			**0.5 % activated biochar**			**1.0 % activated biochar**		
4:2 FTS	<1.0	<1.0	<1.0	<1.0	<1.0	<1.0	<1.0	<1.0	<1.0
6:2 FTS	6.9	7.3	10	1.7	1.8	2.1	1.1	<1.0	1.6
8:2 FTS	3.7	2.6	4	2.2	1.9	2.8	1.2	<1.0	1.4
HPFHpA	<1.0	<1.0	<1.0	<1.0	<1.0	<1.0	<1.0	<1.0	<1.0
PF-3,7-DMOA	<5.0	<5.0	<5.0	<5.0	<5.0	<5.0	<5.0	<5.0	<5.0
PFDeA	<1.0	<1.0	1.2	<1.0	<1.0	<1.0	<1.0	<1.0	<1.0
PFBS	<1.0	<1.0	<1.0	<1.0	<1.0	<1.0	<1.0	<1.0	<1.0
PFBA	21	20	21	<3.0	<3.0	<3.0	<3.0	<3.0	<3.0
PFDoA	<1.0	<1.0	<1.0	<1.0	<1.0	<1.0	<1.0	<1.0	<1.0
PFTrA	2.9	2.6	2.6	1.3	1.4	1.4	<1.0	<1.0	1.1
PFDS	2.2	1.7	1.9	3	2.8	3.7	1.4	1.3	2.3
PFHpA	1.6	1.1	1.5	<1.0	<1.0	<1.0	<1.0	<1.0	<1.0
PFHpS	<1.0	<1.0	<1.0	<1.0	<1.0	<1.0	<1.0	<1.0	<1.0
PFHxA	8	7.5	10	<1.0	<1.0	<1.0	<1.0	<1.0	<1.0
PFHxDA	<1.0	<1.0	<1.0	<1.0	<1.0	<1.0	<1.0	<1.0	<1.0
PFHxS	7.7	5.6	7.5	1.4	1.4	1.6	1.2	<1.0	1.1
PFNA	<1.0	<1.0	<1.0	<1.0	<1.0	<1.0	<1.0	<1.0	<1.0
PFOA	4.6	4.6	7.1	<1.0	<1.0	<1.0	<1.0	<1.0	1.4
PFOS	630	610	600	370	350	460	230	210	290
PFOSA	24	18	23	14	17	18	9.2	8	11
PFPeA	21	20	19	<1.0	<1.0	<1.0	<1.0	<1.0	1.1
PFTA	<1.0	<1.0	<1.0	<1.0	<1.0	<1.0	<1.0	<1.0	<1.0
PFUnA	1.6	1.2	2	<1.0	1.3	1.4	<1.0	<1.0	1
EtFOSA	<1.0	<1.0	<1.0	<1.0	<1.0	<1.0	<1.0	<1.0	<1.0
EtFOSAA	<1.0	<1.0	<1.0	<1.0	<1.0	<1.0	<1.0	<1.0	<1.0
EtFOSE	<1.0	<1.0	<1.0	<1.0	<1.0	<1.0	<1.0	<1.0	<1.0
MeFOSAA	<1.0	<1.0	<1.0	<1.0	<1.0	<1.0	<1.0	<1.0	<1.0
MeFOSE	<1.0	<1.0	<1.0	<1.0	<1.0	<1.0	<1.0	<1.0	<1.0
MeFOSA	<1.0	<1.0	<1.0	<1.0	<1.0	<1.0	<1.0	<1.0	<1.0
FOSAA	1.6	1.4	1.6	<1.0	<1.0	<1.0	<1.0	<1.0	<1.0
PFPeS	<1.0	<1.0	<1.0	<1.0	<1.0	<1.0	<1.0	<1.0	<1.0
PFNS	1.9	1.7	2.1	1.8	2.2	2	1.4	<1.0	1.6
PFDoS	7.8	6	8	3.1	2.6	3.8	1.5	1.8	1.8
Sum PFAS	750	710	720	400	380	500	250	220	320
	1 % ash			***2 % ash***			***5 % ash***		
4:2 FTS	<10	<10	<10	<10	<10	<10	<10	<10	<10
6:2 FTS	1100	1100	1100	910	920	870	940	980	930
8:2 FTS	410	490	440	510	360	430	430	610	420
HPFHpA	<10	<10	<10	<10	<10	<10	<10	<10	<10
PF-3,7-DMOA	<100	<100	<100	<100	<100	<100	<100	<100	<100

	1 % ash			*2 % ash*			*5 % ash*		
PFDeA	94	120	91	110	120	120	110	110	120
PFBS	20	21	22	22	22	23	23	23	19
PFBA	48	55	54	77	57	79	62	81	71
PFDoA	<10	<10	<10	<10	<10	<10	<10	<10	<10
PFTrA	25	<10	<10	<10	<10	<10	<10	<10	<10
PFDS	<20	<20	<20	<20	<20	<20	<20	<20	<20
PFHpA	60	63	63	72	75	79	88	100	98
PFHpS	66	65	77	73	82	66	79	85	69
PFHxA	240	270	280	310	310	500	400	360	360
PFHxDA	<10	<10	<10	<10	<10	<10	<10	<10	<10
PFHxS	610	580	590	590	600	640	620	630	600
PFNA	75	93	110	110	100	120	89	120	87
PFOA	450	470	470	620	610	600	950	900	880
PFOS	110000	100000	97000	110000	110000	95000	90000	93000	88000
PFOSA	3900	4300	3800	4800	4300	4700	4300	4200	4700
PFPeA	200	190	200	220	210	230	220	240	200
PFTA	20	14	18	11	16	18	<10	13	16
PFUnA	48	67	46	77	70	81	55	66	57
EtFOSA	<20	<20	<20	<20	<20	<20	<20	<20	<20
EtFOSAA	<10	<10	<10	<10	<10	<10	<10	<10	<10
EtFOSE	<10	<10	<10	<10	<10	<10	<10	<10	<10
MeFOSAA	20	<10	15	15	16	15	<10	14	<10
MeFOSE	<20	<20	<20	<20	<20	<20	<20	<20	<20
MeFOSA	<20	<20	<20	<20	<20	<20	<20	<20	<20
FOSAA	120	140	120	170	150	120	120	96	99
PFPeS	33	31	35	38	32	41	38	38	36
PFNS	150	150	150	130	110	180	90	110	82
PFDoS	<20	<20	<20	<20	<20	<20	<20	<20	<20
Sum PFAS	120000	110000	100000	120000	120000	100000	99000	100000	97000

	1 % bonemeal			*2 % bonemeal*			*5 % bonemeal*		
4:2 FTS	<10	<10	<10	<10	<10	<10	<10	<10	<10
6:2 FTS	860	810	770	750	700	860	560	820	610
8:2 FTS	280	210	240	150	130	160	44	31	48
HPFHpA	<10	<10	<10	<10	<10	<10	<10	<10	<10
PF-3,7-DMOA	<100	<100	<100	<100	<100	<100	<100	<100	<100
PFDeA	78	46	64	32	35	36	10	12	<10
PFBS	21	22	20	23	24	22	19	22	23
PFBA	52	53	52	43	46	46	43	53	52
PFDoA	<10	<10	<10	<10	<10	<10	<10	<10	<10
PFTrA	<10	<10	<10	<10	<10	<10	<10	<10	<10
PFDS	<20	<20	<20	<20	<20	<20	<20	<20	<20
PFHpA	58	57	50	50	51	49	52	56	45
PFHpS	66	64	77	63	71	58	38	48	37
PFHxA	240	210	200	180	210	200	200	210	200
PFHxDA	<10	<10	<10	<10	<10	<10	<10	<10	<10
PFHxS	610	590	670	610	690	630	540	640	510

	1 % bonemeal			*2 % bonemeal*			*5 % bonemeal*		
PFNA	75	68	88	67	50	58	35	38	28
PFOA	420	380	390	330	370	360	270	370	300
PFOS	89000	66000	75000	43000	37000	49000	17000	22000	20000
PFOSA	760	420	730	330	300	250	140	210	140
PFPeA	160	180	160	170	180	160	180	170	180
PFTA	<10	<10	<10	<10	<10	<10	<10	<10	<10
PFUnA	46	28	34	20	20	14	<10	<10	<10
EtFOSA	<20	<20	<20	<20	<20	<20	<20	<20	<20
EtFOSAA	<10	<10	<10	<10	<10	<10	<10	<10	<10
EtFOSE	<10	<10	<10	<10	<10	<10	<10	<10	<10
MeFOSAA	<10	<10	<10	<10	<10	<10	<10	<10	<10
MeFOSE	<20	<20	<20	<20	<20	<20	<20	<20	<20
MeFOSA	<20	<20	<20	<20	<20	<20	<20	<20	<20
FOSAA	19	18	25	16	14	<10	<10	<10	<10
PFPeS	38	37	40	31	32	32	35	38	32
PFNS	43	33	66	<20	38	<20	<20	22	<20
PFDoS	<20	<20	<20	<20	<20	<20	<20	<20	<20
Sum PFAS	93000	69000	79000	46000	40000	52000	19000	25000	22000

	1 % chitosan			*2 % chitosan*			*5 % chitosan*		
4:2 FTS	<10	<10	<10	<10	<10	<10	<10	<10	<10
6:2 FTS	910	850	900	810	1100	820	960	880	960
8:2 FTS	460	290	330	260	230	230	190	250	230
HPFHpA	<10	<10	<10	<10	<10	<10	<10	<10	<10
PF-3,7-DMOA	<100	<100	<100	<100	<100	<100	<100	<100	<100
PFDeA	110	89	86	76	70	55	54	52	66
PFBS	22	21	20	22	18	18	21	17	17
PFBA	53	53	51	56	43	49	47	44	49
PFDoA	<10	<10	<10	<10	<10	<10	<10	<10	<10
PFTrA	<10	<10	<10	<10	<10	<10	<10	<10	<10
PFDS	<20	<20	<20	<20	<20	<20	<20	<20	<20
PFHpA	55	63	56	63	58	58	60	54	53
PFHpS	61	95	84	79	61	74	53	51	60
PFHxA	280	250	230	270	270	250	260	250	240
PFHxDA	<10	<10	<10	<10	<10	<10	<10	<10	<10
PFHxS	720	710	610	720	610	650	590	540	630
PFNA	100	110	76	110	76	81	69	82	82
PFOA	410	480	460	460	390	460	450	360	370
PFOS	120000	110000	100000	88000	70000	72000	60000	63000	74000
PFOSA	640	700	620	640	470	460	470	590	580
PFPeA	200	220	180	220	170	180	230	160	190
PFTA	<10	<10	<10	<10	<10	<10	<10	<10	<10
PFUnA	58	45	51	34	29	20	18	29	24
EtFOSA	<20	<20	<20	<20	<20	<20	<20	<20	<20
EtFOSAA	<10	<10	<10	<10	<10	<10	<10	<10	<10
EtFOSE	<10	<10	<10	<10	<10	<10	<10	<10	<10
MeFOSAA	13	13	<10	11	<10	<10	<10	<10	<10
MeFOSE	<20	<20	<20	<20	<20	<20	<20	<20	<20

	1 % chitosan			*2 % chitosan*			*5 % chitosan*		
MeFOSA	<20	<20	<20	<20	<20	<20	<20	<20	<20
FOSAA	38	32	37	26	19	20	16	12	19
PFPeS	38	32	35	41	30	31	33	33	35
PFNS	150	130	120	75	66	47	42	45	56
PFDoS	<20	<20	<20	<20	<20	<20	<20	<20	<20
Sum PFAS	120000	110000	100000	92000	74000	76000	64000	66000	78000

	2 % filter dust			*5 % filter dust*			*10 % filter dust*		
4:2 FTS	<10	<10	<10	<10	<10	<10	<10	<10	<10
6:2 FTS	950	1100	1000	930	880	760	750	760	740
8:2 FTS	300	270	300	210	250	220	220	260	200
HPFHpA	<10	<10	<10	<10	<10	<10	<10	<10	<10
PF-3,7-DMOA	<100	<100	<100	<100	<100	<100	<100	<100	<1000
PFDeA	58	59	67	52	51	55	54	54	39
PFBS	22	22	22	22	20	20	24	24	23
PFBA	41	41	49	43	46	39	39	47	45
PFDoA	<10	<10	<10	<10	<10	<10	<10	<10	<10
PFTrA	<10	<10	<10	<10	<10	<10	<10	<10	<10
PFDS	<20	<20	<20	<20	<20	<20	<20	<20	<20
PFHpA	67	74	66	69	67	64	68	74	64
PFHpS	57	53	56	57	57	61	64	57	61
PFHxA	380	410	390	650	590	630	330	270	330
PFHxDA	<10	<10	<10	<10	<10	<10	<10	<10	<10
PFHxS	550	550	560	530	580	550	560	560	540
PFNA	42	47	57	36	57	69	62	70	65
PFOA	430	410	480	570	460	550	470	430	440
PFOS	67000	70000	78000	63000	58000	63000	59000	64000	62000
PFOSA	510	570	740	890	830	980	2000	3100	2500
PFPeA	180	170	180	170	180	170	160	180	160
PFTA	<10	<10	<10	<10	<10	<10	<10	<10	<10
PFUnA	16	16	18	12	<10	15	15	13	12
EtFOSA	<20	<20	<20	<20	<20	<20	<20	<20	<20
EtFOSAA	<10	<10	<10	<10	<10	<10	<10	<10	<10
EtFOSE	<10	<10	<10	<10	<10	<10	<10	<10	<10
MeFOSAA	<10	<10	<10	<10	<10	<10	<10	<10	<10
MeFOSE	<20	<20	<20	<20	<20	<20	<20	<20	<20
MeFOSA	<20	<20	<20	<20	<20	<20	<20	<20	<20
FOSAA	<10	<10	<10	<10	<10	<10	<10	<10	<10
PFPeS	31	31	29	31	33	27	32	34	30
PFNS	29	45	30	53	35	23	23	46	28
PFDoS	<20	<20	<20	<20	<20	<20	<20	<20	<20
Sum PFAS	71000	74000	82000	67000	62000	67000	64000	70000	67000

	1 % LECA			*2 % LECA*			*5 % LECA*		
4:2 FTS	<10	<10	<10	<10	<10	<10	<10	<10	<10
6:2 FTS	950	990	890	930	1000	1000	870	1200	1000
8:2 FTS	420	360	380	440	440	350	410	410	340
HPFHpA	<10	<10	<10	<10	<10	<10	<10	<10	<10

	1 % LECA			*2 % LECA*			*5 % LECA*		
PF-3,7-DMOA	<100	<100	<100	<100	<100	<100	<100	<100	<100
PFDeA	120	120	120	110	130	120	98	110	100
PFBS	22	24	23	23	22	26	22	26	26
PFBA	52	43	55	50	46	46	55	61	66
PFDoA	<10	<10	<10	<10	<10	<10	<10	<10	<10
PFTrA	<10	<10	<10	<10	<10	<10	<10	<10	<10
PFDS	<20	<20	<20	<20	<20	<20	<20	33	<20
PFHpA	62	62	61	62	69	65	62	65	69
PFHpS	78	82	83	82	88	74	76	82	74
PFHxA	240	270	270	240	230	250	240	270	270
PFHxDA	<10	<10	<10	<10	<10	<10	<10	<10	<10
PFHxS	600	690	700	700	660	660	680	720	670
PFNA	120	100	96	100	89	120	130	97	120
PFOA	390	400	420	410	390	420	390	380	400
PFOS	120000	140000	120000	120000	130000	120000	120000	140000	120000
PFOSA	680	820	690	580	730	650	900	810	830
PFPeA	210	200	210	220	210	230	210	250	230
PFTA	<10	<10	<10	<10	<10	<10	<10	<10	<10
PFUnA	77	74	82	70	85	89	66	85	61
EtFOSA	<20	<20	<20	<20	<20	<20	<20	<20	<20
EtFOSAA	<10	<10	<10	<10	<10	<10	<10	<10	<10
EtFOSE	<10	<10	<10	<10	<10	<10	<10	<10	<10
MeFOSAA	<10	12	<10	12	11	<10	12	<10	11
MeFOSE	<20	<20	<20	<20	<20	<20	<20	<20	<20
MeFOSA	<20	<20	<20	<20	<20	<20	<20	<20	<20
FOSAA	63	68	51	52	73	58	74	61	54
PFPeS	35	37	38	35	35	37	35	37	41
PFNS	160	120	130	120	190	110	150	120	79
PFDoS	<20	<20	<20	<20	<20	<20	<20	<20	<20
Sum PFAS	120000	140000	120000	120000	130000	120000	120000	140000	120000

	2 % slag			*5 % slag*			*10 % slag*		
4:2 FTS	<10	<10	<10	<10	<10	<10	<10	<10	<10
6:2 FTS	1600	1500	1300	1000	1100	1100	1000	940	870
8:2 FTS	240	320	330	180	190	180	240	170	160
HPFHpA	<10	<10	<10	<10	<10	<10	<10	<10	<10
PF-3,7-DMOA	<100	<100	<100	<100	<100	<100	<100	<100	<100
PFDeA	57	69	58	48	47	48	55	39	39
PFBS	25	24	25	22	21	23	25	20	22
PFBA	86	60	75	80	73	78	68	68	75
PFDoA	<10	<10	<10	<10	<10	<10	<10	<10	<10
PFTrA	<10	<10	<10	<10	<10	<10	<10	<10	<10
PFDS	<10	<20	<20	<20	<20	<20	<20	<20	<20
PFHpA	92	92	90	93	83	94	82	70	75
PFHpS	74	75	77	70	59	65	67	60	64
PFHxA	1100	780	930	1800	1500	1600	750	690	670
PFHxDA	30	30	31	29	27	32	30	29	29
PFHxS	660	640	640	610	640	660	600	590	620

	2 % slag			*5 % slag*			*10 % slag*		
PFNA	86	81	91	71	70	55	90	64	74
PFOA	530	540	520	660	550	660	490	490	490
PFOS	96000	89000	84000	62000	63000	68000	63000	53000	54000
PFOSA	420	560	450	350	210	240	480	400	460
PFPeA	290	280	250	300	280	310	250	230	230
PFTA	<10	<10	<10	<10	<10	<10	<10	<10	<10
PFUnA	21	25	14	<10	<10	14	15	12	<10
EtFOSA	<20	<20	<20	<20	<20	<20	<20	<20	<20
EtFOSAA	<10	<10	<10	<10	<10	<10	<10	<10	<10
EtFOSE	<10	<10	<10	<10	<10	<10	<10	<10	<10
MeFOSAA	<10	<10	<10	<10	<10	<10	<10	<10	<10
MeFOSE	<20	<20	<20	<20	<20	<20	<20	<20	<20
MeFOSA	<20	<20	<20	<20	<20	<20	<20	<20	<20
FOSAA	<10	<10	<10	<10	<10	<10	<10	<10	<10
PFPeS	34	28	36	35	33	38	34	29	33
PFNS	48	80	67	17	36	20	19	18	34
PFDoS	<20	<20	<20	<20	<20	<20	<20	<20	<20
Sum PFAS	100000	94000	89000	67000	68000	73000	67000	57000	58000

Appendix L Estimated K_d values for batch leaching tests with sorbents

In addition to the K_d values for the soil itself, partition coefficients were calculated for the batch tests where soil had been added sorbents. These values were calculated as described in section 4.4.2 *Partitioning coefficients for describing PFAS sorption*, but with the solid phase concentration including both soil and sorbent. The log K_d values in Table L1 may thereby be seen as "(sorbent+soil)/water" partitioning coefficients.

Table L1. The log K_d values for PFSAs and PFCAs with different perfluorocarbon chain lengths, estimated from the average (n=3) batch leachate PFAS concentration of both the control samples and samples added different concentrations of activated biochar, ash, bonemeal, chitosan, filter dust, LECA and slag. As K_d values were not obtainable from the control batch tests (i.e., unamended soil) for PFCAs of perfluorocarbon chain length 3–5 (see table 4), these compounds were not included.

	Perfluoroalkyl sulfonic acids				Perfluoroalkyl carboxylic acids				
Perfluoroalkyl chain length	*4*	*6*	*7*	*8*	*6*	*7*	*8*	*9*	*10*
0.1 % act. biochar (log K_d)	2.74	3.07	3.33	3.39	2.63	2.86	3.31	3.40	3.28
0.5 % act. biochar (log K_d)	2.74	3.74	3.33	3.58	3.08	3.92	3.31	3.53	3.49
1.0 % act. biochar (log K_d)	2.74	3.97	3.33	3.79	3.08	3.77	3.31	3.53	3.68
1 % ash (log K_d)	0.52	0.56	0.73	0.67	*	*	0.06	0.83	1.66
2 % ash (log K_d)	0.40	0.52	0.65	0.63	*	*	*	0.66	1.47
5 % ash (log K_d)	0.47	0.50	0.57	0.82	*	*	-0.33	0.70	1.61
1 % bonemeal (log K_d)	0.52	0.48	0.74	0.98	-0.11	-0.09	0.51	1.24	1.87
2 % bonemeal (log K_d)	0.34	0.41	0.82	1.40	0.31	0.24	0.88	1.60	2.20
5 % bonemeal (log K_d)	0.49	0.64	1.20	1.82	0.21	0.47	1.32	2.28	2.77
1 % chitosan (log K_d)	0.52	0.28	0.52	0.56	-0.40	*	-0.08	0.90	1.69
2 % chitosan (log K_d)	0.65	0.36	0.69	0.98	-0.97	*	0.21	1.19	1.99
5 % chitosan (log K_d)	0.72	0.58	0.98	1.11	-0.08	-0.23	0.52	1.29	2.07
2 % filter dust (log K_d)	0.43	0.67	0.97	1.04	*	*	1.05	1.25	2.23
5 % filter dust (log K_d)	0.55	0.67	0.92	1.16	*	*	0.96	1.35	2.33
10 % filter dust (log K_d)	0.26	0.67	0.88	1.16	*	*	0.76	1.39	2.33
1 % LECA (log K_d)	0.34	0.34	0.50	0.26	*	-0.49	*	0.62	1.46
2 % LECA (log K_d)	0.26	0.31	0.49	0.33	*	-0.62	-1.56	0.62	1.43
5 % LECA (log K_d)	0.13	0.24	0.58	0.26	*	-0.17	*	0.82	1.51
2 % slag (log K_d)	0.13	0.40	0.62	0.83	*	*	0.30	1.25	2.15
5 % slag (log K_d)	0.43	0.43	0.81	1.12	*	*	0.76	1.41	2.31
10 % slag (log K_d)	0.40	0.53	0.83	1.22	*	*	0.56	1.45	2.33
0 % sorbent (log K_d)	0.55	0.54	0.64	0.56	-0.47	-0.17	-0.44	0.70	1.51

* Log K_d could not be estimated in cases where the PFAS concentration of the leachate (c_w) exceeded the initial soil concentration ($c_{s,i}$), thus making K_d negative when calculating $c_s = c_{s,i} - c_w$ (see eq. 5).

Appendix M Electrical conductivity and pH of batch eluates

Table M1. The measured pH and electrical conductivity (EC) values in one-step batch leachates from Soil A samples mixed with ash, LECA, bonemeal, chitosan, activated biochar, slag and filter dust at different concentrations (% of soil dw). The pH and EC measurements were carried out on triplicate samples, and a control (unamended soil) and a blank sample (deionized water) were measured as well.

	pH			**EC (µS/cm)**		
Ash (1%)	8.48	8.57	8.67	194	197	193
Ash (2%)	9.63	9.69	9.58	280	275	282
Ash (5%)	10.84	10.83	10.9	550	569	540
LECA (1%)	6.52	6.67	6.6	46.1	52.4	47.2
LECA (2%)	6.55	6.64	6.56	46.7	49.4	46.1
LECA (5%)	6.79	6.68	6.77	58.8	57.3	63.5
Bonemeal (1%)	6.58	6.64	6.58	360.7	371.6	364.6
Bonemeal (2%)	6.48	6.41	6.34	655.9	643.8	635.4
Bonemeal (5%)	6.22	6.26	6.23	1158	1210	1323
Chitosan (1%)	6.42	6.45	6.59	74.08	59.85	65.17
Chitosan (2%)	6.56	6.3	6.19	70.82	145.1	199.1
Chitosan (5%)	6.48	6.47	6.52	157.9	147.3	111.1
Act. biochar (0.1%)	6.61	6.58	6.59	41.57	41.68	47.48
Act. biochar (0.5%)	6.81	6.81	6.8	48.87	47.74	50.66
Act. biochar (1.0%)	6.93	6.95	6.89	60.95	55.56	54.08
Slag (2%)	6.53	6.56	6.48	496.6	442.9	437.5
Slag (5%)	6.78	6.31	6.3	722.6	801	757.5
Slag (10%)	6.6	6.59	6.64	1072	1082	1046
Filter dust (2%)	6.57	6.59	6.64	667.1	659.7	659.8
Filter dust (5%)	7.02	6.94	6.98	1145	1127	1161
Filter dust (10%)	7.31	7.39	7.36	1485	1406	1429
Control	*6.44*	*6.59*	*6.4*	*40.6*	*47.3*	*43.2*
Blank	*6.00*	*5.90*	*5.94*	*1.08*	*1.07*	*1.39*

Appendix N Dissolved organic carbon (DOC)

Table N1. The measured DOC values in the triplicate batch leachates of Soil A amended with different sorbent doses (% of soil dw), in addition to control and blank samples. All tests were performed in triplicate, and the certified reference material (SAGAMON) was well within its certified value. The averages (n=3) are adjusted for blank values and uncertainties are given as standard deviations.

Sample type	**DOC (mg/L)**			***Average DOC (mg/L)***
Blank	0.25	0.25	0.49	*0.3 ± 0.14*
Control	9.1	11	8.8	*9 ± 1.2*
1 % ashes	23	24	23	*23.0 ± 0.58*
2 % ashes	17	16	17	*16.3 ± 0.58*
5 % ashes	27	26	27	*26.3 ± 0.58*
1 % LECA	11	11	11	*10.7 ± 0*
2 % LECA	11	11	11	*10.7 ± 0*
5 % LECA	12	12	13	*12.0 ± 0.58*
1 % bonemeal	39	78	72	*60 ± 21*
2 % bonemeal	200	170	180	*180 ± 15*
5 % bonemeal	500	550	650	*570 ± 76*
1 % chitosan	2.2	2.1	1.9	*1.74 ± 0.15*
2 % chitosan	1.7	11	32	*15 ± 16*
5 % chitosan	28*	29*	2.3	*19 ± 15*
0.1 % biochar	7.8	7.8	7.9	*7.50 ± 0.058*
0.5 % biochar	3.4	3.3	3.2	*3.0 ± 0.10*
1.0 % biochar	1.9	2.0	2.0	*1.64 ± 0.058*
2 % slag	4.0	4.6	3.8	*3.8 ± 0.42*
5 % slag	4.7	3.5	3.5	*3.6 ± 0.69*
10 % slag	4.6	4.7	4.7	*4.34 ± 0.058*
2 % filter dust	4.9	4.9	5.5	*4.8 ± 0.35*
5 % filter dust	6.4	5.7	6.9	*6.0 ± 0.60*
10 % filter dust	10	11	10	*10.0 ± 0.58*
CRM (SAGAMON)	4.5			

* Filtrated due to flocculation in the sample

Appendix O Anion analyses of batch leachates

Table O1. The measured anion (chloride, nitrate and sulphate) concentrations in the batch leachates of soils amended with different sorbent doses (% of soil dw). All batch tests were performed in triplicate, and the certified reference materials for the IC-analysis (ION-96.4) was well within its certified values. An in-house standard (REF IC) was measured as well, and the results matched the standard's specified concentration values.

Sample type	Anions (mg/L)								
	Chloride			Nitrate			Sulphate		
1 % ash	9.0	9.4	9.3	0.21	0.21	0.22	31	31	31
2 % ash	18	18	18	0.20	0.21	0.22	52	51	53
5 % ash	43	43	43	0.13	0.14	0.11	59	68	51
1 % LECA	0.31	0.40	0.37	0.28	0.30	0.29	6.0	6.5	6.4
2 % LECA	0.36	0.34	0.39	0.30	0.33	0.35	6.5	6.6	6.8
5 % LECA	0.37	0.43	0.43	0.27	0.34	0.42	7.5	7.5	7.7
1 % bonemeal	5.4	5.1	5.1	<0.020	<0.020	<0.020	<0.080	<0.080	<0.080
2 % bonemeal	*	*	*	*	*	*	*	*	*
5 % bonemeal	23	24	25	<0.020	<0.020	<0.020	0.86	0.38	1.2
1 % chitosan	0.93	0.94	0.92	0.22	0.36	0.35	1.6	3.7	4.3
2 % chitosan	1.6	1.5	1.4	0.32	<0.020	<0.020	2.9	0.47	<0.080
5 % chitosan	3.5	3.5	3.5	<0.020	<0.020	<0.020	2.0	2.3	3.8
0,1 % biochar	0.39	0.41	0.39	0.28	0.26	0.27	5.7	5.6	5.6
0,5 % biochar	0.76	0.78	0.84	0.18	0.2	0.21	5.6	5.7	5.6
1,0 % biochar	1.2	1.3	1.3	0.12	0.13	0.11	5.4	5.4	5.1
2 % slag	0.55	0.50	0.50	<0.020	<0.020	<0.020	290	250	250
5 % slag	0.45	0.55	0.55	<0.020	<0.020	<0.020	500	700	700
10 % slag	0.60	0.60	0.65	<0.020	<0.020	<0.020	1130	1180	1170
2 % filter dust	0.65	0.70	1.1	<0.020	<0.020	<0.020	460	470	450
5 % filter dust	1.2	1.3	1.3	<0.020	<0.020	<0.020	1140	1140	1140
10 % filter dust	2.5	2.4	2.4	<0.020	<0.020	<0.020	1700	1700	1700
Control	*0.33*	*0.31*	*0.31*	*0.29*	*0.26*	*0.11*	*6.1*	*6.1*	*6.1*
ION-96.4	76			2.9			81		
In-house standard (REF IC)	5.1			2.1			10		

* Anion values were not determinable for the batch leachates of the soil sample with 2 % bonemeal.

Appendix P Element concentrations of batch leachates

Table P1. The average element concentrations (n=3) in batch leachates of Soil A samples amended with different doses (% soil dw) of ash (ASH), LECA, bonemeal (BONE), chitosan (CHI), activated biochar (ACT), slag (SLAG) and filter dust (FILT). The batch leachates of a control sample (unamended soil) and a blank (deionized water) were analysed as well. The LOD values for each element were based on triplicate values and estimated as described in Appendix D.

	Na (mg/L)	**Mg (mg/L)**	**Sb (µg/L)**	**P (mg/L)**	**K (mg/L)**	**Ca (mg/L)**
LOD	*0.06*	*0.002*	*0.008*	*0.0004*	*0.007*	*0.002*
Blank	*< LOD*	*< LOD*	*< LOD*	*0.00065 ± 0*	*0.0125 ± 0*	*0,00365 ± 0*
Control	*0.35 ± 0.031*	*0.37 ± 0.074*	*0.36 ± 0*	*0.15 ± 0.012*	*0.53 ± 0.036*	*7 ± 1,2*
1 % ASH	1.23 ± 0.058	0.61 ± 0.035	8.50 ± 0.099	0.31 ± 0.012	1.53 ± 0.058	36,3 ± 0,58
2 % ASH	1.5 ± 0	0.15 ± 0.012	10.3 ± 0.58	0.13 ± 0.012	1.57 ± 0.058	58 ± 1,7
5 % ASH	2.23 ± 0.058	0.015 ± 0.0015	7.2 ± 0.66	0.213 ± 0.0058	1.93 ± 0.058	113 ± 5,8
1 % LECA	0.38 ± 0.015	0.69 ± 0.015	0.38 ± 0.012	0.177 ± 0.0058	0.51 ± 0.015	7,5 ± 0,72
2 % LECA	0.48 ± 0.02	0.90 ± 0.050	0.39 ± 0.015	0.167 ± 0.0058	0.53 ± 0.025	6,8 ± 0,25
5 % LECA	0.71 ± 0.026	1.7 ± 0.12	0.413 ± 0.0058	0.17 ± 0.015	0.56 ± 0.032	7,6 ± 0,38
1 % BONE	5.2 ± 0.12	1.67 ± 0.058	0.32 ± 0.031	0.76 ± 0.065	4.07 ± 0.058	27 ± 1,2
2 % BONE	9.9 ± 0.23	2.73 ± 0.058	0.36 ± 0.068	1.67 ± 0.058	7.4 ± 0.21	40,3 ± 0,58
5 % BONE	23.3 ± 0.58	5.97 ± 0.058	0.50 ± 0.052	5.8 ± 0.36	17 ± 0	59 ± 2
1 % CHI	0.56 ± 0.015	0.52 ± 0.051	0.22 ± 0.050	0.10 ± 0.012	0.9 ± 0.17	8,5 ± 0,68
2 % CHI	0.77 ± 0.021	0.91 ± 0.20	0.25 ± 0.042	0.078 ± 0.0075	1.3 ± 0.37	13 ± 5,3
5 % CHI	1.433 ± 0.058	1.4 ± 0.12	0.18 ± 0.084	0.05 ± 0.010	1.3 ± 0.21	14 ± 2
0.1 % ACT	0.37 ± 0.026	0.40 ± 0.084	0.61 ± 0.026	0.183 ± 0.0058	0.59 ± 0.012	6,3 ± 0,62
0.5 % ACT	0.56 ± 0.021	0.57 ± 0.040	1.8 ± 0	0.173 ± 0.0058	0.87 ± 0.049	6,8 ± 0,26
1.0 % ACT	0.84 ± 0.023	0.85 ± 0.025	3.3 ± 0.10	0.17 ± 0.012	1.33 ± 0.058	7,7 ± 0,74
2 % SLAG	0.39 ± 0.015	4.5 ± 0.51	0.20 ± 0.023	0.015 ± 0.0017	0.80 ± 0.021	90 ± 7,8
5 % SLAG	0.45 ± 0.021	10 ± 1.7	0.15 ± 0.070	0.011 ± 0.0029	0.9 ± 0.17	200 ± 17
10 % SLAG	0.493 ± 0.0058	17.7 ± 0.58	0.13 ± 0.028	0.013 ± 0.0020	0.64 ± 0.055	340 ± 11
2 % FILT	0.51 ± 0.045	6.9 ± 0.26	0.46 ± 0.035	0.027 ± 0.0029	1.17 ± 0.058	147 ± 5,8
5 % FILT	0.833 ± 0.0058	16.7 ± 0.58	0.52 ± 0.042	0.022 ± 0.0012	1.27 ± 0.058	367 ± 5,8
10 % FILT	1.33 ± 0.058	24 ± 2	0.64 ± 0.096	0.023 ± 0.0017	1.7 ± 0.12	573 ± 5,8
	Cr (µg/L)	**Mn (µg/L)**	**Fe (mg/L)**	**Ni (µg/L)**	**Cu (µg/L)**	**Zn (µg/L)**
LOD	*0.06*	*0.05*	*0.0001*	*0.01*	*0.1*	*0.2*
Blank	*< LOD*	*< LOD*	*< LOD*	*0.056 ± 0.004*	*< LOD*	*< LOD*
Control	*0.83 ± 0.068*	*9 ± 2.5*	*0.23 ± 0.08*	*2.5 ± 0.15*	*4.2 ± 0.15*	*1,6 ± 0,67*
1 % ASH	41 ± 0.58	0.6 ± 0.22	0.014 ± 0.0015	1.07 ± 0.058	12.3 ± 0.58	< LOD
2 % ASH	48 ± 2.3	1.17 ± 0.058	0.015 ± 0.0015	1 ± 0	22.3 ± 0.58	< LOD
5 % ASH	81 ± 2	0.87 ± 0.025	0.0079 ± 0.00070	2.63 ± 0.058	100 ± 0	0,73 ± 0,061
1 % LECA	0.98 ± 0.12	16 ± 1.2	0.45 ± 0.038	2.7 ± 0.10	4.37 ± 0.058	1,2 ± 0,15
2 % LECA	0.86 ± 0.03	13 ± 0	0.35 ± 0.035	2.80 ± 0.010	4.3 ± 0.12	1,06 ± 0,069
5 % LECA	0.8 ± 0.14	13 ± 5.1	0.4 ± 0.15	3.3 ± 0.23	4.77 ± 0.058	0,9 ± 0,24
1 % BONE	0.80 ± 0.015	2000 ± 100	15 ± 2.1	8.2 ± 0.12	0.52 ± 0.035	1,6 ± 0,67
2 % BONE	0.70 ± 0.015	1900 ± 100	16 ± 1	10 ± 1.5	0.55 ± 0.081	3,5 ± 0,46
5 % BONE	0.63 ± 0.058	1400 ± 100	16 ± 2.6	12 ± 1.0	0.8 ± 0.17	5,3 ± 0,31
1 % CHI	< LOD	10 ± 18	0.06 ± 0.013	0.6 ± 0.13	< LOD	0,8 ± 0,18
2 % CHI	< LOD	600 ± 550	0.5 ± 0.49	1.2 ± 0.61	< LOD	1,8 ± 0,28
5 % CHI	< LOD	300 ± 170	0.07 ± 0.052	0.8 ± 0.19	< LOD	0,79 ± 0,11
0.1 % ACT	0.69 ± 0.046	12 ± 4.0	0.3 ± 0.10	1.7 ± 0.12	2.07 ± 0.058	1,2 ± 0,21
0.5 % ACT	0.36 ± 0.031	10 ± 1.3	0.25 ± 0.026	0.69 ± 0.047	0.66 ± 0.044	0,84 ± 0,092
1.0 % ACT	0.24 ± 0.028	5.3 ± 0.60	0.14 ± 0.012	0.50 ± 0.040	0.49 ± 0.040	0,74 ± 0,090
2 % SLAG	1 ± 1.5	1400 ± 150	0.018 ± 0.0088	4.4 ± 0.70	3 ± 1.2	2,8 ± 0,40
5 % SLAG	0.25 ± 0.014	3400 ± 900	10 ± 10	7 ± 3.5	< LOD	12 ± 6,9
10 % SLAG	< LOD	5170 ± 58	82 ± 3.5	3.1 ± 0.68	< LOD	5,0± 0,93
2 % FILT	0.30 ± 0.078	920 ± 55	0.020 ± 0.0085	3.1 ± 0.21	1.7 ± 0.17	3,8 ± 0,42
5 % FILT	< LOD	1300 ± 100	0.016 ± 0.0094	2.6 ± 0.46	1.1 ± 0.59	3 ± 1,2
10 % FILT	0.28 ± 0.042	440 ± 80	0.06 ± 0.053	2.4 ± 0.32	< LOD	2,3 ± 0,32

	As (µg/L)	Se (µg/L)	Cd (µg/L)	Al (mg/L)	Pb (µg/L)
LOD	*0.003*	*0.02*	*0.001*	*0.001*	*0.001*
Blank	*< LOD*	*< LOD*	*< LOD*	*0.00137 ± 0.000058*	*0.0016 ± 0*
Control	*0.49 ± 0.041*	*0.17 ± 0.030*	*0.019 ± 0.0031*	*0.21 ± 0.053*	*0.27 ± 0.096*
1 % ASH	6.6 ± 0.10	0.74 ± 0.07	0.0053 ± 0.00071	1.0 ± 0.12	0.029 ± 0.0042
2 % ASH	4.03 ± 0.058	1.1 ± 0.12	< LOD	18.7 ± 0.58	0.036 ± 0.0044
5 % ASH	2.7 ± 0.15	1.4 ± 0.10	0.0052 ± 0	56 ± 5.1	0.066 ± 0.0029
1 % LECA	0.68 ± 0.031	0.20 ± 0.040	0.018 ± 0.0023	0.32 ± 0.031	0.55 ± 0.035
2 % LECA	0.67 ± 0.026	0.18 ± 0.040	0.017 ± 0.0021	0.27 ± 0.030	0.42 ± 0.042
5 % LECA	0.78 ± 0.021	0.23 ± 0.041	0.014 ± 0.0015	0.27 ± 0.090	0.4 ± 0.18
1 % BONE	9.5 ± 0.44	0.48 ± 0.032	0.0048 ± 0.00078	0.085 ± 0.0036	0.17 ± 0.015
2 % BONE	9.2 ± 0.31	0.46 ± 0.047	0.0065 ± 0.00052	0.067 ± 0.0029	0.15 ± 0.042
5 % BONE	9.1 ± 0.83	0.51 ± 0.035	0.014 ± 0.0017	0.053 ± 0.0044	0.28 ± 0.075
1 % CHI	0.31 ± 0.046	< LOD	0.013 ± 0.0064	0.04 ± 0.010	0.08 ± 0.018
2 % CHI	0.4 ± 0.20	0.14 ± 0.042	< LOD	0.01 ± 0.014	0.03 ± 0.015
5 % CHI	0.5 ± 0.19	< LOD	< LOD	0.011 ± 0.0053	0.02 ± 0.011
0.1 % ACT	0.69 ± 0.049	0.11 ± 0.016	0.016 ± 0.0015	0.22 ± 0.056	0.4 ± 0.14
0.5 % ACT	1.2 ± 0	0.074 ± 0.0021	0.007 ± 0.0025	0.14 ± 0.015	0.31 ± 0.032
1.0 % ACT	1.93 ± 0.058	0.08 ± 0.016	0.005 ± 0.0012	0.09 ± 0.010	0.18 ± 0.020
2 % SLAG	0.14 ± 0.019	0.15 ± 0.070	0.087 ± 0.013	0.011 ± 0.0014	0.016 ± 0.0081
5 % SLAG	0.137 ± 0.0058	0.183 ± 0.0058	0.03 ± 0.021	0.011 ± 0.0024	0.02 ± 0.015
10 % SLAG	0.17 ± 0.012	0.2 ± 0.14	< LOD	0.013 ± 0.0036	0.011 ± 0.0027
2 % FILT	0.23 ± 0.025	0.15 ± 0.035	0.060 ± 0.0072	0.016 ± 0.0035	0.12 ± 0.077
5 % FILT	0.32 ± 0.026	0.5 ± 0.31	0.023 ± 0.0035	0.013 ± 0.0032	0.12 ± 0.070
10 % FILT	0.65 ± 0.055	3.9 ± 0.49	< LOD	0.05 ± 0.017	0.11 ± 0.099

Appendix Q ANOVA tests

In addition to the data plot of the sum leached PFAS concentrations by sorbent type (fig. 20), the ANOVA test resulted in the ANOVA table (table Q1) and the means table (table Q2) below. The low p-value (< 0.05) confirms that the effect of the different sorbent concentrations on PFAS leaching is not the same for all groups.

Table Q1. The one-way ANOVA table for sum PFAS concentration in eluates added different sorbents (n=7) at three different concentrations. The table contains information on source, degrees of freedom (DF) sum of squares, mean square, F Ratio and p-value (Prob > F).

Source	DF	Sum of Squares	Mean Square	F Ratio	Prob > F
Sorbent type	20	9.9822e+10	4.9911e+9	95.1683	<.0001
Error	42	2202681067	52444787		
C. Total	62	1.0202e+11			

Table Q2. Means of total [PFAS] for each sorbent dose in the one-way ANOVA. This table includes information on the sorbent doses' PFAS concentration means, standard errors (Std Error) and both lower endpoint (Lower 95 %) and upper endpoint (Upper 95 %) for a 95 % confidence interval. The standard error uses a pooled estimate of error variance.

Level	Number	Mean	Std Error	Lower 95%	Upper 95%
Act. biochar 0.1 %	3	727	4181,1	-7711	9164
Act. biochar 0.5 %	3	427	4181,1	-8011	8864
Act. biochar 1.0 %	3	263	4181,1	-8174	8701
Ash 1 %	3	110000	4181,1	101562	118438
Ash 2 %	3	113333	4181,1	104896	121771
Ash 5 %	3	98667	4181,1	90229	107104
Bonemeal 1 %	3	80333	4181,1	71896	88771
Bonemeal 2 %	3	46000	4181,1	37562	54438
Bonemeal 5 %	3	22000	4181,1	13562	30438
Chitosan 1 %	3	110000	4181,1	101562	118438
Chitosan 2 %	3	80667	4181,1	72229	89104
Chitosan 5 %	3	69333	4181,1	60896	77771
Filter dust 2 %	3	75667	4181,1	67229	84104
Filter dust 5 %	3	65333	4181,1	56896	73771
Filter dust 10 %	3	67000	4181,1	58562	75438
LECA 1 %	3	126667	4181,1	118229	135104
LECA 2 %	3	123333	4181,1	114896	131771
LECA 5 %	3	126667	4181,1	118229	135104
Slag 2 %	3	94333	4181,1	85896	102771
Slag 5 %	3	69333	4181,1	60896	77771
Slag 10 %	3	60667	4181,1	52229	69104

To investigate the assumption that the dependent variable (total PFAS concentrations) was normally distributed in each group, a normal quantile plot was made over the centred values (fig. Q1). As seen in Figure Q1, the residuals are more or less on a straight line. While some values deviate towards the confidence bounds, the model assumptions were still assumed to be acceptable.

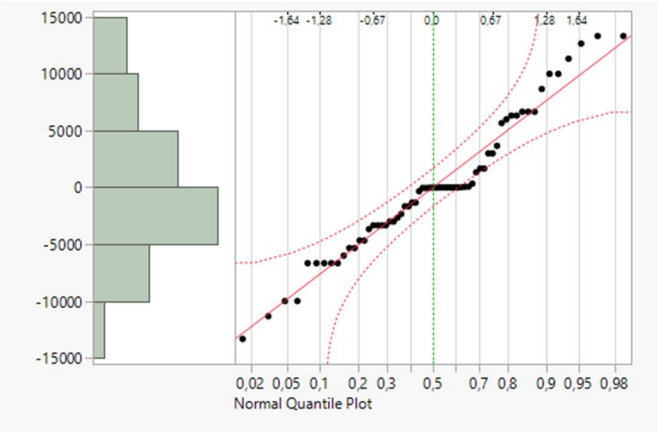

Figure Q1. The normal quantile plot of the total PFAS concentration values centred by sorbent type (residuals), combined with a histogram. The y-axis shows the column values, the top x-axis shows the normal quantile scale, and the bottom x-axis shows each value's empirical cumulative probability. The confidence bounds are marked with red lines.

Another one-way ANOVA test was performed as well to investigate the eluate's total PFAS concentrations for batch tests with different sorbents. This resulted in the ANOVA table (table Q3) and data plot (fig. Q2) displayed below.

Table Q3. ANOVA table with information on source, degrees of freedom (DF) sum of squares, mean square, F Ratio and p-value (Prob > F).

Source	DF	Sum of Squares	Mean Square	F Ratio	Prob > F
Sorbent type	6	8.9626e+10	1.494e+10	67.4694	<.0001
Error	56	1.2398e+10	221399031		
C. Total	62	1.0202e+11			

As indicated by the low p-value (table Q2) and observed in Figure Q2, the sorbents differed from each other in their ability to reduce PFAS concentration.

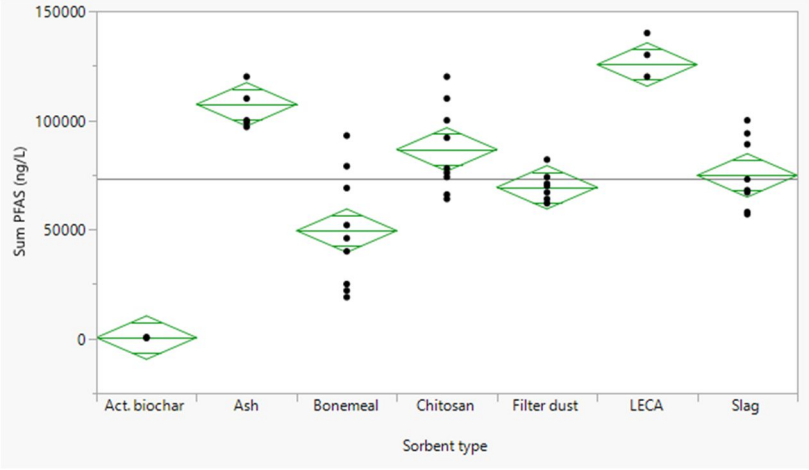

Figure Q2. Plot of Σ33-PFAS concentration by sorbent type. The confidence intervals (95 %) of the concentration averages are given as green rhombuses, and the concentration values (n=9) for each sorbent are given as black dots.

Appendix R Stepwise regression analysis

A backwards stepwise regression was performed using BIC (Bayes Information Criterion) as the stopping criteria and EC, DOC, P, Mg, Ca and Fe as variables for PFOS concentration. Data from the ash, bonemeal, chitosan, filter dust, LECA and slag batch tests were used. Information on the resulting estimates and step history is given in Figure R1.

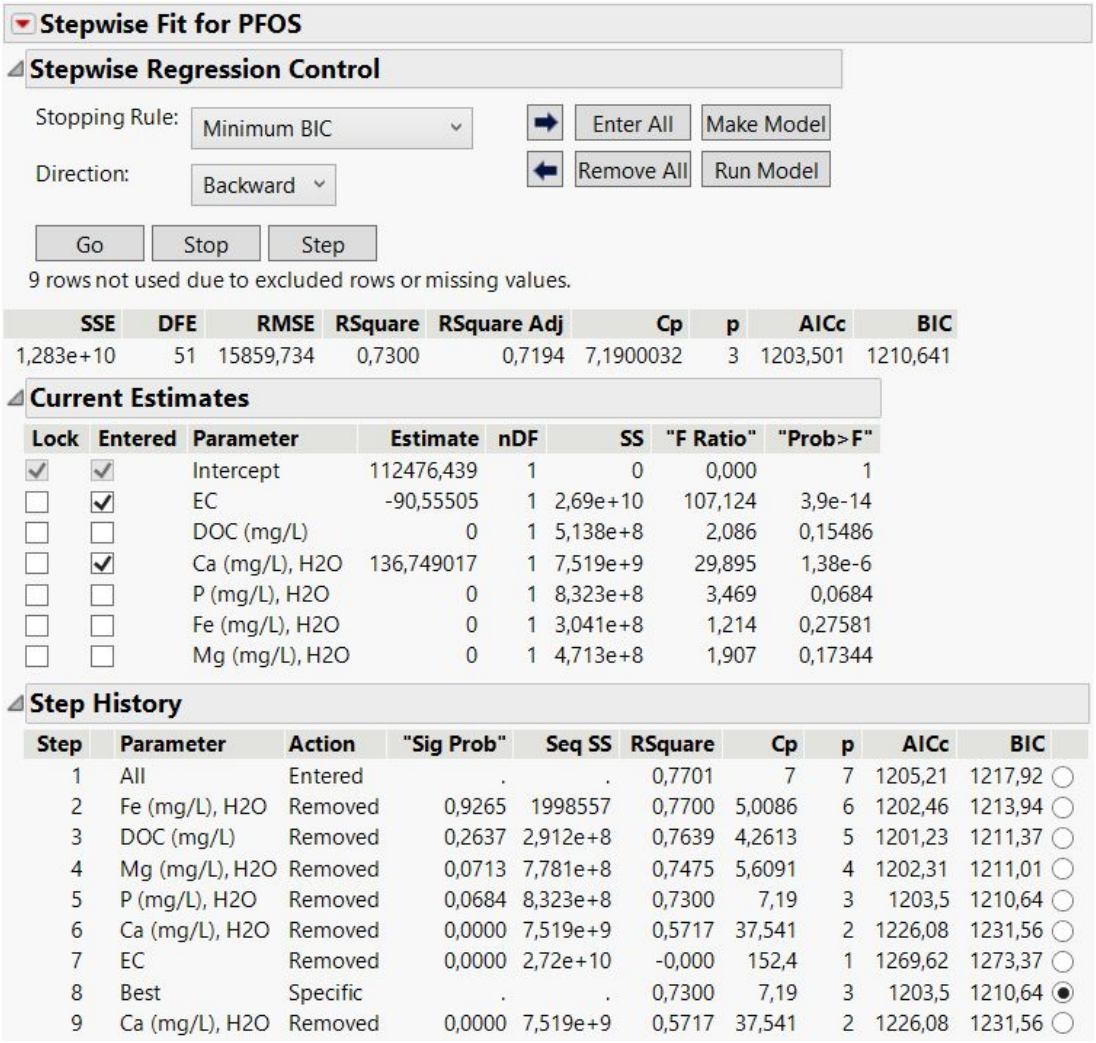

Stepwise Fit for PFOS

Stepwise Regression Control

Stopping Rule: Minimum BIC — Enter All — Make Model

Direction: Backward — Remove All — Run Model

Go — Stop — Step

9 rows not used due to excluded rows or missing values.

SSE	DFE	RMSE	RSquare	RSquare Adj	Cp	p	AICc	BIC
1,283e+10	51	15859,734	0,7300	0,7194	7,1900032	3	1203,501	1210,641

Current Estimates

Lock	Entered	Parameter	Estimate	nDF	SS	"F Ratio"	"Prob>F"
☑	☑	Intercept	112476,439	1	0	0,000	1
☐	☑	EC	-90,55505	1	2,69e+10	107,124	3,9e-14
☐	☐	DOC (mg/L)	0	1	5,138e+8	2,086	0,15486
☐	☑	Ca (mg/L), H2O	136,749017	1	7,519e+9	29,895	1,38e-6
☐	☐	P (mg/L), H2O	0	1	8,323e+8	3,469	0,0684
☐	☐	Fe (mg/L), H2O	0	1	3,041e+8	1,214	0,27581
☐	☐	Mg (mg/L), H2O	0	1	4,713e+8	1,907	0,17344

Step History

Step	Parameter	Action	"Sig Prob"	Seq SS	RSquare	Cp	p	AICc	BIC	
1	All	Entered	.	.	0,7701	7	7	1205,21	1217,92	○
2	Fe (mg/L), H2O	Removed	0,9265	1998557	0,7700	5,0086	6	1202,46	1213,94	○
3	DOC (mg/L)	Removed	0,2637	2,912e+8	0,7639	4,2613	5	1201,23	1211,37	○
4	Mg (mg/L), H2O	Removed	0,0713	7,781e+8	0,7475	5,6091	4	1202,31	1211,01	○
5	P (mg/L), H2O	Removed	0,0684	8,323e+8	0,7300	7,19	3	1203,5	1210,64	○
6	Ca (mg/L), H2O	Removed	0,0000	7,519e+9	0,5717	37,541	2	1226,08	1231,56	○
7	EC	Removed	0,0000	2,72e+10	-0,000	152,4	1	1269,62	1273,37	○
8	Best	Specific	.	.	0,7300	7,19	3	1203,5	1210,64	◉
9	Ca (mg/L), H2O	Removed	0,0000	7,519e+9	0,5717	37,541	2	1226,08	1231,56	○

Figure R1. The stepwise regression results—including the stepwise regression control panel, the resulting estimates and the step history for performing the regression in the backwards direction. The elements' measured batch leachate concentrations (i.e., mg/L of P, Mg, Ca and Fe) were the values employed in the analysis. With an RSquare value of 0.73, the EC and Ca variables were found to explain 73 % of the variance seen in PFOS leachate concentrations. Removing Ca (thus only having EC as a parameter) gave an RSquare value of 0.57.

Running a model with *PFOS concentration* as the response variable and both *EC* and *Ca concentration* as predictor variables led to the parameter estimates displayed in Table R1. Information on the analysis of variance (ANOVA) and a summary of fit are given in Table R2 and Table R3, respectively.

Table R1. The parameter estimates for PFOS (ng/L) leachate concentration

Term	Estimate	Std Error	t Ratio	Prob>|t|	VIF
Intercept	112476,44	3423,927	32,85	<,0001*	.
EC	-90,55505	8,749223	-10,35	<,0001*	3,1874425
Ca (mg/L), H2O	136,74902	25,01082	5,47	<,0001*	3,1874425

Table R2. Analysis of variance (ANOVA) table providing information on the degrees of freedom (DF), sum of squares, mean square, F ratio and p-value (Prob > F).

Source	DF	Sum of Squares	Mean Square	F Ratio
Model	2	3,4682e+10	1,734e+10	68,9423
Error	51	1,2828e+10	251531171	**Prob > F**
C. Total	53	4,751e+10		<,0001*

Table R3. Table displaying the summary of fit—including RSquare values, root mean square error, mean of response and observation number.

RSquare	0,729994
RSquare Adj	0,719405
Root Mean Square Error	15859,73
Mean of Response	81740,74
Observations (or Sum Wgts)	54

Due to the very small p-value reported in the ANOVA table (table R2), at least one term in the model should be significant. As further seen in Table R1, the p-values for both EC and Ca are very small as well. Thus, EC and CA are both highly significant. While the parameter estimate of Ca was positive, the EC had a negative parameter estimate—implying that an increase in EC would give a decrease in the response value (PFOS concentration). Additionally, that all VIF (variance inflation factors) were < 4 (table R1) indicated that multicollinearity between the predictors was not an issue.

[This is the last page left blank intentionally]

Norges miljø- og biovitenskapelige universitet
Noregs miljø- og biovitskapelege universitet
Norwegian University of Life Sciences

Postboks 5003
NO-1432 Ås
Norway